TECHNISCHE UNIVERSITÄT DRESDEN

Faculty of Environmental Sciences Institute of Urban Water Management

Variable reaction rate models for chlorine decay and trihalomethanes formation in drinking and swimming pool waters

Dissertation zur Erlangung des akademischen Grades

Doktoringenieur (Dr.-Ing.)

an der Fakultät Umweltwissenschaften der Technischen Universität Dresden

vorgelegt von

M. Sc. Pei Hua

geboren am 15. Januar 1985 in Chengdu, China

Verteidigt am 22. September 2016

Gutachter:

Prof. Dr. sc. techn. Peter Krebs, Technische Universität Dresden, Germany

Prof. Dr. Gongduan Fan, Fuzhou University, China

Prof. Dr.-Ing. Wolfgang Uhl, Norwegian Institute for Water Research, Norway

ACKNOWLEDGEMENT

During my Ph.D. study, I received supports and helps from many people. First and foremost, I am profoundly indebted to my doctoral supervisor, Prof. Dr.-Ing. Wolfgang Uhl, who was very generous with his time and knowledge, assisted me in each step of my Ph.D. experience. His encouragements and supports inspired me and gave me the confidence to make my Ph.D. study more productive and creative.

Dipl.-Ing. Klaus Ripl is sincerely thanked for his constructive suggestions and helpful discussion at the early stage of my modeling research. Thanks to Dr. Ekaterina Vasyukova for her patience to review my countless pages of manuscripts and her invaluable suggestions. I would like to express my gratitude to them again not only for the work related helps, but also for their intensive personal helps to made me integrate to the environment easily and quickly.

Thanks to Dr.-Ing. Irene Slavik, Nadine Siebdrath, Bertram Skibinski, Javier Farias and Wei Ding for their academic advices and discussions. Thanks to Gerit Orzechowski who provided me the laboratory and technical support. In particular, I am grateful to Prof. Dr. Peter Krebs. His helps and supports encouraged me to go through the final Ph.D. phase.

Certainly, I gratefully acknowledge all the students who I supervised and worked with, Xiao Chen, Sai Ma, Liyeen Chen, for their great assistances with my research studies. Thanks also go to all the staff from our institute for giving me all the necessary assistance and friendly atmosphere.

I would like to gratefully acknowledge the state-sponsored scholarship program provided by China Scholarship Council (CSC) which offered me a four-year stipend for study abroad. Thanks also to Completion grants - sponsored by the German Academic Exchange Service (DAAD, Deutschen Akademischen Austauschdienstes) in the frame of the STIBET funding program which supported the last phase of my Ph.D. program.

Finally, but not least, I would like to thank my family. I am deeply indebted to my parents who gave an important and indispensable source of spiritual support. Thanks to Jin Zhang for his endless encouragement and support throughout the whole period. He understood every difficulty I had during my PhD journey, trusted my ability and inspired me to keep going.

Pei Hua

Dresden, Germany

December, 2015

STATEMENT OF ORIGINAL AUTHORSHIP

I hereby confirm that this copy conforms to the original dissertation on the topic:

"Variable reaction rate models for chlorine decay and trihalomethanes formation in drinking and swimming pool waters"

Die Übereinstimmung dieses Exemplars mit dem Original der Dissertation zum Thema:

„Variable reaction rate models for chlorine decay and trihalomethanes formation in drinking and swimming pool waters"

wird hiermit bestätigt.

Signed:

Pei Hua

Date: Place

ABSTRACT

An important aspect of modeling water quality in water distribution system (WDS) is to predict the temporal and spatial distribution of disinfectant, and the formation of disinfection byproducts (DBP). Consistent efforts have been made to investigate the kinetics of chlorine decay and trihalomethanes (THM) formation in WDS, which are caused by the reaction of chlorine with natural organic matter (NOM). NOM is a heterogeneous mixture of complex compounds. Each specific compound shows individual reactivity with chlorine. Therefore, to better understand and predict the kinetics of chlorine decay and THM formation, the core assumption of this study was established. That is, the variable reactivity of NOM should be involved into the second order kinetics model. Specifically, each single reactive site provided by NOM shows its individual reactivity towards chlorine decay and THM formation, which can be expressed by its individual reaction rate constant, while the mixture compounds of NOM shows the overall reactivity with respect to chlorine decay and THM formation, which should be expressed by an overall reaction rate coefficient. With the reaction progress, the overall reaction rate coefficient was assumed to be continuously decreasing with the reaction time due to the decreased concentration and reactivity of NOM. The decreased overall reaction rate coefficient was referred as a variable reaction rate coefficient (VRRC) in this dissertation. The VRRC was calculated as an exponential function with limited model parameters, which was only related to the characteristics of NOM but independent of chlorine concentration. By introducing the VRRC, the required model parameters were reduced, calibration was simplified and therefore the models showed abilities for a wider application.

Consequently, a systematic work has been carried out to develop VRRC models of chlorine decay and THM formation based on the above mentioned assumption, and further extend and validate the models under different chlorination conditions. The following specific topics were addressed.

- A VRRC model of chlorine decay was developed and validated under different conditions, including different initial chlorine dosages, different temperature,

rechlorination and water mixing conditions.

- Based on the identical assumption applied in the chlorine decay model, a VRRC model of THM formation was also developed and also validated under different chlorination conditions, such as, different initial chlorine dosages, changeable temperature condition and rechlorination.
- The model application was extended from bulk reaction to wall reaction by considering the presence of pipe deposits in the WDS. Both the chlroine decay and THM formation models were advanced and validated when pipe deposits were present in water.
- To further validate the core assumption proposed in this dissertation and also validate the proposed models have a wide application, the residual chlorine and THM concentrations in chlorinated swimming pools were predicted.

Both the model accuracy and model adequacy were evaluated through statistical analysis. The results showed that the proposed models were well suited for application in water quality modeling for distribution systems.

KEYWORDS

Body fluid analogue; chlorine decay; dissolved organic matter; drinking water distribution system; kinetic model; pipe deposits; rechlorination; swimming pool; trichloromethanes formation; variable reaction rate coefficient; water mixing

TABLE OF CONTENTS

LIST OF FIGURES

LIST OF TABLES

ABBREVIATIONS

BP	Biopolymer
BFA	Body fluid analogue
BB	Building blocks
BSF	Bromine substitution factor
CV	Coefficient of variation
Cl	Chlorine
DBP	Disinfection byproducts
DOC	Dissolved organic carbon
DOM	Dissolved organic matter
DPD	N, N-diethyl-p-Phenylenediamine
FO	First order
HA	Humic acid
HS	Humic substances
HAA	Haloacetic acids
HOC	Hydrophobic organic carbon
ICC	Initial chlorine concentration
LMW-neutrals	Low molecular weight neutrals
LMW-acid	Low molecular weight acids
NOM	Natural organic matter
PDs	Pipe deposits
RMSE	Root-mean-square error
R^2	Coefficient of determination
SO	Second order
SP	Swimming pool
SSE	Sum of square error
THM	Trihalomethanes
TTHM	Total trihalomethanes
THMFP	Trihalomethanes formation potential
TCM	Trichloromethane

TOC		Total organic carbon
UV_{254}		UV absorbance at 254 nm
VRRC		Variable reaction rate coefficient
WDS		Water distribution system
X		Fractional conversion
2R		Two-reactant
$c_{Cl}(t)$	[mg/L]	Chlorine concentration at time t
$c_{Ri,Cl}(t)$	[mg/L]	Concentration of i^{th} reactive site R_i with respect to chlorine decay at time t
$c_{Ri,TCM}(t)$	[µM]	Concentration of the available reactive site R_i at time t with respect to TCM formation
$c_{R,Cl}(t)$	[mg/L]	Concentration of all reactive sites with respect to chlorine decay at time t
$c_{sj,Cl}(t)$	[mg/L]	Concentration of all reactive sites provided by substance S_j with respect to chlorine decay
$c_{mix,Cl}(t)$	[mg/L]	Concentration of reactive sties provided by the mixtures with respect to chlorine decay at time t
$c_{R,TCM}(t)$	[µM]	Concentration of all available reactive site at time t with respect to TCM formation
$c_{sj,TCM}(t)$	[µM]	Concentration of all reactive sites provided by substance S_j with respect to TCM formation at time t
$c_{mix,TCM}(t)$	[µM]	Concentration of reactive sties provided by the mixtures with respect to TCM formation at time t
$k_{i,Cl}(t)$	[L/mg/h]	Reaction rate constant of chlorine decay for the i^{th} reactive-site at time t
$k_{i,TCM}(t)$	[L/µmol/h]	Reaction rate constant of TCM formation for the i^{th} reactive-site at time t
$k_{i,Br\text{-}THM}(t)$	[L/µmol/h]	Reaction rate constant of brominated THM formation for i^{th} reactive site at time t
$k_{ov,Cl}(t)$	[L/mg/h]	Overall (variable) reaction rate coefficient of chlorine at time t
$k_{ov,TCM}(t)$	[L/µmol/h]	Overall (variable) reaction rate coefficient of TCM formation at time t
$k_{ov,TTHM}(t)$	[L/µmol/h]	Overall (variable) reaction rate coefficient of TTHM formation at time t
$k_{mix,Cl}(t)$	[L/mg/h]	Overall (variable) rate coefficient of chlorine decay for mixtures at time t

$k_{ov,Cl}^{S_j}$	[L/mg/h]	Overall reaction rate coefficient of chlorine decay for j^{th} substance
$k_{ov,TCM}^{S_j}$	[L/µmol/h]	Overall reaction rate coefficient of TCM formaiton for j^{th} substance
P_i		Disinfection by-product of a specific reaction
P		The collection of all disinfection by-products
R_i		The i^{th} chlorine-reactive site with $i = 1, \ldots, n$
$R_{i,Cl}$		The i^{th} reactive site with respect to chlorine decay
$R_{i,TCM}$		The i^{th} reactive site with respect to TCM formation
R		The collection of all chlorine-reactive sites
$R_{i,Cl}^{S_j}$		The i^{th} reactive sites provided by j^{th} substance (S_j) for chlorine consumption
$R_{i,\mathrm{TCM}}^{S_j}$		The i^{th} reactive sites provided by j^{th} substance (S_j) for TCM formation
$\Delta c_{Cl,max}$	[mg/L]	Total (or maximum) chlorine demand
$\Delta c_{Cl}(t)$	[mg/L]	Consumed chlorine at time t
$\Delta c_{TCM}(t)$	[µM]	Concentration of TCM at time t
Δc_{TCMFP}	[µM]	Trichloromethane formation potential
Δc_{THMFP}	[µM]	Trihalomethanes formation potential
α	[L/mg/h]	Model parameter with respect to chlorine decay
β		Model parameter with respect to chlorine decay
φ	[L/µmol/h]	Model parameter with respect to TCM formation
χ		Model parameter with respect to TCM formation
γ		Substitution-rate ratio of chlorine to bromine

LIST OF PUBLICATIONS FROM THIS RESEARCH

Peer Reviewed Journal and Book Chapter Publications

[1] **Pei Hua**, E. Vasyukova and W. Uhl (2015). A variable reaction rate model for chlorine decay in drinking water due to the reaction with dissolved organic matter. *Water Research*, 75 (0): 109-122

[2] **Pei Hua**, X. Chen, E. Vasyukova and W. Uhl (2015). Reaction kinetics of chlorine with human body fluids present in swimming pool water. *The Royal Society of Chemistry. ISBN:978-1-78262-0884*, pages 322-329

Peer Reviewed Conference Publications

[3] **Pei Hua**, S. Ma, W. Ding, J. Zhang and W. Uhl (2016). Towards a better design of the pipe section reactor based on computational fluid dynamics analysis (accepted as Poster presentation). In: Proc. "IWA World Water Congress & Exhibition", Brisbane, Queensland, October 09-13.

[4] **Pei Hua**, E. Vasyukova and W. Uhl (2014). Effects of pipe deposits on chlorine consumption and trihalomethanes formation in drinking water distribution system (oral presentation). In: Proc. "IWA World Water Congress", Lisbon/Portugal, September 21-26.

[5] **Pei Hua**, E. Vasyukova and W. Uhl (2014). Assessing the reactivity of natural organic matter upon chlorination through chlorine decay and THM formation model (poster presentation). In: "Wasser 2014 - Jahrestagung der Wasserchemischen Gesellschaft", Haltern am See, Germany, May 26-28, 384-387. ISBN: 978-3-936028-83-6.

[6] **Pei Hua**, E. Vasyukova and W. Uhl (2013). Variable reactivity modeling for predicting the disinfection by-product formation in drinking water distribution systems. In: Proc. "Am. Water Works Ass. Water Qual. Technol. Conf." Long Beach/USA, November 3-7.

[7] **Pei Hua**, E. Vasyukova and W. Uhl (2012). Variable reactivity modeling for chlorine decay and THM formation in drinking water distribution systems (oral presentation). In: Proc. "Disinfection of Water, Wastewater and Biosolids conference", Mexico City, Mexico, November 26-29.

CHAPTER 1

General introduction

1 GENERAL INTRODUCTION

1.1 BACKGROUND

The management of drinking water distribution system (WDS) is a complex engineering challenge. On the one hand, the large spatial extent of WDS, multiple flow paths, variable retention time, retention time distribution and flow rate are the causes for the management complexities of WDS. On the other hand, a good WDS management requires not only the hydraulics controlling but also the water quality maintenance during the water distribution. Mathematic models of WDS have reached operational status for various purposes. Generally, the flows and velocities in links and pressures at nodes can be determined by a hydraulic model, while the contaminant concentrations throughout the distribution system can be simulated by a water quality model. Usually, the water quality model is combined with the output of hydraulic model, and thus, these two models become an integrated package (Shang et al. 2007).

An important aspect of modeling water quality in WDS is the ability to predict the temporal and spatial distribution of disinfectant residuals, as well as the formation of disinfection byproducts. Chlorine has been widely used as disinfectant to protect against contamination and to limit bacterial regrowth in WDS. However, it also reacts with natural organic matter (NOM) to produce literally hundreds of halogenated byproducts. Some of these disinfection byproducts (DBP) exhibit cancer risks and other adverse effects on human health (Hebert et al. 2010, Hrudey 2009, Richardson et al. 2002, Villanueva et al. 2004, Xu and Weisel 2004). Among the detected DBPs, trihalomethanes (THM) are accounted for the greatest quantities. Therefore, predicting the residual chlorine and THM concentration in WDS through reliable water quality models is of particular interest. Moreover, the predicted concentrations at the end points of WDS, which in turn, provide suggestions to minimize the chlorine dosage at waterworks or optimize the booster doses (rechlorination) at intermediate locations (Kurek and Ostfeld 2013, Ohar and Ostfeld 2014).

To simplify the modeling approaches, the water quality models are developed separately with regard to bulk reaction and wall reaction. As shown in **Fig. 1-1**, the bulk reaction reflects the interaction of chlorine with NOM remaining in bulk water after the drinking water treatment. The wall reaction indicates the reaction of chlorine with pipe particulate, biofilm, and pipe materials etc. The following section will review the historical and current research focuses which is regarding the development of kinetics models for both bulk reaction and wall reaction. Based on the literature review, the motivation and objectives of this research study are revealed. The structure of the dissertation will be explained in the following sections as well.

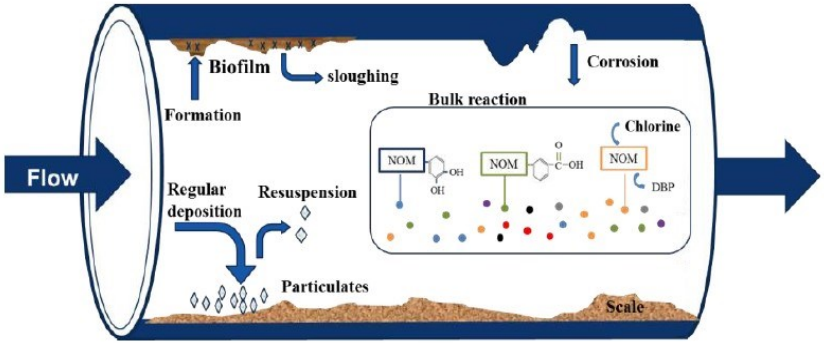

Figure 1-1. Bulk reaction and wall reaction in drinking water distribution system (revised based on Vreeburg et al. (2008)).

1.1.1 Model development with respect to bulk reaction

As addressed above in **Fig. 1-1**, the bulk reaction represents the reaction of chlorine with NOM in bulk water. Due the reaction and the relative long retention time in WDS, harmful DBP may be formed at a high concentration (Brown et al. 2011, Elshorbagy et al. 2000). It is widely known that NOM is a heterogeneous mixture of complex compounds, including humic substances (fulvic acid and humic acid), amino acid, lipids, amino sugars, proteins, and polysaccharides (Fabris et al. 2008, Vasyukova et al. 2013). These compounds exhibit different chemical properties and therefore have different reactivity with chlorine (Cooper et al. 2008, Świetlik et al. 2004, Zhang et al. 2009).

To investigate the characteristics of an individual NOM compound or to determine the rate constants of chlorine decay and THM formation for a fraction (species) of NOM, consistent efforts have been made by chlorination of a specific NOM isolates. The aforementioned NOM isolates were either obtained from separation technologies, such as resin adsorption and membrane fractionation, or acquired from synthesizing samples of specific organic matter (Assemi et al. 2004, Ma et al. 2013, Marhaba et al. 2003, Marhaba et al. 2000, Matilainen et al. 2011). The experiment results validate the importance of NOM characterization for the kinetics of chlorine decay and THM formation. Gallard et al. (2004) reported that resorcinol-type structures are the fast reacting species for the THM formation, while the phenolic compounds may belong to the slow reacting species. Gang et al. (2003) reported that the total THM (TTHM) formation increased with the decreased molecular weight of NOM. Yang et al. (2008) concluded that aromatic contents contributed to the THM formation mostly. Collectively, the specific reactive site provided by NOM has its own reactivity with respect to chlorine decay and THM formation. From modeling standpoint, the individual reactivity of a single reactive site can be expressed by a specific reaction rate constant, while the reactivity of NOM mixture should be expressed by an overall reaction rate coefficient.

Based on the above discussion, the core assumption is established. For the second order reaction rate model, which considers two reactants in water, i.e. chlorine and reactive site provided by NOM, it is important to take the variable reactivity of NOM into account (Jonkergouw et al. 2008). Specifically, the overall reaction rate coefficient for the NOM (heterogeneous mixture) is related to the individual reactivity and concentration of each specific reactive site. With the reaction progress, the overall reaction rate coefficient of the NOM is assumed to be continuously decreasing with reaction time. Therefore, the decreased overall reaction rate coefficient is referred as variable reaction rate coefficient (VRRC) in this research study.

The introduction of VRRC is expected to reduce the model calibration efforts. AWWA (2014) conducted a survey on the trends in WDS modeling, it is concluded

that model calibration and parameter estimation technology are the most challenging tasks of WDS modeling. The VRRC enables the proposed model to have wider application in different scenarios, such as the variable initial chlorine dosages (Gibbs et al. 2006), rechlorination (Boccelli et al. 2003, Lee et al. 2007, Ohar and Ostfeld 2014), water mixing and different temperature conditions (Chen et al. 2008, Fisher et al. 2012, McKay et al. 2013, Vieira et al. 2004, Zhang et al. 2013). **Fig. 1-2** shows the general presentation of different scenarios in WDS. In this research study, the developed models would be applied in different scenarios with invariant parameters (**Chapter 2**).

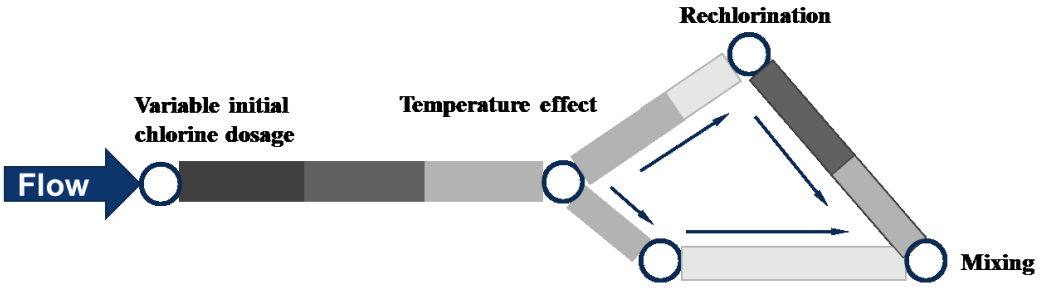

Figure 1-2. Schematic representation of different operation condition in WDS.

For the development of TTHM formation model in bulk water, not only the reactivity of NOM but also the effect of bromide concentration should be taken into account, as THM is a group of DBP contains chloroform and brominated THM. It is widely accepted that the bromide remaining in treated water is oxidized by chlorine to bromine very fast. A great deal of efforts has been made to investigate the incorporation of bromide ion on TTHM formation (Chowdhury et al. 2010, Fabbricino and Korshin 2009, Hua et al. 2006, Tian et al. 2013). A so-called bromine incorporation factor was introduced and further extended to a bromine substitution factor. However, these factors are usually constant and indicate the incorporation of bromine to the maximum TTHM formation, i.e. TTHM formation potential, whereas the bromine substitution factor during the TTHM formation progress is usually ignored. Specifically, during the TTHM formation progress, the brominated THM accounts for the large proportion of TTHM at the beginning phase of reaction progress as the substitution rate of bromine is faster than chlorine with NOM (Chang

et al. 2001, Uyak and Toroz 2007). Nevertheless, the bromine concentration is much lower than chlorine concentration in practice; the chloroform becomes a prevalent substance of TTHM in a later phase of reaction progress. Therefore, both the bromine incorporation factor and the bromine substitution factor should decrease with the reaction progress rather than remaining a constant value. Therefore, the effect of bromine on the kinetics of TTHM formation is modelled in this research study (**Chapter 3**).

1.1.2 Model development with respect to wall reaction

As shown in **Fig. 1-1**, free chlorine reacts not only with NOM remaining in the bulk water, but also with biofilm (Chandy and Angles 2001, Lu et al. 1999, Teng et al. 2008), pipe materials (Al-Jasser 2007), and pipe deposits (PDs) (Hassan et al. 2006, Zhang and Andrews 2012) which is termed as the wall reaction (Vikesland 2000). The wall reaction also includes the mass transfer of disinfectant from the bulk water to the pipe wall at different flow rates (Reynolds number). As reported in the literature, the wall reaction rate was usually indirectly determined from in-situ field measurements in the WDS (Maier et al. 2000). Specifically, the loss of disinfectant and the TTHM formation are measured between two sampling points while the contribution by the bulk water is subtracted. Although this method has been applied with some success, it lacks a firm foundation in the description of kinetic principles of wall reaction as the physical and chemical conditions within the WDS are seldom constant (Mouly et al. 2010, Wert et al. 2012).

Therefore, the investigation of the wall reaction under well-controlled laboratory condition provides a prerequisite for the model development with regard to the wall reaction (Digiano and Zhang 2005, Westbrook and Digiano 2009, Zhang and Andrews 2013). In this research study (**Chapter 4**), the effects of pipe deposits on the chlorine decay and THM formation are investigated and quantified from modeling standpoint. Generally, the developed models for bulk reaction are extended to simulate the chlorine and THM concentrations in the presence of pipe deposits.

1.1.3 Model application in swimming pool

Chlorine is widely used as disinfectant and oxidant to control the microbial activity in the swimming pool (SP) water (Casanovas-Massana and Blanch 2013, Goeres et al. 2004). Not only the NOM that comes from the filling water reacts with chlorine to form THM in the SP water, the human body fluids that are excreted by swimmers may also result in THM formation (Chu and Nieuwenhuijsen 2002, Dyck et al. 2011, Kim et al. 2002).

The filling water is usually tap water obtained from a WDS which contains the remaining NOM after the water treatment, while the human body fluids are composed of urine, sweat and some synthetic chemicals. Previous studies reported the introduction rates of sweat per each swimmer per event ranging from 200 to 1760 mL and introduction rates of urine per each swimmer ranging from 25 to 117 mL/event (Lian et al. 2014).

Using the same models, which are originally developed for WDS, to simulate the chlorine consumption and THM formation in SP water is a special model application in this research study. The reasons of this application are listed as follows: (1) the NOM in the filling water and the human body fluids have very different characteristics, i.e. exhibit different reactivity towards chlorine consumption and THMs formation; (2) the NOM in the filling water is assured to completely mix with human body fluids in the SP water, which is similar as the water mixing condition existed in WDS; and (3) to maintain a certain level of chlorine concentration in the SP, the chlorine is continuously dosed into SP water, which can be treated as a rechlorination condition. Therefore, it is interesting to apply the same models to the SP water to test whether or not the model has a wide application, and further validate the reliability of the proposed model. Specifically, in **Chapter 5**, the reactivity of individual human body analogue in the SP water was quantified firstly; the overall reactivity of organic matter in the SP water towards chlorine consumption and THM formation are predicted by using the modeling techniques.

1.2 OBJECTIVES AND INNOVATIONS

The general objective of this research was to develop water quality models regarding the kinetics of chlorine decay and THM formation in WDS. The models extended the existing second order kinetics models by taking into account (1) the variable reactivity of reactant (NOM); (2) the variable bromine substitution factor during the reaction progress; and (3) the effects of pipe deposits. Based on this approach, the models are expected to reduce the required number of parameters, simplify the calibration process, and enable the model to have wider application under different chlorination conditions in WDS as well as in swimming pool.

To clarify the systematic development of study, **Fig. 1-3** shows a schematic structure. The research was started with the development of model with respect to the bulk reaction. The main novelty was to taking the variable reactivity of NOM into account. The variable reactivity of NOM was expressed by the variable reaction rate coefficient which was calculated by an exponential function with two model parameters. The proposed models were applied in different chlorination conditions in WDS, such as different initial chlorine concentrations dosed in waterworks, seasonal temperature variation, rechlorination and water mixing condition. It should be illustrated that the invariant two parameters were used for all above mentioned scenarios as long as the water comes from the same origin.

Following that, the models, which were developed for the bulk reaction, were extended for the wall reaction by considering the effects of pipe deposits on reaction kinetics. Similar as the models for the bulk reaction, the models developed for wall reaction were also required to simulate residual chlorine and THM concentrations under different conditions by applying invariant parameters. Finally, the models were applied in one special application, i.e. to predict the kinetics of chlorine consumption and THM formation in the SP.

Generally, the objectives and respective innovations are summarized as follows,

(1) Development of a chlorine decay model for the bulk reaction by considering the variable reactivity of NOM. Applying the models under different conditions,

such as different initial chlorine concentrations, different temperature, rechlorination and mixing conditions;

(2) Development of THM formation model for the bulk reaction by taking into account not only the variable reactivity of NOM but also the changing bromine substation factor into account. Applying the models under different conditions, such as different initial chlorine concentrations, different temperature, rechlorination condition;

(3) Extend the chlorine decay and THM formation kinetics models for wall reaction, i.e. pipe deposits are present; and

(4) Applying the models to simulate chlorine consumption and THM formation in the SP water. To quantify the reaction rate coefficient of individual body fluids analogue (BFA) and to predict the chlorine consumption and THM formation of BFA mixture as well as the mixture of BFA and NOM in the filling water.

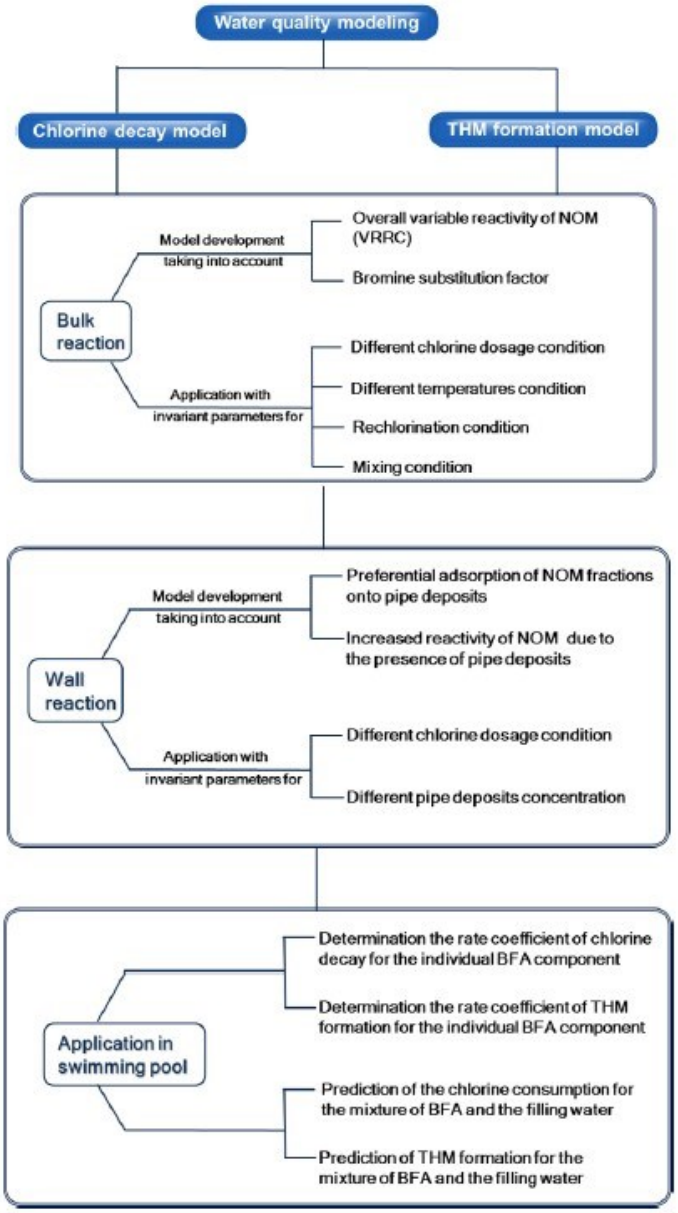

Figure 1-3. Schematic structure of research objectives and innovations.

1.3 OUTLINE OF THIS THESIS

This thesis is structured into seven chapters.

Chapter 1 provides the general introduction of the research topic and the prevailing research problems in this research area.

Chapter 2 includes the introduction of a variable reaction rate model for chlorine decay in drinking water due to the reaction with the dissolved organic matter (bulk reaction).

In Chapter 3, a variable reaction rate model for THM formation in drinking water due to the reaction with the dissolved organic matter (bulk reaction) is presented.

In Chapter 4, the variable reaction rate models for chlorine decay and THM formation were extended to the wall reaction when the pipe deposits are present in drinking water.

In Chapter 5, the chlorine decay and THM formation models were applied to the prediction of chlorine consumption and THM formation in the SP water.

Chapter 6 provides a summary of this study.

Chapter 7 provides the supplementary information.

References

Al-Jasser, A.O. (2007) Chlorine decay in drinking-water transmission and distribution systems: Pipe service age effect. Water Research 41(2), 387-396.

Assemi, S., Newcombe, G., Hepplewhite, C. and Beckett, R. (2004) Characterization of natural organic matter fractions separated by ultrafiltration using flow field-flow fractionation. Water Research 38(6), 1467-1476.

AWWA (2014) Committee Report: Trends in water distribution system modeling.

Boccelli, D.L., Tryby, M.E., Uber, J.G. and Summers, R.S. (2003) A reactive species model for chlorine decay and THM formation under rechlorination conditions. Water Research 37(11), 2654-2666.

Brown, D., Bridgeman, J. and West, J.R. (2011) Predicting chlorine decay and THM formation in water supply systems. Reviews in Environmental Science and Bio/Technology 10(1), 79-99.

Casanovas-Massana, A. and Blanch, A.R. (2013) Characterization of microbial populations associated with natural swimming pools. International Journal of Hygiene and Environmental Health 216(2), 132-137.

Chandy, J.P. and Angles, M.L. (2001) Determination of nutrients limiting biofilm formation and the subsequent impact on disinfectant decay. Water Research 35(11), 2677-2682.

Chang, E.E., Lin, Y.P. and Chiang, P.C. (2001) Effects of bromide on the formation of THMs and HAAs. Chemosphere 43(8), 1029-1034.

Chen, C., Zhang, X.-j., Zhu, L.-x., Liu, J., He, W.-j. and Han, H.-d. (2008) Disinfection by-products and their precursors in a water treatment plant in North China: Seasonal changes and fraction analysis. Science of The Total Environment 397(1–3), 140-147.

Chowdhury, S., Champagne, P. and James McLellan, P. (2010) Investigating effects of bromide ions on trihalomethanes and developing model for predicting bromodichloromethane in drinking water. Water Research 44(7), 2349-2359.

Chu, H. and Nieuwenhuijsen, M. (2002) Distribution and determinants of trihalomethane concentrations in indoor swimming pools. Occupational and Environmental Medicine 59(4), 243-247.

Cooper, W., Song, W., Gonsior, M., Kalnina, D., Peake, B. and Mezyk, S. (2008) Recent advances in structure and reactivity of dissolved organic matter in natural waters. Water Science & Technology: Water Supply 8(6).

Digiano, F.A. and Zhang, W. (2005) Pipe section reactor to evaluate chlorine-Wall reaction. Journal - American Water Works Association, 74-85.

Dyck, R., Sadiq, R., Rodriguez, M.J., Simard, S. and Tardif, R. (2011) Trihalomethane exposures in indoor swimming pools: A level III fugacity model. Water Research 45(16), 5084-5098.

Elshorbagy, W.E., Abu-Qdais, H. and Elsheamy, M.K. (2000) Simulation of THM species in water distribution systems. Water Research 34(13), 3431-3439.

Fabbricino, M. and Korshin, G.V. (2009) Modelling disinfection by-products formation in bromide-containing waters. Journal of Hazardous Materials 168(2–3), 782-786.

Fabris, R., Chow, C.W.K., Drikas, M. and Eikebrokk, B. (2008) Comparison of NOM character in selected Australian and Norwegian drinking waters. Water Research 42(15), 4188-4196.

Fisher, I., Kastl, G. and Sathasivan, A. (2012) A suitable model of combined effects of temperature and initial condition on chlorine bulk decay in water distribution systems. Water Research 46(10), 3293-3303.

Gallard, H., Leclercq, A. and Croué, J.-P. (2004) Chlorination of bisphenol A: kinetics and by-products formation. Chemosphere 56(5), 465-473.

Gang, D., Clevenger, T.E. and Banerji, S.K. (2003) Relationship of chlorine decay and THMs formation to NOM size. Journal of Hazardous Materials 96(1), 1-12.

Gibbs, M.S., Morgan, N., Maier, H.R., Dandy, G.C., Nixon, J.B. and Holmes, M. (2006) Investigation into the relationship between chlorine decay and water distribution parameters using data driven methods. Mathematical and Computer Modelling 44(5–6), 485-498.

Goeres, D.M., Palys, T., Sandel, B.B. and Geiger, J. (2004) Evaluation of disinfectant efficacy against biofilm and suspended bacteria in a laboratory swimming pool model. Water Research 38(13), 3103-3109.

Hassan, K.Z., Bower, K.C. and Miller, C.M. (2006) Iron oxide enhanced chlorine decay and disinfection by-product formation. Journal of Environmental Engineering 132(12), 1609-1616.

Hebert, A., Forestier, D., Lenes, D., Benanou, D., Jacob, S., Arfi, C., Lambolez, L. and Levi, Y. (2010) Innovative method for prioritizing emerging disinfection by-products (DBPs) in drinking water on the basis of their potential impact on public health. Water Research 44(10), 3147-3165.

Hrudey, S.E. (2009) Chlorination disinfection by-products, public health risk tradeoffs and me. Water Research 43(8), 2057-2092.

Hua, G., Reckhow, D.A. and Kim, J. (2006) Effect of Bromide and Iodide Ions on the Formation and Speciation of Disinfection Byproducts during Chlorination. Environmental Science & Technology 40(9), 3050-3056.

Jonkergouw, P.M.R., Khu, S.-T., Savic, D.A., Zhong, D., Hou, X.Q. and Zhao, H.-B. (2008) A variable rate coefficient chlorine decay model. Environmental Science & Technology 43(2), 408-414.

Kim, H., Shim, J. and Lee, S. (2002) Formation of disinfection by-products in chlorinated swimming pool water. Chemosphere 46(1), 123-130.

Kurek, W. and Ostfeld, A. (2013) Multi-objective optimization of water quality, pumps operation, and storage sizing of water distribution systems. Journal of Environmental Management 115(0), 189-197.

Lee, J., Lee, D. and Sohn, J. (2007) An experimental study for chlorine residual and trihalomethane formation with rechlorination. Water science and technology 55(1-2), 307-313.

Lian, L., E, Y., Li, J. and Blatchley, E.R. (2014) Volatile Disinfection Byproducts Resulting from Chlorination of Uric Acid: Implications for Swimming Pools. Environmental Science & Technology 48(6), 3210-3217.

Lu, W., Kiéné, L. and Lévi, Y. (1999) Chlorine demand of biofilms in water distribution systems. Water Research 33(3), 827-835.

Ma, D., Gao, B., Sun, S., Wang, Y., Yue, Q. and Li, Q. (2013) Effects of dissolved organic matter size fractions on trihalomethanes formation in MBR effluents during chlorine disinfection. Bioresource Technology 136(0), 535-541.

Maier, S.H., Powell, R.S. and Woodward, C.A. (2000) Calibration and comparison of chlorine decay models for a test water distribution system. Water Research 34(8), 2301-2309.

Marhaba, T.F., Pu, Y. and Bengraine, K. (2003) Modified dissolved organic matter fractionation technique for natural water. Journal of Hazardous Materials 101(1), 43-53.

Marhaba, T.F., Van, D. and Lippincott, R.L. (2000) Changes in NOM fractionation through treatment: A comparison of ozonation and chlorination.

Matilainen, A., Gjessing, E.T., Lahtinen, T., Hed, L., Bhatnagar, A. and Sillanpää, M. (2011) An overview of the methods used in the characterisation of natural organic matter (NOM) in relation to drinking water treatment. Chemosphere 83(11), 1431-1442.

McKay, G., Sjelin, B., Chagnon, M., Ishida, K.P. and Mezyk, S.P. (2013) Kinetic study of the reactions between chloramine disinfectants and hydrogen peroxide: Temperature dependence and reaction mechanism. Chemosphere 92(11), 1417-1422.

Mouly, D., Joulin, E., Rosin, C., Beaudeau, P., Zeghnoun, A., Olszewski-Ortar, A., Munoz, J.F., Welté, B., Joyeux, M., Seux, R., Montiel, A. and Rodriguez, M.J. (2010) Variations in trihalomethane levels in three French water distribution systems and the development of a predictive model. Water Research 44(18), 5168-5179.

Ohar, Z. and Ostfeld, A. (2014) Optimal design and operation of booster chlorination stations layout in water distribution systems. Water Research 58(0), 209-220.

Richardson, S.D., Simmons, J.E. and Rice, G. (2002) Peer Reviewed: Disinfection Byproducts: The Next Generation. Environmental Science & Technology 36(9), 198A-205A.

Shang, F., Uber, J.G. and Rossman, L.A. (2007) Modeling Reaction and Transport of Multiple Species in Water Distribution Systems. Environmental Science & Technology 42(3), 808-814.

Świetlik, J., Dąbrowska, A., Raczyk-Stanisławiak, U. and Nawrocki, J. (2004) Reactivity of natural organic matter fractions with chlorine dioxide and ozone. Water Research 38(3), 547-558.

Teng, F., Guan, Y.T. and Zhu, W.P. (2008) Effect of biofilm on cast iron pipe corrosion in drinking water distribution system: Corrosion scales characterization and microbial community structure investigation. Corrosion Science 50(10), 2816-2823.

Tian, C., Liu, R., Guo, T., Liu, H., Luo, Q. and Qu, J. (2013) Chlorination and chloramination of high-bromide natural water: DBPs species transformation. Separation and Purification Technology 102(0), 86-93.

Uyak, V. and Toroz, I. (2007) Investigation of bromide ion effects on disinfection by-products formation and speciation in an Istanbul water supply. Journal of Hazardous Materials 149(2), 445-451.

Vasyukova, E., Proft, R., Jousten, J., Slavik, I. and Uhl, W. (2013) Removal of natural organic matter and trihalomethane formation potential in a full-scale drinking water treatment plant. Water Science & Technology: Water Supply 13(4).

Vieira, P., Coelho, T. and Loureiro, D. (2004) Accounting for the influence of initial chlorine concentration, TOC, iron and temperature when modelling chlorine decay in water supply. Journal of Water Supply: Research and Technology-AQUA 53, 453-467.

Vikesland, P.J. (2000) The role of the pipe water interface in DBP formation and disinfectant loss, American Water Works Association, U.S.A.

Villanueva, C.M., Cantor, K.P., Cordier, S., Jaakkola, J.J., King, W.D., Lynch, C.F., Porru, S. and Kogevinas, M. (2004) Disinfection byproducts and bladder cancer: a pooled analysis. Epidemiology 15(3), 357-367.

Vreeburg, J.H.G., Schippers, D., Verberk, J.Q.J.C. and van Dijk, J.C. (2008) Impact of particles on sediment accumulation in a drinking water distribution system. Water Research 42(16), 4233-4242.

Wert, E.C., Bolding, J., Rexing, D.J. and Zegers, R.E. (2012) Real-time modeling of trihalomethane formation in a full-scale distribution system. Journal of Water Supply: Research and Technology—AQUA 61(6), 352-363.

Westbrook, A. and Digiano, F.A. (2009) Rate of chloramine decay at pipe surfaces. Journal: American Water Works Association 101(7).

Xu, X. and Weisel, C.P. (2004) Human respiratory uptake of chloroform and haloketones during showering. J Expo Anal Environ Epidemiol 15(1), 6-16.

Yang, X., Shang, C., Lee, W., Westerhoff, P. and Fan, C. (2008) Correlations between organic matter properties and DBP formation during chloramination. Water Research 42(8–9), 2329-2339.

Zhang, H. and Andrews, S.A. (2012) Catalysis of copper corrosion products on chlorine decay and HAA formation in simulated distribution systems. Water Research 46(8), 2665-2673.

Zhang, H. and Andrews, S.A. (2013) Effects of pipe materials, orthophosphate, and flow conditions on chloramine decay and NDMA formation in modified pipe loops. Journal of Water Supply: Research and Technology—AQUA 62(2), 107-119.

Zhang, H., Qu, J., Liu, H. and Wei, D. (2009) Characterization of dissolved organic matter fractions and its relationship with the disinfection by-product formation. Journal of Environmental Sciences 21(1), 54-61.

Zhang, X.L., Yang, H.W., Wang, X.M., Fu, J. and Xie, Y.F. (2013) Formation of disinfection by-products: Effect of temperature and kinetic modeling. Chemosphere 90(2), 634-639.

CHAPTER 2

A variable reaction rate model for chlorine decay in drinking water due to the reaction with dissolved organic matter

---

THIS CHAPTER IS REPRODUCED BASED ON

A variable reaction rate model for chlorine decay in drinking water due to the reaction with dissolved organic matter

Hua P, Vasyukova E and Uhl W

Water Research 75(0), 109-122, 2015

2 A VARIABLE REACTION RATE MODEL FOR CHLORINE DECAY IN DRINKING WATER DUE TO THE REACTION WITH DISSOLVED ORGANIC MATTER

ABSTRACT

A second order kinetic model for simulating chlorine decay in bulk water due to the reaction with dissolved organic matter (DOM) was developed. It takes into account the decreasing reactivity of dissolved organic matter using a variable reaction rate coefficient (VRRC) which decreases with an increasing conversion. The concentration of reducing species is surrogated by the maximum chlorine demand. Temperature dependency, respectively, is described by the Arrhenius-relationship. The accuracy and adequacy of the proposed model to describe chlorine decay in bulk water were evaluated and shown for very different waters and different conditions such as water mixing or rechlorination by applying statistical tests. It is thus very well suited for application in water quality modeling for distribution systems.

KEYWORDS

Chlorine decay model; drinking water; rechlorination; variable reaction rate coefficient; water mixing

2.1 INTRODUCTION

Chlorine is widely used for the disinfection of drinking water due to its relatively low cost and ability to maintain a disinfectant residual throughout drinking water distribution systems (WDS). However, due to the reaction of chlorine with dissolved organic matter and bromide ion, potentially harmful disinfection by-products (DBPs) can be produced, such as trihalomethanes (THM) and haloacetic acids (HAA), which may have adverse effects on human health (Nieuwenhuijsen et al. 2000, Richardson et al. 2007). Furthermore, a high dose of chlorine at the entry of WDS to maintain a desired level of chlorine residual at the system endpoints, will generate taste or odor complaints from upstream consumers and may require booster doses (rechlorination) at intermediate locations to reduce the initial dose. Accordingly, the chlorine dose and residual should be kept low to limit DBPs formation. Meanwhile, it is required to maintain sufficient chlorine residual to protect against contamination and to limit bacterial regrowth.

To optimize the chlorine dose at the DWDS entry and limit DBPs formation, or to properly place booster stations in DWDS, an accurate and widely applicable kinetic model for chlorine decay is needed (Clark 1998, Kastl et al. 1999, Kastl et al. 2003, Kiéné et al. 1998, Ohar and Ostfeld 2014). In practice, the kinetic model of chlorine decay is required to be compatible with hydraulic models, such as EPANET (Rossman 2000, Rossman et al. 1994, Shang et al. 2007). Even for unchlorinated DWDS, which are often found in European countries such as The Netherlands, Denmark and Germany, chlorine decay models are needed as well. For these DWDS, it is important to know how chlorine depletes in case of application after an accidental contamination.

It is generally agreed that the chlorine decay model ideally should describe two mechanisms: homogeneous decay due to the reaction between chlorine and reactants in bulk water (bulk decay) and wall decay due to the reaction between chlorine and pipe materials, and biofilm etc. Fisher et al. (2011) emphasized the need for an accurate model of bulk decay prior to any attempt to characterize the wall decay, and pointed out that separating chlorine decay into bulk and wall decay

minimizes the effort required for calibration. Therefore, this study is focused on the bulk reaction.

Chlorine bulk decay models have been developed as first order (FO) and as second order (SO) models. The latter considers two reactants in water: chlorine and chlorine-reactive species (Clark 1998, Kastl et al. 1999). The FO models are shown to be highly unsuited for modeling, while the SO models show potential capability to simulate chlorine profiles in DWDS (Fisher et al. 2011, Jegatheesan et al. 2006). Kastl et al. (1999) proposed a SO model, which is based on the assumption that chlorine reacts with two classes of reactants. Namely notional fast and slow reducing agents with individual fast and slow rate coefficients which are considered being constant over the reaction period, respectively. Hereafter, this is termed as the two-reactant (2R) model (Fisher et al. 2011). In this 2R model, the so-called fast or slow notional reducing agents are used to represent the complex mixture of (unknown) reactants, and the respective fast or slow reaction rate coefficient is an alternative interpretation of the collection of corresponding reactants. It is assumed that the fast and slow reaction rate coefficients remain constant during the respective reaction periods. However, chlorine disappears in bulk water due to concurrent reactions with a multitude of aqueous constituents with individual reactivity, and should not be simply treated as a fast or slow reducing agent (Deborde and von Gunten 2008, Qualls and Johnson 1983). In fact, the reactivity and concentration of all chlorine-reactive species decrease with reaction time. Therefore, to better predict chlorine bulk decay and minimize recalibration, an overall variable reaction rate coefficient (VRRC) should be introduced to replace separated fast and slow reaction rate coefficients, which is related to the reaction progress and is an alternative interpretation of the collective individual rate constants. Furthermore, to simplify the calibration process, the fast and slow reducing agents which were estimated by the 2R model should be replaced by a sum of the chlorine-reactive reactants.

Jonkergouw et al. (2008) proposed a variable rate coefficient model with an empirical equation for concentration-weighted rate coefficient calculation. However, the model

efficiency in accordance with its complexity is being questioned and some of the parameters are not readily interpretable. Specifically, systematically lower calibrated initial chlorine concentrations (ICCs), rather than those experimentally determined, were used in order to improve the data fit during model validation. Supposedly, the authors had to use such a method due to the straightforward approach they chose which assumed the initial concentration of all reactants to be equal to the total or dissolved organic carbon concentration of a water sample multiplied by 5 or 10 (arbitrarily chosen). Although the accuracy of the model was evaluated at different temperatures, the model parameters were derived for different temperatures, rather than using invariant parameters for the entire data set (Fisher et al. 2011, 2012).

Consequently, the objectives of this work were to (1) develop a SO model for chlorine decay due to the reaction with dissolved organic matter which takes into account the decreasing reactivity of the reactants in water, (2) derive an overall variable reaction rate coefficient k_{ov}, which is described as a function of chlorine consumed, to reflect the decreasing reactivity of reactants (therefore, the model is referred to as VRRC model in this work), (3) show the applicability of the model to chlorination of several water samples collected from different sources and with different organic matter contents, and (4) show the applicability of the model to chlorination of identical water samples at a wide range of ICCs, chlorination at different temperatures, as well as to rechlorination and water mixing by using invariant parameters.

2.2 MODEL DEVELOPMENT

2.2.1 Variable reaction rate coefficient derivation

Chlorine depletion occurs in bulk water due to concurrent reactions with a multitude of aqueous constituents which include dissolved organic matter, particulate organic matter, and inorganic substances (Deborde and von Gunten 2008, Gallard and von Gunten 2002, Vasconcelos et al. 1997, Warton et al. 2006). Each chlorine-reactive species has its own characteristic reaction or reactivity with chlorine. For example, Deborde and von Gunten (2008) reported that, compared to the low chlorine reactivity

of Mn(II) in a homogeneous solution, a faster transformation by chlorine was found for ammonia, halides (Br^- and I^-), SO_3^{2-}, CN^-, NO_2^-, As(III) and Fe(II). Gallard and von Gunten (2002) found that resorcinol-type structures may be responsible for fast reacting species, while phenolic compounds may belong to slow reacting species.

The reaction between chlorine and a single reactive site *i* provided by the reactant can be expressed as follows:

$$Cl + R_{i,Cl} \xrightarrow{k_{i,Cl}} \nu_i P_i \qquad \text{Equation 2-1}$$

where *Cl* represents chlorine either in the form of dissolved chlorine (Cl_2, aq), hypochlorous acid (HOCl) or hypochlorite ions (OCl^-), $R_{i,Cl}$ denotes different reactive sites *i* for chlorine (*i* = 1, 2, …, *n*), P_i is a DBP of the respective reaction, and ν_i is the stoichiometric coefficient for the product P_i. It needs to be pointed out that R_i represents a single reactive site. Thus, the stoichiometric coefficient is equal to one. Furthermore, it is assumed to be of first order with chlorine and first order with a single reactive site provided by the reactant. The reaction rates of chlorine with the individual reactive site R_i are given by:

$$\frac{dc_{Cl_i}(t)}{dt} = \frac{dc_{R_{i,Cl}}(t)}{dt} = -k_{i,Cl} \cdot c_{Cl}(t) \cdot c_{R_{i,Cl}}(t) \qquad \text{Equation 2-2}$$

where $c_{Cl}(t)$ is the concentration of chlorine at time *t* in the bulk water, $c_{Ri,Cl}(t)$ is the concentration of the i^{th} reactive site R_i with respect to chlorine decay at time *t*, and $k_{i,Cl}$ is the reaction rate constant for the i^{th} reactive site.

Thus, chlorine consumption for all reactive sites is obtained as follows:

$$\frac{dc_{Cl}(t)}{dt} = \sum_{i=1}^{n} -k_{i,Cl} \cdot c_{Cl}(t) \cdot c_{R_{i,Cl}}(t) = -c_{Cl}(t) \cdot \sum_{i=1}^{n} \left[k_{i,Cl} \cdot c_{R_{i,Cl}}(t) \right] \qquad \text{Equation 2-3}$$

However, individual rate constants $k_{i,Cl}$ and the concentration of each reactive site R_i are not measureable. Therefore, an alternative form to express **Eq. 2-3** needs to be developed.

Clark (1998) and Clark and Sivaganesan (2002) proposed an equation for chlorine decay based on the second order kinetic and the reaction equation is represented by:

$$Cl + R \rightarrow P$$ Equation 2-4

where R represents the collection of all reactive sites with different reactivity, and P is the collection of all DBPs. The reaction rate is given by:

$$\frac{dc_{Cl}(t)}{dt} = -k_{ov,Cl} \cdot c_{Cl}(t) \cdot c_R(t) = -k_{ov,Cl}(t) \cdot c_{Cl}(t) \cdot \sum_{i=1}^{n} c_{R_{i,Cl}}(t)$$ Equation 2-5

where $c_{R,Cl} = \sum_{i=1}^{n} c_{R_{i,Cl}}$ is the concentration of all reactive sites at time t. In their second order model, $k_{ov,Cl}$ is constant over the whole reaction period.

However, as discussed previously, the reactive sites are consumed as the reaction proceeds and the reactivity of available total reactive sites is also decreasing with reaction time. Thus, $k_{ov,Cl}$ should represent the overall collection of all second order rate constants ($k_{i,Cl}$) and decrease with the progress of the reaction. Consequently, in this work, the decreasing reactivity is taken into account and $k_{ov,Cl}$ is referred to as VRRC.

For each water sample, there is a certain concentration of reactive sites which is reflected in the maximum chlorine demand. It is therefore convenient to describe the reaction progress using the concentration of consumed chlorine as a function of the maximum chlorine demand. Thus, the fractional conversion $X(t)$ is defined as follows:

$$X(t) = \frac{-\Delta c_{Cl}(t)}{\Delta c_{Cl,\max}}$$ Equation 2-6

where $\Delta c_{Cl}(t)$ is the chlorine which has been consumed at time t. It calculated as $c_{Cl}(t)$ minus the initial chlorine concentration $c_{Cl}(0)$, and therefore it is negative. $\Delta c_{Cl,max}$ is the total (maximum) chlorine demand, which is a positive value. By combining **Eq. 2-3** and **Eq. 2-5**, the k_{ov} is expressed by **Eq. 2-7**:

$$k_{ov,Cl}(t) = \frac{\sum_{i=1}^{n}\left[k_{i,Cl} \cdot c_{R_{i,Cl}}(t)\right]}{\sum_{i=1}^{n} c_{R_{i,Cl}}(t)}$$ Equation 2-7

It can be seen from **Eq. 2-7** that the initial $k_{ov,Cl}(0)$ only depends on the rate constants of the individual reactions $k_{i,Cl}$ and the initial concentrations of all chlorine-reactive sites $c_{Ri,Cl}$, and is independent of the ICCs. In other words, the initial $k_{ov,Cl}(0)$ is a constant for an individual water sample. Although the overall VRRC k_{ov} is expressed numerically, it cannot be determined directly from **Eq. 2-7** because the concentration of reactive sites $c_{Ri,Cl}(t)$ and the individual rate coefficients $k_{i,Cl}$ for each chlorine-reactive site cannot be measured or determined. Hence, a new approach to determine $k_{ov,Cl}(t)$ is required. In order to further explore the behavior of k_{ov}, differentiation of **Eq. 2-7** provides:

$$\frac{dk_{ov,Cl}(t)}{dt} = c_{Cl}(t) \cdot \left[k_{ov,Cl}^2(t) - \frac{\sum_{i=1}^{n} k_{i,Cl}^2 c_{R_{i,Cl}}(t)}{c_{R,Cl}(t)} \right]$$ Equation 2-8

The detailed derivation of **Eq. 2-8** is provided in appendix (**Eq. 7-1 to 7-7**). According to **Eq. 2-8**, the change rate of $k_{ov,Cl}$ over time is: (1) negative (validated in appendix **Eq. 7-8 to 7-10**), which indicates that the $k_{ov,Cl}(t)$ decreases. This finding is in accordance with the decreasing reactivity of the reactive sites with reaction progress as reported in the literature, (2) related to the chlorine concentration, i.e. $k_{ov,Cl}(t)$ decreases faster at higher ICCs compared to lower ICCs and, (3) tends to zero when the concentration of chlorine tends to zero.

These characteristics of $k_{ov,Cl}$ obtained from **Eq. 2-7** and **Eq. 2-8** are criteria for the proposition of an empirical equation to calculate $k_{ov,Cl}$. Based on the above theoretical discussion, phenomenologically, an exponential equation may be appropriate to describe the $k_{ov,Cl}(t)$ as given in **Eq. 2-9**:

$$k_{ov,Cl}(t) = \alpha \cdot e^{-\beta \cdot \left[\frac{-\Delta c_{Cl}(t)}{\Delta c_{Cl,\max}}\right]} = \alpha \cdot e^{-\beta \cdot [X(t)]}$$ Equation 2-9

where α and β are model parameters, which should be positive to meet the characteristics of $k_{ov,Cl}$. The unit of α is L/mg/h while the β is dimensionless.

According to **Eq. 2-9**, $k_{ov,Cl}$ always equals α at the beginning of the reaction, i.e. $\Delta c_{Cl}(0) = 0$ and $X(0) = 0$. Thus, the first criterion obtained from **Eq. 2-7** that the initial $k_{ov,Cl}$ is independent of ICCs is met. In other words, α represents initial $k_{ov,Cl}$. **Eq. 2-9** also shows that the $k_{ov,Cl}$ is decreasing with the increasing fractional conversion (X), i.e. the progress of the reaction, which is consistent with the discussion above.

Differentiation of **Eq. 2-9** provides:

$$\frac{dk_{ov,Cl}(t)}{dt} = -\frac{\beta}{\Delta c_{Cl,\max}} \cdot k_{ov,Cl}^2(t) \cdot c_{Cl}(t) \cdot c_{R,Cl}(t) \qquad \text{Equation 2-10}$$

The detailed derivation process regarding **Eq. 2-10** is provided in the supplementary information (**Eq. 7-11 to 7-13**). Comparing **Eq. 2-8** and **Eq. 2-10**, it can be concluded that the proposed exponential equation meets all three criteria related to the changing rate of k_{ov}. Thus, the exponential equation **Eq. 2-9** is suitable to describe k_{ov} from a theoretical point of view. This will be further addressed and validated below by applying experimental data sets.

Substituting **Eq. 2-9** into **Eq. 2-5** yields:

$$\frac{dc_{Cl}}{dt} = -\alpha \cdot e^{-\beta \cdot \left[\frac{-\Delta c_{Cl}(t)}{\Delta c_{Cl,\max}}\right]} \cdot c_{Cl} \cdot c_{R,Cl} \qquad \text{Equation 2-11}$$

Based on the principle of mass conservation as well as the assumption that the stoichiometric coefficients for chlorine and for the reactive sites are equal to one (**Eq. 2-1**), the following relationships are established:

$$c_{Cl}(t) = c_{Cl}(0) + \Delta c_{Cl}(t)$$
$$c_{R,Cl}(t) = c_{R,Cl}(0) + \Delta c_{Cl}(t) \qquad \text{Equation 2-12}$$

where $c_{R,Cl}(0)$ is the initial concentration of chlorine-reactive sites R at time $t = 0$, and $c_{Cl}(0)$ is the ICC, Δc_{Cl} is the consumed chlorine at time t, which is negative. The initial reactant concentration $c_{R,Cl}(0)$ is surrogated by the total (or maximum) chlorine

demand $\Delta c_{Cl,max}$ which can be stoichiometrically and linearly linked to the initial concentration of all chlorine-reactive sites, i.e. $c_{R,Cl}(0) = \Delta c_{Cl,max}$. The latter can be determined experimentally.

Combining **Eq. 2-11** and **Eq. 2-12** yields the final VRRC model:

$$\frac{dc_{Cl}}{dt} = -\alpha \cdot e^{-\beta \cdot \left[\frac{-\Delta c_{Cl}(t)}{\Delta c_{Cl,\max}}\right]} \cdot c_{Cl} \cdot \left[\Delta c_{Cl,\max} + \Delta c_{Cl}(t)\right] \qquad \text{Equation 2-13}$$

Considering the fraction conversion, the final VRRC model expressed as follows:

$$\frac{dX(t)}{dt} = \alpha \cdot e^{-\beta \cdot X(t)} \cdot c_{Cl} \cdot \left[1 - X(t)\right] \qquad \text{Equation 2-14}$$

2.2.2 Model application to chlorination at different temperatures

For successful planning and management of a real distribution system, seasonal water temperatures must be taken into account. Therefore, the proposed VRRC model is extended to simultaneously account for the impact of temperature variations across a typical system. The effect of temperature on chemical reaction rate can be expressed by the classical Arrhenius equation:

$$k_T = F \cdot e^{\frac{-E_A}{R \cdot T}} \qquad \text{Equation 2-15}$$

where k_T is the reaction rate coefficient at absolute temperature T (K), F is the frequency factor (same unit as k_T). E_A is the activation energy and R is the ideal gas constant. If the rate coefficient is known for a reference temperature T_1, then it can be calculated for another temperature T_2 when E_A/R is known. Assuming that the activation energies for the reaction of all reactive sites i are approximately equal with each other, the VRRC at temperature T_2 can be obtained as follows:

$$k_{ov,Cl,T_2}\left[X(t)\right] = k_{ov,Cl,T_1}\left[X(t)\right] \cdot \exp\left[\frac{-E_A / R \cdot (T_1 - T_2)}{T_1 \cdot T_2}\right] \qquad \text{Equation 2-16}$$

Since the $k_{ov,Cl,T1}$ is the reference, the E_A/R ratio becomes the only parameter which is needed to be determined from experiments. In the literature, large differences of

E_A/R are given for different waters. For example, Kastl et al. (2003) estimated an E_A/R of 14.700 K in water, while Powell et al. (2000) suggested E_A/R values ranging between 7.500 and 9.600 K.

2.2.3 Model application to rechlorination and water mixing condition

For the application of the VRRC model to rechlorination conditions, the model parameters of α, β, and $k_{ov,Cl}$ should be independent of the new chlorine concentration after the booster station. It means that the booster doses do not influence $k_{ov,Cl}$, because the latter depends only on the reactivity and concentration of the chlorine-reactive sites (**Eq. 2-7**). It is obvious that available reactive sites C_R are constant at the rechlorination point, and therefore, recalibration of the VRRC model is not needed.

However, when mixing of different waters is taking place, e.g. in pipe junctions, a new $k_{ov,Cl}$ needs to be calculated. This is due to the fact that each water package contains different concentrations of chlorine-reactive substances and thus, the overall reactivity changes after the mixing. Assuming that two or more different water packages (inflow packages) mix completely, $k_{ov,Cl}$ of the mixture is calculated as a function of mass-weighted average rate coefficient by using **Eq. 2-17**, yielding:

$$k_{mix,Cl}[X(t)] = \sum_{j=1}^{n}\left[k_{ov,Cl,j}[X(t)_j]\cdot\left(\frac{c_{R_{j,Cl}}\cdot V_j}{\sum_{j=1}^{n}\left(c_{R_{j,Cl}}\cdot V_j\right)}\right)\right] \qquad \text{Equation 2-17}$$

where $k_{ov,Cl,j}[X(t)]$ and $c_{Rj,Cl}$ are the (overall) VRRC and the chlorine-reactive substances concentration related to the water volume V_j (j^{th} water package), respectively.

2.3 MATERIALS AND METHODS

2.3.1 Chlorination experiment

2.3.1.1 Water samples

In order to determine the model parameters and evaluate the accuracy of the developed VRRC model, various chlorine decay data sets were used. These data sets were obtained from chlorination of several water samples with different origins and organic matter contents. In the authors' own experiments, treated water samples prior to final disinfection were collected between January and June 2012 from the Altenberg drinking water treatment (AWT) and Hosterwitz drinking water treatment (HWT) plants located in the state of Saxony, Germany. The Altenberg waterworks treats organic-rich, low-turbidity reservoir water by means of coagulation/flocculation using iron chloride, followed by sedimentation, rapid sand filtration, ozonation, biological activated carbon filtration and finally chlorine disinfection. The Hosterwitz waterworks infiltrates surface water from the Elbe River, which is further treated by granular activated carbon filtration and chlorine disinfection.

To determine the water quality characteristics, both HWT and AWT water samples were pre-filtered through 0.45 µm polycarbonate filters (Nuclepore Track-Etch Membrane, Whatman, Germany) and then analyzed for dissolved organic carbon (DOC) and UV absorbance at wavelength 254 nm (UV_{254}). The DOC concentration was determined by the catalytic combustion method using a LiquiTOC II organic carbon analyzer (Elementar Analysensystem GmbH, Germany) while UV_{254} was measured with a UV-VIS Genesys 10 UV spectrophotometer (Thermo Spectronic, USA) using a 5-cm cuvette. The specific UV-absorbance (SUVA), which is an indicator of aromatic molecules in water, was calculated by dividing the UV_{254} by the corresponding DOC concentration. pH value was determined by a pH meter 340i (WTW, Germany). Total chlorine demand of water samples was determined by preliminary chlorination experiments according to a Standard Method 2350 B of the American Public Health Association (APHA 2005a). **Table 2-1** summarizes the characteristics of the water samples.

The experimental design used to obtain the chlorine decay test data included chlorination of HWT and AWT water samples with different ICCs, chlorination of HWT water sample at different temperatures, rechlorination of HWT water samples and mixing of HWT and AWT water samples.

2.3.1.2 Chlorination of identical water with different ICCs and at different temperatures

Chlorine stock solution, made up by diluting concentrated sodium hypochlorite solution with ultrapure water, was added to a series of pre-cleaned, chlorine-demand-free amber glass bottles with HWT or AWT water samples. The volumes of the amber glass bottles were determined firstly using a mass balance before and after adding samples. Then, based on the volume of glass bottles and the required initial chlorine concentration, the corresponding calculated volume of chlorine stock solution was added by using a pipette. The ICCs were 0.6, 2 and 4 mg/L based on the ratio of ICC-to-DOC in the range of 0.5 to 2 mg/mg. In total, 5 independent experiments for chlorination of AWT and HWT water samples with different ICCs were conducted at 20 °C. To evaluate the effect of temperature, additional 4 independent decay tests were performed, i.e. HWT water sample was spiked with target ICCs and incubated at constant temperatures of 5 and 12 °C. Following each dose, the residual chlorine concentration was measured at the end of the reaction time over a maximum period of 120 h by using a pipette to take samples out of the corresponding bottles. The frequency of grab sampling was higher at the beginning and decreased gradually over time, ranging from 5 to 30 min during the first hour and from 1 to 8 h beyond the first hour during the first day, and from 24 h thereafter. Free chlorine concentrations were determined according to the N, N-diethyl-p-Phenylenediamine (DPD) Standard Colorimetric Method 4500-Cl G from the APHA (2005b).

2.3.1.3 Rechlorination

Rechlorination experiments were conducted 24 and 36 h after the initial chlorination of HWT water sample with ICCs of 0.6 mg/L at 20 °C, times chosen according to the previous studies (Boccelli et al. 2003, Lee et al. 2007, Mouly et al. 2010). A rechlorination dose was calculated which would increase the residual chlorine

concentration of the water to 0.4 mg/L or to 0.6 mg/L. The residual chlorine concentration was measured after times of 10 min, 30 min, 1 h and to maximum 160 h.

2.3.1.4 Mixing of chlorinated water

As water mixing (in a real distribution system) could be considered as rechlorination of a water package containing relatively low residual chlorine concentration by another containing more chlorine, the water mixing experiments were performed by mixing AWT and HWT water samples 36 h after the initial chlorination at 20 °C.

In the first experiment, HWT water sample spiked with 0.6 mg/L chlorine was mixed with AWT sample spiked with 1.9 mg/L chlorine at 1:1 (v:v, volume:volume). The second experiment was performed by mixing a HWT sample spiked with 0.6 mg/L chlorine with AWT sample spiked with 2.5 mg/L chlorine at 1:2 (v:v). The residual chlorine concentrations were measured periodically after mixing point.

2.3.1.5 Literature data sets

Except for the experimental data from this section, five data sets were extracted from studies published by Gang (2003) and Jabari Kohpaei (2010). In Gang (2003), one sample of raw lake water (LWR) was spiked with 12.2 mg/L chlorine; while two alum-treated river and lake water samples (CWT and GWT) were spiked with 3.6 and 4.0 mg/L chlorine, respectively. Experiments were conducted in the dark for 5 days at 25 °C and pH 8.0. Jabari Kohpaei (2010) spiked ''Pilbara dam water'' (PDW) with chlorine in the range of 2.11 to 11.2 mg/L and incubated in the dark for maximum 7 days. For chlorination of PDW, 5 independent data sets were obtained. Six decay data sets regarding chlorination of the identical water sample, labelled as PRW, at different temperatures were also obtained from Jabari Kohpaei (2010). The concentration in these studies was determined by the DPD colorimetric method. **Table 2-1** shows the characteristics of the water samples.

2.3.2 Data analysis

The proposed model requires the calibration to obtain the optimal values for the model parameters α and β, which allows the model to best represent chlorine decay. The optimal parameters should be invariant for any ICCs, which is an important criterion for a suitable chlorine decay model to reduce the model recalibration and extend the model application. In this study, the VRRC model was first calibrated against each data set for six distinctly different waters (AWT, HWT, CWT, GWT, LWR, and PDW), by minimizing the sum of squared differences between the experimentally-determined chlorine concentrations and simulations at corresponding times, namely, sum of the squared errors (SSE). In this study, Excel Solver was employed to minimize the SSE based on the generalized reduced gradient algorithm.

Then, to validate that the parameters for identical water, which were obtained from different experiments with a particular ICC, were not significantly different, the coefficient of variation (CV) was calculated. We accepted that the parameters were not significantly different from each other when the CV was less than 10%.

Table 2-1. Characteristics of water samples.

Abbr.	Sample description	pH	DOC	UV_{254}	$SUVA_{254}$	Chlorine demand	NH_4^+	Data source
			mg/L	m^{-1}	L/mg/m	mg/L	mg/L	
AWT	Treated reservoir water	7.3	1.8±0.1	2.64	1.45	2.8±0.4	< 0.05	Authors
HWT	Treated river water	7.2	1.7±0.2	2.72	1.57	3.5±0.4	< 0.05	Authors
CWT	Alum-treated river water	-	3.1	5.18	1.68	4.46	n. a.	Gang et al. (2003)
GWT	Alum-treated lake water	-	2.8	2.84	1.01	4.11	n. a.	Gang et al. (2003)
LWR	Raw lake water	-	9.9	15.74	1.60	15.78	n. a.	Gang et al. (2003)
PDW	Reservoir water	-	-	-	-	5.88	n. a.	Jabari Kohpaei (2010)
PRW	Pilbara raw water	8.5	3.87	6.4	1.67	4.04	n. a.	Jabari Kohpaei (2010)

After proofing that the model parameters were not different from each other, the average parameters for the corresponding type of water were then used for model validation under different conditions. The model with average parameters was validated by predicting the decay curves with a wide range of ICCs (2.1 to 12.2 mg/L, PDW water sample), at different temperatures (5 to 20 °C, HWT water sample and 15 to 40 °C, PRW water sample), rechlorination (HWT water sample) and water mixing conditions. It is important to note that no additional model calibrations or parameter recalculations were required for rechlorination. For model validation under water mixing conditions, the VRRC of the mixed water was calculated according to **Eq. 2-17** and no recalibration was required. Since the proposed model did not have an analytical solution, the Euler method was adopted to solve the model numerically with a numerical time interval of 2 min. The details of the calculation process are described elsewhere (Butcher 2008).

The VRRC model was evaluated by the coefficient of determination (R^2) and the root-mean-square error (RMSE). All the methods were often used as measures of difference between the predicted data and those obtained experimentally (Piñeiro et al. 2008). The R^2 shows the unexplained variance of model while the RMSE evaluates the prediction capability of the model, with a smaller RMSE value indicating a greater predictive capability. The obtained RMSE is also expected to be of similar magnitude to the measurement error, which indicates a reasonable fit. Furthermore, the model adequacy was evaluated by the *F* test for the goodness-of-fit. If an appropriate model has been found, the calculated *F* value will be greater than the critical *F* value at the given level of significance, i.e. 0.05 in this study and the corresponding probability *p* value should be lower than 0.05. Therefore, the goodness-of-fit test is derived to be statistically significant (Otto 2007).

2.4 RESULTS AND DISCUSSION

2.4.1 Model parameters estimation

The individual optimal α_i and β_i for six different water samples by applying respective decay data sets are shown in **Table 2-2**. In total, two groups of $\alpha_{AWT,i}$ and $\beta_{AWT,i}$, i = 1,

2, were determined for the AWT water sample chlorinated at ICCs of 1.9 and 2.5 mg/L. Three groups of best-fit parameters were obtained for the HWT water sample by using three data sets with ICCs of 0.6, 2 and 4 mg/L, respectively. Similar to the HWT water sample, five groups of parameters were determined for PDW water sample by applying decay data sets with ICCs ranging from 2.1 to 11.2 mg/L. The original experiment data sets with respect to the PDW water sample are from Jabari Kohpaei (2010). As addressed in section 2.2 (Model development), the VRRC $k_{ov,Cl}$ is independent of the ICC (**Eq. 2-7**), i.e. for each water, the α and β were independent of ICCs. Therefore, it is expected that the difference between the obtained group of parameters (α_i and β_i) is negligible for identical water samples, which would confirm that the model parameters are independent of any ICC and further validate that the VRRC k_{ov} is independent of the ICCs.

For the identical water samples, the differences between the obtained groups of α_i and β_i were evaluated based on the CV. It can be seen from **Table 2-2** that the CV with respect to α and β were equal to or smaller than 10%, which shows that there were no noticeable differences between the groups of optimal α_i and β_i for the same water sample even if a wide range of ICCs was applied. Thus, the VRRC k_{ov} was validated to be independent of the ICCs. The value of VRRC at the end of individual experimental time was calculated based on **Eq. 2-9** and shown in the appendix **Table 7-1**.

As the optimal α_i and β_i for the same water sample were not significantly different, the average values of parameters ($\bar{\alpha}$ and $\bar{\beta}$) were applied and the corresponding accuracy as well as adequacy test results are also shown in **Table 2-2**. For AWT, HWT and PDW water samples, the relationship between the measured and simulated results were satisfactory with R^2 ranging from 0.91 to 0.99. The obtained RMSE is of similar magnitude to the measurement error with a typical precision (95%), e.g. ± 0.05 at 1 mg/L free chlorine and ± 0.2 at 5 mg/L, which indicates a good fit. As for the model adequacy assessed by *F*-test for the goodness-of-fit, all the *p* values were lower than the significance level of 0.05 considered in this study,

and the test is therefore significant, which gives additional evidence that the model provides an adequate fit to the experimental data.

Table 2-2. Best-fit model parameters α and β for each data set, average parameters $\overline{\alpha}$ and $\overline{\beta}$, and corresponding R^2, SSE and RMSE, *F* value, *p* value and number of measurements (n).

Water	ICC mg/L	α L/mg/h	β	R^2	SSE	RMSE mg/L	*F* value	*p* value	n
AWT	1.9	0.14	4.51	0.95	0.33	0.10	243.7	2.9E-10	16
	2.5	0.17	4.08	0.94	0.41	0.18	119.7	6.9E-7	9
CV (%)		9.68	5.01						
Average parameters		0.150	4.295	0.91	1.33	0.25	165.9	1.0E-11	
HWT	0.6	0.19	15.60	0.98	0.04	0.05	201.6	5.8E-7	10
	2.0	0.21	15.72	0.98	0.11	0.05	332.3	9.1E-6	8
	4.0	0.19	16.05	0.98	0.07	0.07	339.2	1.6E-6	9
CV (%)		5.99	1.50						
Average parameters		0.196	15.786	0.99	0.24	0.09	2587.5	2.4E-16	
PDW	2.1	0.10	7.59	0.97	0.03	0.10	304.8	2.9E-8	11
	4.5	0.10	7.32	0.98	0.15	0.17	476.2	4.2E-9	11
	6.7	0.10	7.60	0.97	0.45	0.21	340.9	1.8E-8	11
	8.8	0.095	7.62	0.97	0.82	0.25	298.5	3.2E-8	11
	11.2	0.096	7.60	0.97	0.73	0.28	265.6	5.4E-8	11
CV (%)		2.26	1.70						
Average parameters		0.098	7.546	0.98	2.18	0.23	10216	0	
CWT	3.6	0.07	3.83	0.98	0.50	0.13	454.6	2.46E-8	11
GWT	4.0	0.06	3.51	0.98	0.61	0.18	360.3	6.14E-8	11
LWR	12.2	0.02	4.17	0.98	4.52	0.59	309	1.11E-7	11

Fig.2-1 shows the goodness of curve fitting for chlorination of different water samples with different ICCs. It can be seen that the proposed VRRC model

described the experimental data well although the water samples represented a wide range of DOC concentrations between 1.7 to 9.9 mg/L (**Table. 2-1**).

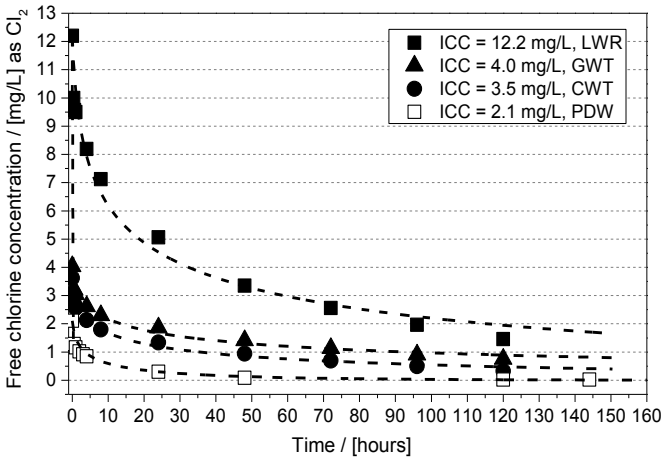

Figure 2-1. Decay test and VRRC model calibration for six water samples in the DOC range of 2.8 to 9.9 mg/L. Points represent experimental data and dashed lines represent the VRRC model fitted to the experimental data.

Fig.2-2(a) and (b) illustrate the goodness of model simulations for HWT and PDW water samples upon different ICCs, respectively. As can be seen, the VRRC model performed well under chlorination conditions at a relatively wide range of ICCs from 0.6 to 12.2 mg/L. On the basis of the graphical and quantitative analysis discussed above, the VRRC model was confirmed to provide an adequate fit to the data.

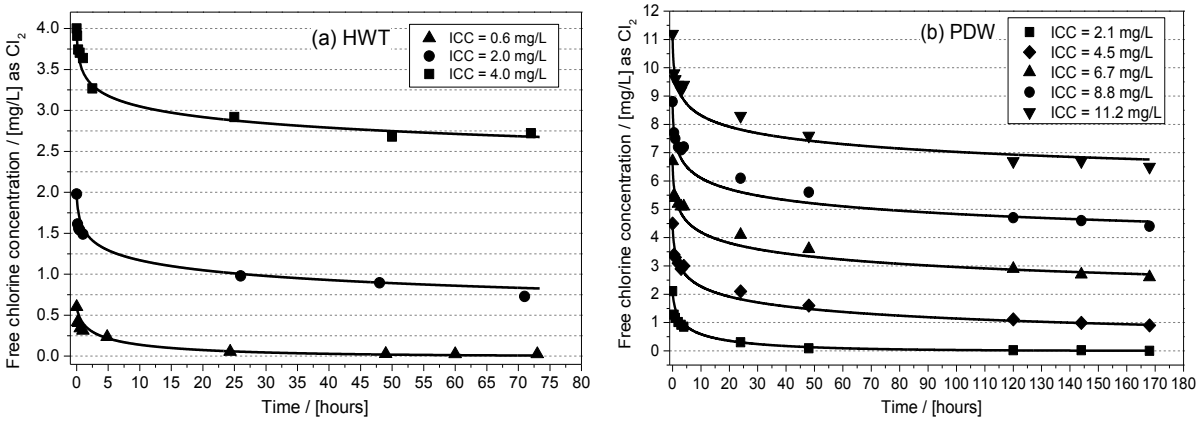

Figure 2-2. Decay test and VRRC model simulation for HWT (a) and PDW (b) with different ICCs at 20 °C. Points represent experimental data and solid curves are the VRRC model predicting results by applying invariant average parameters.

2.4.2 Model validation for chlorination at different temperatures

In this study, several combinations of ICCs and temperatures referred to as ICCs/temperatures were conducted on the HWT water sample. To illustrate that the model was able to provide reliable predictive results for chlorination of other types of water at different temperatures, i.e. whatever the water matrix or water quality, six additional decay sets regarding the PRW water sample, which were reported in the literature (Jabari Kohpaei 2010), were tested in this study as well. For the HWT water sample, the combinations included 0.6 mg/L/20 °C, 0.6 mg/L /12 °C, 0.6 mg/L /5 °C, 2 mg/L/5 °C and 4 mg/L/5 °C. The PRW water sample was chlorinated at an ICC of 3 mg/L and incubated at temperatures ranging from 15 to 40 °C with an interval of 5 °C.

The individual group of optimal parameter estimates (α_i and β_i) were obtained and described separately for all data sets, which are shown in appendix **Table 7-2**. It was found that the optimal β_i for both HWT and PRW water samples were generally not significant different. However, there were some noticeable changes between the optimal estimates of α_i for decay sets conducted at different temperatures.

As addressed above in section 2.2, it is expected that the differences of α_i with associated $k_{ov,Cl}(X)$ at different temperatures are in conformity with Arrhenius theory. Thus, **Fig. 2-3** shows an Arrhenius plot of $k_{ov,Cl}(X)$ for different conversions against $1/(T\,[\mathrm{K}])$.

A straight line was obtained with R^2 of 0.997 for $k_{ov,Cl}(0\%)$ regarding HWT and 0.992 for $k_{ov,Cl}(0\%)$ regarding PRW water. The straight lines were also obtained for other $k_{ov,Cl}(X)$, which indicates that the Arrhenius equation is suitable to describe the effects of temperature on the VRRC $k_{ov,Cl}$. It needs to be pointed out that the conversion fraction X shown in **Fig. 2-3(a) and (b)** were corresponding to the respective experimental condition. Specifically, the maximum conversion was 17% when ICC = 0.6 mg/L was applied for HWT water while maximum conversion fraction was 74% when ICC = 3 mg/L was applied for PRW water.

It was found that the E_A/R, which was obtained from the Arrhenius plot shown in **Fig. 2-3**, increased slightly with the increasing percentages of chlorine consumption (X). In other words, E_A/R was increasing with the progress of the reaction. **Fig. 7-3** shows more details regarding the ratio of E_A/R (X) to E_A/R (0) as a function of the conversion X for the HWT and PRW samples. The results indicate that there is an increasing influence of temperature on the VRRC k_{ov} (X) with the progress of the reaction. This is in agreement with the observation by others that the rate constant of slow reacting NOM species is more sensitive to temperature than that of fast reacting ones (Jabari Kohpaei 2010). Although E_A/R increased slightly with the progress of the reaction, the change of E_A/R (X) is less than 2% and thus can be ignored. Specifically, the obtained average E_A/R was 8727 K ± 26 for HWT while 8203 K ± 32 for PRW water samples.

In this context, $k_{ov,20}$ was used as reference VRRC, and the $k_{ov,T}$ were obtained from **Eq. 2-16** for other temperatures by applying E_A/R of 8727 K for HWT water sample and 8203 K for PRW water sample. This implies that the $k_{ov,T}$ increases about 2.5 times when temperature increases by 10 °C.

As for the model accuracy evaluation, the R^2 ranged from 0.93 to 0.98 indicating a good to excellent match of experimental data. The F-test ($p < 0.05$) is significant, which confirmed the adequacy of the VRRC model. Graphically, good agreement for residual chlorine concentration was found between experimental data and model predictions at all ICCs/temperatures combinations for both the HWT and PRW water samples, which are presented in appendix **Fig. 7-1 and 7-2**. The VRRC k_{ov} (X) for each data set was calculated based on obtained model parameters and the range of k_{ov} (X) was shown in appendix **Table 7-1** as well.

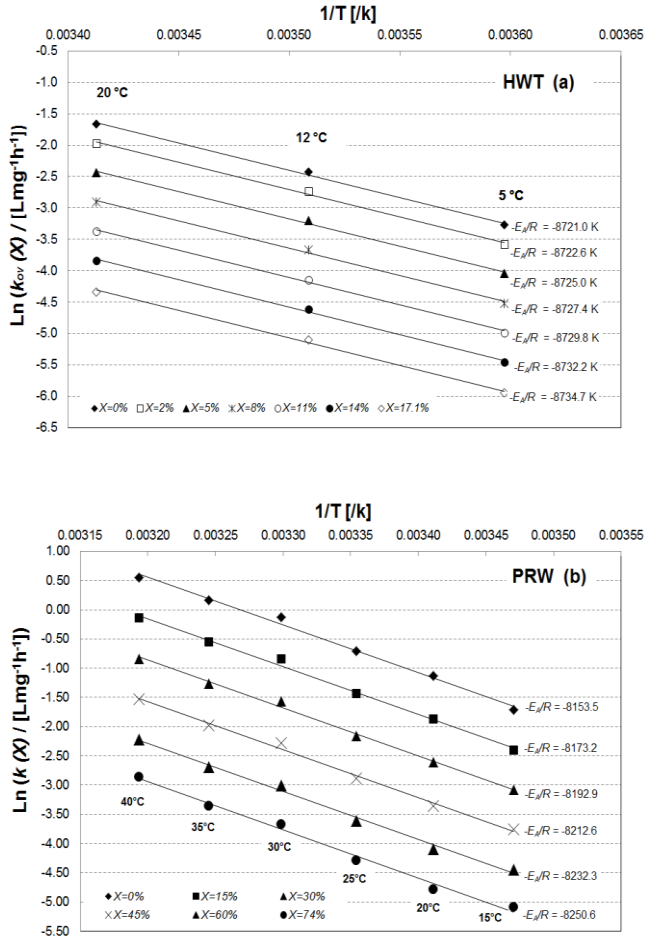

Figure 2-3. Arrhenius plot of VRRC $k_{ov,Cl}(X)$ derived by applying VRRC models to HWT at ICC of 0.6 mg/L (a) and to PRW at ICC of 3 mg/L (b) at different temperatures. X represents the percentage of chlorine consumption. E_A/R can be derived from the straight line equation.

2.4.3 Model validation for water mixing

The chlorinated AWT and HWT water samples were mixed in different proportions. For the mixtures, the $k_{ov,mix}$ was calculated according to **Eq. 2-17** and chlorine decay in the mixture was predicted. **Fig. 2-4** shows the results and illustrates graphically the accuracy of the VRRC model for water mixing at 36 h after initial chlorination with HWT:AWT mixing ratio at 1:1 as shown in **Fig. 2-4(a)** and 1:2 as shown in **Fig. 2-4(b)**.

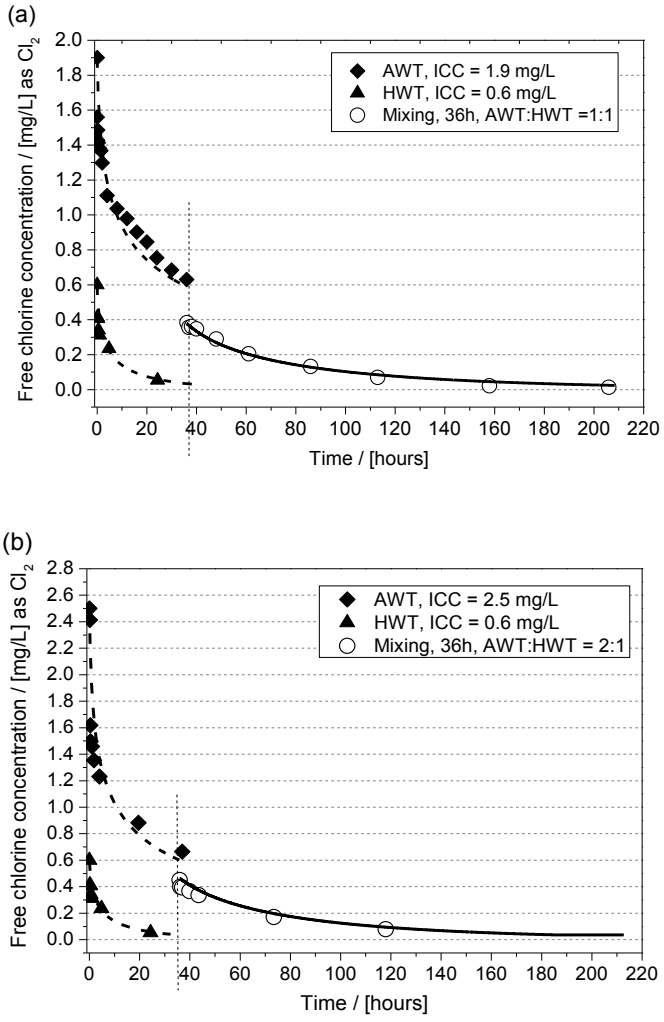

Figure 2-4. Decay test and VRRC model prediction for water mixing at 36 h after initial chlorination with HWT:AWT mixing ratio of 1:1 (a) and of 1:2 (b). Point represent experimental data, dash lines represent the calibration results, and solid curves are the VRRC model predicting results.Vertical dash-dot lines indicate the mixing time.

The R^2 for the model accuracy evaluation was 0.97, i.e. 3% of variance is unexplained, while the RMSE was 0.028. As for the model adequacy test, the *p* value was lower than the significant level of 0.05 showing the test is significant, which proves that the model provides a very good prediction of experimental data.

2.4.4 Model validation for rechlorination

Fig. 2-5 demonstrates that the model provides reliable simulation results for two independent rechlorination conditions with respect to different rechlorination dosages as well as different booster times. The first experiment was conducted at

24 h after the initial chlorination where the chlorine concentration was raised to 0.65 mg/L, which corresponded to the ICCs. Another rechlorination experiment was conducted 36 h after the initial chlorination and the chlorine concentration raised to 0.4 mg/L. The results show a high adequacy of the prediction with an average R^2 of 0.98, i.e. only less than 2% of variances are unexplained. Similar with other chlorination scenarios, the *F* test for the goodness-of-fit showed that the prediction was statistically significant. In summary, the VRRC model enables very good predictions of the chlorine residuals that were measured over time in bulk water under rechlorination condition.

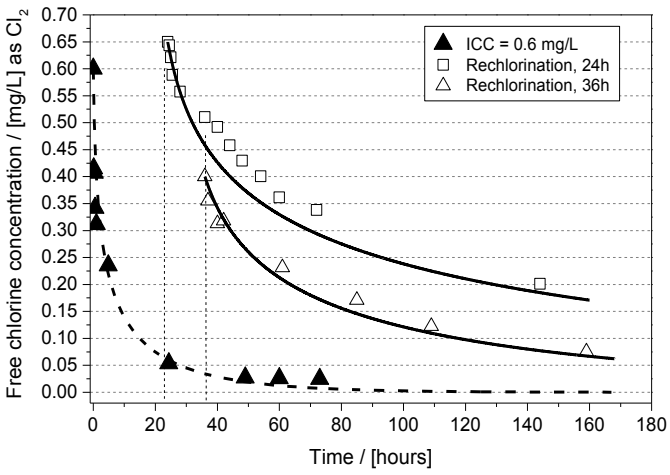

Figure 2-5. Decay test and VRRC model prediction for rechlorination of HWT water 24 h and 36 h after initial chlorination with 0.6 mg/L chlorine. Point represent experimental data, dash lines represent the calibration results, and solid curves are the VRRC model predicting results, dash-dot lines emphasize the rechlorination time.

2.5 CONCLUSION

Fisher et al. (2011) critically reviewed the commonly applied chlorine decay models and listed five suitability criteria of bulk chlorine decay models to assist disinfection planning and management in a water distribution network. These five criteria are: (1) accurate prediction of chlorine residual over typical maximum system travel times, (2) simplicity with least number of state variables and parameters, (3) the real initial chlorine concentration is applied as initial chlorine concentrations (ICCs) in the model, rather than some lower concentration being applied after an initial loss period to

improve the fit to data, (4) parameter values invariant over the maximum time taken for water to travel through the distribution system, and (5) parameter values invariant for any ICCs in the operation range.

Here a second order chlorine decay model was introduced which fulfills all the five criteria stated. In the new model, named variable reaction rate coefficient (VRRC) model, the overall concentration of reactive species besides chlorine is surrogated by the maximum chlorine demand which can easily be determined experimentally. The maximum chlorine demand in turn results from a mixture of different unknown species with different reactivity. Naturally, species with high reactivity are converted at first and those with low reactivity last. That is taken into account by the variable second order rate coefficient k_{ov} which is described by an exponential function decreasing with increasing conversion X of the maximum chlorine demand. k_{ov} is maximum at the beginning of the reaction ($X = 0$) and is approaching to zero ($X = 1$) when the maximum chlorine demand has been turned over. Only two parameters are needed to describe k_{ov} as a function of conversion and can easily be determined by curve fitting from a few batch experiments.

The VRRC model was shown to describe the chlorine decay rate as a function of conversion or time with high quality applying statistical goodness of fit tests for different waters. Furthermore, without any further calibration, the model can excellently describe chlorine decay rates after rechlorination or after water mixing. Additionally, temperature dependency of the overall variable second order rate coefficient k_{ov} is perfectly described by the Arrhenius relationship. It was shown that the temperature sensitivity increases with increasing turnover which is in accordance to the findings of others. However, these differences are so small that they can be neglected for most cases.

Generally, the model is effective for describing bulk chlorine decay within a broad range of ICCs (ranging from 0.6 to 12.2 mg/L), a wide range of temperatures (5 to 40 °C) and for typical conditions such as rechlorination and water mixing. Thus, it can very well be applied to model chlorine decay in distribution systems by bulk reactions. For future research, it could attempt to predict the residual chlorine

concentration in water sample with high ammonia concentrations and to test the model compatibility with hydraulic models, such as EPANET-MSX.

REFERENCES

APHA (2005a) 2350 B: Standard Method for determination of chlorine demand, American Water Works Association and Water Environment Federation, Washington, D.C.

APHA (2005b) 4500-Cl G: Standard method for determination of chlorine (residual), American Water Works Association and Water Environment Federation, Washington, D.C.

Boccelli, D.L., Tryby, M.E., Uber, J.G. and Summers, R.S. (2003) A reactive species model for chlorine decay and THM formation under rechlorination conditions. Water Research 37(11), 2654-2666.

Butcher, J.C. (2008) Numerical methods for ordinary differential equations. Second edition, John Wiley & Sons, West Sussex, England.

Clark, R.M. (1998) Chlorine demand and TTHM formation kinetics: a second-order model. Journal of Environmental Engineering 124(1), 16-24.

Clark, R.M. and Sivaganesan, M. (2002) Predicting Chlorine Residuals in Drinking Water: Second Order Model. Journal of Water Resources Planning and Management 128(2), 152-161.

Deborde, M. and von Gunten, U. (2008) Reactions of chlorine with inorganic and organic compounds during water treatment—Kinetics and mechanisms: A critical review. Water Research 42(1–2), 13-51.

Fisher, I., Kastl, G. and Sathasivan, A. (2011) Evaluation of suitable chlorine bulk-decay models for water distribution systems. Water Research 45(16), 4896-4908.

Fisher, I., Kastl, G. and Sathasivan, A. (2012) A suitable model of combined effects of temperature and initial condition on chlorine bulk decay in water distribution systems. Water Research 46(10), 3293-3303.

Gallard, H. and von Gunten, U. (2002) Chlorination of phenols: Kinetics and formation of chloroform. Environmental Science & Technology 36(5), 884-890.

Gang, D.C., Clevenger, T.E. and Banerji, S.K. (2003) Modeling Chlorine Decay in Surface Water. Journal of Environmental Informatics 1(1), 21-27.

Jabari Kohpaei, A. (2010) Development of an analytical solution for the parallel second order reaction scheme for chlorine decay modelling. Master Thesis, Curtin University of Technology, Australia.

Jegatheesan, V., Kim, S. and Joo, C. (2006) Evaluating the drinking water quality through an efficient chlorine decay model. Water Science and Technology: Water Supply 6(4), 1-7.

Jonkergouw, P.M.R., Khu, S.-T., Savic, D.A., Zhong, D., Hou, X.Q. and Zhao, H.-B. (2008) A variable rate coefficient chlorine decay model. Environmental Science & Technology 43(2), 408-414.

Kastl, G., Fisher, I. and Jegatheesan, V. (1999) Evaluation of chlorine decay kinetics expressions for drinking water distribution systems modelling. Journal of Water Supply: Research and Technology - AQUA (48), 219-226.

Kastl, G., Fisher, I., Jegatheesan, V., Chandy, J. and Clarkson, K. (2003) Prediction of chlorine and trihalomethanes concentration profile in bulk drinking water distribution systems from laboratory data. Water Science and Technology: Water Supply 3(1-2), 239-246.

Kiéné, L., Lu, W. and Lévi, Y. (1998) Relative importance of the phenomena responsible for chlorine decay in drinking water distribution systems. Water science and technology 38(6), 219-227.

Lee, J., Lee, D. and Sohn, J. (2007) An experimental study for chlorine residual and trihalomethane formation with rechlorination. Water science and technology 55(1-2), 307-313.

Mouly, D., Joulin, E., Rosin, C., Beaudeau, P., Zeghnoun, A., Olszewski-Ortar, A., Munoz, J.F., Welté, B., Joyeux, M., Seux, R., Montiel, A. and Rodriguez, M.J. (2010) Variations in trihalomethane levels in three French water distribution systems and the development of a predictive model. Water Research 44(18), 5168-5179.

Nieuwenhuijsen, M.J., Toledano, M.B., Eaton, N.E., Fawell, J. and Elliott, P. (2000) Chlorination disinfection byproducts in water and their association with adverse

reproductive outcomes: a review. Occupational and Environmental Medicine 57(2), 73-85.

Ohar, Z. and Ostfeld, A. (2014) Optimal design and operation of booster chlorination stations layout in water distribution systems. Water Research 58(0), 209-220.

Otto, M. (2007) Chemometrics: Statistics and Computer Application in Analytical Chemistry, Wiley-VCH, Weinheim, Germany.

Piñeiro, G., Perelman, S., Guerschman, J.P. and Paruelo, J.M. (2008) How to evaluate models: Observed vs. predicted or predicted vs. observed? Ecological Modelling 216(3–4), 316-322.

Powell, J.C., Hallam, N.B., West, J.R., Forster, C.F. and Simms, J. (2000) Factors which control bulk chlorine decay rates. Water Research 34(1), 117-126.

Qualls, R.G. and Johnson, J.D. (1983) Kinetics of the short-term consumption of chlorine by fulvic acid. Environmental Science & Technology 17(11), 692-698.

Richardson, S.D., Plewa, M.J., Wagner, E.D., Schoeny, R. and Demarini, D.M. (2007) Occurrence, genotoxicity, and carcinogenicity of regulated and emerging disinfection by-products in drinking water: a review and roadmap for research. Mutation Research 636(1-3), 178-242.

Rossman, L. (2000) EPANET 2 users manual, U.S. Environmental protection agency, Cincinnati, Ohio.

Rossman, L., Clark, R. and Grayman, W. (1994) Modeling Chlorine Residuals in Drinking-Water Distribution Systems. Journal of Environmental Engineering 120(4), 803-820.

Shang, F., Uber, J.G. and Rossman, L.A. (2007) Modeling Reaction and Transport of Multiple Species in Water Distribution Systems. Environmental Science & Technology 42(3), 808-814.

Vasconcelos, J.J., Rossman, L.A., Grayman, W.M., Boulos, P.F. and Clark, R.M. (1997) Kinetics of chlorine decay. Journal-American Water Works Association 89(7), 54-65.

Warton, B., Heitz, A., Joll, C. and Kagi, R. (2006) A new method for calculation of the chlorine demand of natural and treated waters. Water Research 40(15), 2877-2884.

CHAPTER 3

A variable reaction rate model for trihalomethanes formation in drinking water due to the reaction with dissolved organic matter

---

THIS CHAPTER IS REPRODUCED BASED ON

Variable reactivity modeling for predicting the disinfection by-product formation in drinking water distribution systems

Hua P, Vasyukova E and Uhl W

American Water Works Association Water Quality and Technology Conference, November 3-7, 2013, Long Beach, California

3 A VARIABLE REACTION RATE MODEL FOR TRIHALOMETHANES FORMATION IN DRINKING WATER DUE TO THE REACTION WITH DISSOLVED ORGANIC MATTER

ABSTRACT

The kinetic of the trichloromethane (TCM) and total trihalomethanes (TTHM) formation in the bulk water were simulated in this study by a second order model. The kinetics model was related to two reactants, the residual chlorine and the THM formation precursors. A variable formation coefficient was introduced to replace the constant formation coefficient as the former one took the decreasing reactivity of THM precursors into account. Such a coefficient decreased with the reaction progress and was influenced by the temperatures following the Arrhenius theory. The applicability of proposed models was evaluated under different chlorination conditions, i.e. chlorination with different initial chlorination concentrations, and rechlorination conditions. With an average R^2 of 0.94, the model predicts of TTHM matched closely with the THM test data set in the range of initial chlorine concentrations from 8.5 to 52 μM, at temperatures ranged from 10 to 20 °C, and under rechlorination conditions by applying the invariant parameters for given waters.

KEYWORDS

Chlorine decay; kinetics model; trichloromethane formation, trihalomethanes formation

3.1 INTRODUCTION

Trihalomethanes (THM) is one of the first identified carcinogenicity DBP which is regulated by most of countries worldwide. A great deal of research efforts has been paid toward developing prediction models to monitor THM concentrations simultaneously under different scenarios in WDS, such as variable initial chlorine dose, season induced temperature changes and rechlorination (Chowdhury et al. 2009).

In terms of modeling approach, the THM formation models are classified into two categories, which based on the multiple regression or reaction kinetic approaches. Specifically, the first category of models is developed using the multiple regression analysis among THM concentrations and different parameters (Golfinopoulos and Arhonditsis 2002, Hong et al. 2007, Sohn et al. 2004, Uyak et al. 2007). These incorporated parameters include water quality parameters, e.g. TOC or DOC, bromide ion (Br^-) etc., and operational parameters, e.g. pH and temperature. The applicability of these multivariate regression models is limited, because they are derived or dependent on the specific water quality and operational parameters. The second category of models, which based on the reaction kinetics approach, has higher degree of flexibility as it is independent of water quality and operation parameters (Chowdhury et al. 2009).

Clark (1998) carried out one of influential early study regarding the kinetics of total THM (TTHM) formation, which provided a hypothesis that the TTHM formation was proportional to the chlorine consumption. Based on the hypothesis, more TTHM formation models coupled with chlorine decay models were developed. For example, a so-called parallel first order model for the TTHM prediction was developed as the chlorine consumption was determined by a parallel first order model (Gang et al. 2003); a second order model for the TTHM formation was developed by combining it with second order models for chlorine decay (Boccelli et al. 2003).

However, the linear relationship between chlorine consumption and TTHM concentration is questionable, because not all of the consumed chlorine contributes

to the TTHM formation (Deborde and von Gunten 2008). Therefore, some studies introduced a THM formation potential (THMFP) to replace the chlorine consumption and surrogate the THM formation precursors (Gallard et al. 2004, Li and Zhao 2006, Zhang et al. 2013). The TTHM formation model is based on a reaction theory by considering two reactants: residual chlorine and THMFP. The second order THM formation model is able to simulate a long-term reaction period and usually ignore a short-term reaction period, e.g. the first 4 – 8 hours (Gallard and von Gunten 2002b). This might due to the fact that the THM formation pattern starts with a fast reaction period follows by a slow reaction period, which brings about the difficulties for the model simulation.

Indeed, THM formation precursor is a collection of different types of NOM that have individual structures and reactivity with chlorine. In the literature, some studies have shown the importance of NOM characteristics in the formation of TTHM (Chang et al. 2001a). Gallard et al. (2004) reported that resorcinol-type structures are the fast reacting species for the THM formation, while the phenolic compounds may belong to the slow reacting species. Gang et al. (2003) reported that the TTHM formation increased as the molecular weight of NOM decreased. Yang et al. (2008) concluded that aromatic contents contributed to the THM formation mostly. These results indicate that the different reactivity of individual THM precursors and the changing reactivity of the overall THM precursors should be taken into account for the model development. In other words, due to the consideration of different NOM characteristics, the proposed model is expected to predict the whole reaction periods by applying the minimum model parameters.

In addition to the different NOM characteristics, another challenge for modeling the kinetics of TTHM formation is the incorporation of bromide. Intensive studies investigated the effect of bromide on the TTHM formation from experimental standpoints by varying the bromide dosage to the synthesized sample (Chang et al. 2001b, Hua and Reckhow 2012, Hua et al. 2006). It is widely accepted that hypobromous acid (HOBr) is a more powerful halogenating agent than hypochlorous acid (HOCl), which results in reactions that incorporating bromine into NOM is faster

than incorporating chlorine. However, the substitution competition between bromine and chlorine was ignored in most reported kinetics models (Gallard et al. 2004, Gallard and von Gunten 2002b, Zhang et al. 2013). In practical waterworks operation, the bromide concentration in raw water is relative stable while the initial chlorine doses may be variable, which indicates the bromide-to-chlorine ratio is changing. The changeable bromide-to-chlorine ratio affects the kinetics of TTHM formation and generates a challenge of model simulation by applying invariant model parameters.

For successful planning and management of a real DWDS, seasonal water temperature changes should be also considered. However, limited studies involved the temperature effects into the TTHM model. Moreover, to reduce the initial chlorine dose, booster does (rechlorination) at intermediate locations is usually required. Therefore, the proposed TTHM model should be not only extended to simultaneously account for the impact of temperature changes but also needed to predict TTHM formation after rechlorination.

Generally, the study of this chapter is intended to propose a universal model to predict the concentration of trichloromethane (TCM), as well as TTHM concentration as a function of time by applying invariant model parameters. As addressed previously, the model should take into account two factors: different reactivity of reactive sites provided by NOM and the incorporating competition between bromine and chlorine for the TTHM formation. Furthermore, the model was further extended to chlorination at different temperature and rechlorinaiton condition. Consequently, the objectives of this work were to (1) propose a novel equation to calculate the variable reaction rate coefficient of THM formation, and improve a second order model of THM formation by introducing this coefficient, (2) apply the model to simulate the TCM formation at different ICC, (3) apply the model to predict the TTHM formation at ICCs, (4) apply the model to the prediction of TCM and TTHM formation under chlorination at different temperatures and rechlorination condition.

3.2 MODEL DEVELOPMENT

3.2.1 Trichloromethane (TCM) formation model

TTHM contains TCM and brominated THM. In order to simplify the TTHM model derivation process, the TCM formation model was developed initially. This is because the bromide concentration (the ratio of bromide-to-chlorine) can be ignored when developing TCM model and then the different NOM characteristics upon chlorination become the only considered factor.

As discuss previously, the DOM is a prerequisite for the TCM formation and can be roughly classified into complicated heterogenous humic solutes and non-humic solutes including carbohydrates, hydrocarbons, lipids and amino acids (Fabris et al. 2008). Although humic and non-humic solutes are not entirely distinguishable from each other, the individual NOM compound indeed has its own reaction characteristics or reactivity with chlorine to form TCM, i.e. single reactive site *i* provided by the NOM shows the reaction rate constant $k_{i,TCM}$. Therefore, the reaction between chlorine and a single reactive site *i* can be expressed as follow:

$$Cl + R_{i,TCM} \xrightarrow{k_{i,TCM}} \delta_i TCM_i \qquad \text{Equation 3-1}$$

where *Cl* represents chlorine either in the form of dissolved chlorine (Cl_2, aq), hypochlorous acid (HOCl) or hypochlorite ions (OCl^-). $R_{i,TCM}$ denotes the i^{th} reactive site provided by the TCM formation precursors, i = 1, 2, … , n. As the $R_{i,TCM}$ represents a single i^{th} reactive site, thus, the stoichiometric coefficient δ_i is one. The second order reaction rate of TCM formation is given by:

$$\frac{dc_{TCM,i}(t)}{dt} = k_{i,TCM} \cdot c_{Cl}(t) \cdot c_{R_{i,TCM}}(t) \qquad \text{Equation 3-2}$$

where $c_{Ri,TCM}(t)$ is the concentration of the available TCM formation site *i* at time *t*, $c_{Cl}(t)$ is the chlorine concentrations at time *t* in bulk water, $k_{i,TCM}$ is TCM formation rate constant with respect to the i^{th} TCM formation site.

Summing up the concentrations of all available sites for TCM formation yields:

$$\frac{\sum_{i=1}^{n} dc_{TCM,i}(t)}{dt} = \frac{dc_{TCM}(t)}{dt} = \sum_{i=1}^{n} k_{i,TCM} \cdot c_{Cl}(t) \cdot c_{R_{i,TCM}}(t) \qquad \text{Equation 3-3}$$

Considering an overall second order model, the TCM formation rate is usually proposed according to the following expression in the literature (Gallard and von Gunten 2002a):

$$\frac{dc_{TCM}(t)}{dt} = k_{ov,TCM}(t) \cdot c_{Cl}(t) \cdot c_{R_{TCM}}(t) \qquad \text{Equation 3-4}$$

where $c_{R,TCM}$ is the concentration of all available TCM formation site at time t, Combining **Eq. 3-3** and **3-4**, the overall rate coefficient of TCM formation is expressed as follows:

$$k_{ov,TCM}(t) = \frac{\sum_{i=1}^{n} \left[k_{i,TCM} \cdot c_{R_{i,TCM}}(t) \right]}{\sum_{i=1}^{n} c_{R_{i,TCM}}(t)} \qquad \text{Equation 3-5}$$

where $k_{ov,TCM}$ is an overall rate coefficient of TCM formation.

To further explore the characteristics of $k_{ov,TCM}(t)$, differentiation of **Eq. 3-5** provides:

$$\frac{dk_{ov,TCM}(t)}{dt} = c_{Cl}(t) \cdot \left[k_{ov,TCM}^2(t) - \frac{\sum_{i=1}^{n} {k_{i,TCM}}^2 \cdot c_{R_{i,TCM}}(t)}{\sum_{i=1}^{n} c_{R_{i,TCM}}(t)} \right] \qquad \text{Equation 3-6}$$

Since $k_{i,TCM}$ for each specific reactive site in NOM cannot be measured directly, hence, **Eq. 3-5** and **Eq. 3-6** provide several criteria to develop a new analytical solution for solving $k_{ov,TCM}(t)$. Similar with the derivation of $k_{ov,Cl}(t)$ addressed in the **Chapter 2**, the criteria obtained from **Eq. 3-5** includes: (1) the $k_{ov,TCM}$ depends on the individual TCM formation rate constant $k_{i,TCM}$ and the concentrations of TCM formation precursors $c_{Ri}(t)$, indicating the initial $k_{ov,TCM}(0)$ is independent of ICCs, (2) when one species $c_{Ri}(t)$ is in large excess with respect to all other species, the $k_{ov,Cl}$ tends to be stable. The criteria obtained from **Eq. 3-6** is regarding the change rate of $k_{ov,TCM}$ over time, which includes (3) it is negative, which indicates that the $k_{ov,TCM}$

decreases with the reaction progress, (4) is related to the chlorine concentration, i.e. $k_{ov,TCM}$ decreases faster at higher ICC compared to a lower ICC, (5) tends to zero when the concentration of chlorine tends to zero, and (6) second order with respect to $k_{ov,TCM}$.

As listed above, these characteristics of $k_{ov,TCM}$ obtained from **Eq. 3-5** and **Eq. 3-6** are the criteria for the proposition of an empirical equation. Similar to the chlorine decay (**Eq. 2-9**), phenomenologically, an exponential equation could be appropriate to describe $k_{ov,TCM}$ as given in **Eq. 3-7**:

$$k_{ov,TCM}(t) = \varphi \cdot e^{-\chi \cdot \left[\frac{\Delta c_{TCM}(t)}{\Delta c_{TCMFP}}\right]} = \varphi \cdot e^{-\chi \cdot [X_{TCM}(t)]} \qquad \text{Equation 3-7}$$

where φ and χ are independent and positive model parameters, which are obtained from the model calibration and invariant for a given water. The unit of φ is L/µmol/h while χ is dimensionless. $X_{TCM}(t)$ is the fractional conversion ranging from 0 to 1, which represents the progress of TCM formation. Δc_{TCM} is the TCM concentration formed at time t (µM). Δc_{TCMFP} is the maximum TCM formation, i.e. the formation potential of TCM (µM).

Differentiation of **Eq. 3-7** provides:

$$\frac{dk_{ov,TCM}(t)}{dt} = -\frac{\varphi}{\Delta c_{TCMFP}} \cdot k_{ov,TCM}^2(t) \cdot c_{Cl}(t) \cdot c_{TCMFP}(t) \qquad \text{Equation 3-8}$$

According to **Eq. 3-7** and **Eq. 3-8**, it is found that $k_{ov,TCM}$ always equals to φ at the beginning of the reaction. Thus, the first criterion, which regarding the initial $k_{ov,TCM}(0)$ is independent of ICC, was met. **Eq. 3-7** also shows that the $k_{ov,TCM}$ is decreasing with the increased fractional conversion (X), which is consistent with the criteria 2. Based on **Eq. 3-8**, it can be concluded that the proposed exponential equation meets all the other criteria related to the change rate of $k_{ov,TCM}$ (criteria 3 -6). Therefore, the proposed exponential equation **Eq. 3-7** is suitable to describe $k_{ov,TCM}$ from a theoretical point of view. This will be further addressed and validated below by applying experimental data sets.

Substituting **Eq. 3-7** into **Eq. 3-4** yields:

$$\frac{dc_{TCM}(t)}{dt} = \varphi \cdot e^{-\chi \cdot \left[\frac{\Delta c_{TCM}(t)}{\Delta c_{TCMFP}}\right]} \cdot c_{Cl}(t) \cdot c_{TCMFP}(t) \qquad \text{Equation 3-9}$$

where $c_{TCMFP}(t)$ is the concentration of TCM formation precursors remaining in water at time *t*, which can be expressed as the difference between initial TCMFP and TCM concentration at time *t*. It can be determined as follows:

$$c_{TCMFP}(t) = \Delta c_{TCMFP}(0) - \Delta c_{TCM}(t) \qquad \text{Equation 3-10}$$

Substituting **Eq. 3-10** to **Eq. 3-9** yields the final equation to calculate the TCM concentrations for chlorination at different ICCs.

3.2.2 Total trihalomethanes (TTHM) formation model

In the study of this chapter, although the water sample was not intendedly spiked with different bromide concentrations to investigate the role of bromine in the kinetics formation of TTHM, the ratio of bromine to chlorine concentration also changed because different initial chlorine dosages were applied to identical waters. The changeable reaction rate of TTHM formation caused by changeable bromine to chlorine ratio becomes a challenge when applying invariant model parameters for the TTHM simulation.

Similar as **Eq. 3-1**, the bromine reacted with a single reactive site *i* provided by the NOM and intermediates after halogenation step to form the brominated THM (*Br-THM*) was expressed as follows:

$$Br + R_{i,Br-THM} \xrightarrow{k_{i,Br-THM}} \delta_i Br - THM_i \qquad \text{Equation 3-11}$$

The TTHM is the sum of TCM and *Br-THM*:

$$\frac{\sum_{i=1}^{n} dc_{TTHM}(t)}{dt} = \sum_{i=1}^{n} k_{i,TCM} \cdot c_{Cl}(t) \cdot c_{TCMFP_i}(t) + \sum_{i=1}^{n} k_{i,Br-THM} \cdot c_{Br}(t) \cdot c_{Br-THMFP_i}(t) \qquad \text{Equation 3-12}$$

where $k_{i,Br\text{-}THM}$ is the rate constant for the i^{th} reactive site to form *Br-THM* and $c_{Br}(t)$ is the bromine concentration at time *t*. $c_{Br\text{-}THMFP}$ is the concentration of reactive sites for the *Br-THM* formation. It is assumed that the reactive sites in NOM that available for

TCM formation are the same as the sites available for *Br-THM* formation. To reduce the number of model parameters, the TCM formation potential c_{TCMFP} is equal to *Br-THM* formation potential $c_{Br\text{-}THMFP}$.

Moreover, as the reactions incorporating bromine into NOM being faster than those incorporating chlorine, for each specific NOM reactive site, defining the ratio of the rate constant of $k_{i,Br\text{-}THM}$ to rate constant of $k_{i,TCM}$ as γ.

Incorporation the substitution ratio γ and rearrange the equation, the **Eq. 3-12** can be rearranged as follows:

$$\frac{\sum_{i=1}^{n} dc_{TTHM}(t)}{dt} = \left[1+\gamma\cdot\frac{c_{Br}(t)}{c_{Cl}(t)}\right]\cdot c_{Cl}(t)\cdot\sum_{i=1}^{n} k_{i,Cl}\cdot c_{THMFP_i}(t) \qquad \text{Equation 3-13}$$

Furthermore, substituting **Eq. 3-9** to **Eq. 3-13** yields:

$$\frac{dc_{TTHM}(t)}{dt} = \left[1+\gamma\cdot\frac{c_{Br}(t)}{c_{Cl}(t)}\right]\cdot\varphi\cdot e^{-\chi\cdot\left[\frac{\Delta c_{TCM}(t)}{\Delta c_{TCMFP}}\right]}\cdot c_{Cl}(t)\cdot c_{TCMFP}(t) \qquad \text{Equation 3-14}$$

Eq. 3-14 is the final equation for the TTHM prediction. $K_{ov,TTHM}(t)$ is defined as the overall coefficient with respect to the TTHM formation, which is expressed as follows:

$$k_{ov,TTHM}(t) = \left[1+\gamma\cdot\frac{c_{Br}(t)}{c_{Cl}(t)}\right]\cdot\varphi\cdot e^{-\chi\cdot\left[\frac{\Delta c_{TCM}(t)}{\Delta c_{TCMFP}}\right]} \qquad \text{Equation 3-15}$$

As $k_{ov,TTHM}(t)$ is not constant, which is therefore referred to as a variable reaction rate coefficient (VRRC) of TTHM formation in this study.

It can be seen from **Eq. 3-15,** the optimum model parameters φ and χ can be determined through TCM model calibration. Therefore, the TTHM model calibration is not required, which improves the TTHM model applicability. The value of γ used in **Eq. 3-15** was chosen as 9 for model simulation (Nokes et al. 1999). Moreover, it is assumed that the initial bromine concentration $c_{Br}(0)$ to be equal to the bromide

concentration in water. This is because chlorine is usually orders of magnitude higher than bromide in concentration, and the oxidation of bromide by chlorine is very rapid (Kumar and Margerum 1987), i.e. nearly all of the bromide typically present in a chlorinated water becomes oxidized to bromine and reacts with NOM. If the bromide concentration in raw water is below the detection limit but the brominated THM are detected, it is assumed that the initial bromide concentration (initial bromine concentration) is the same as the minimum detective concentration (Obolensky and Singer 2005). The bromine concentration at time t ($c_{Br}(t)$) is derived from the standpoint of fundamental chemistry, i.e. the ratio of the consumed bromine to the consumed chlorine should be most directly related to the bromine substitution factor (BSF) (Hua and Reckhow 2012). Thus, $c_{Br}(t)$ used in **Eq. 3-15** is determined based on the consumed chlorine and the BSF, which can be expressed as follows:

$$c_{Br}(t) = c_{Br}(0) - \Delta c_{Cl}(t) \cdot BSF \qquad \text{Equation 3-16}$$

where BSF is bromine substitution factor. Theoretically, the BSF is decreasing with the reaction time as the bromination is faster than chlorination, and more TCM formed during the long reaction period. To simplify the model simulation process, the BSF is treated as one constant parameter in this study.

Generally, the overall rate coefficient $k_{ov,TTHM}(t)$ is decreasing with the reaction progress, which takes into account the overall decreasing reactivity of NOM in water. The influences of the bromine-to-chlorine concentration ratio and the substitution ratio γ on the TTHM formation rate were also reflected by the $k_{ov,TTHM}(t)$. Therefore, when the model is applied to simulate TTHM concentration at different ICCs, the model is able to provide reliable results by using invariant model parameters.

3.2.3 TCM and TTHM model application to chlorination at different temperatures

The effect of temperatures on the TCM and TTHM formation rate were illustrated in Chapter 2 (**Eq. 2-15**). Similarity, the VRRC of TCM and TTHM formation at different temperatures can be expressed as **Eq. 3-17** and **3-18**, respectively:

$$k_{ov,TCM,T_2}[X(t)] = k_{ov,TCM,T_1}[X(t)] \cdot \exp\left[\frac{-E_A/R \cdot (T_1 - T_2)}{T_1 \cdot T_2}\right] \quad \text{Equation 3-17}$$

$$k_{ov,TTHM,T_2}[X(t)] = k_{ov,TTHM,T_1}[X(t)] \cdot \exp\left[\frac{-E_A/R \cdot (T_1 - T_2)}{T_1 \cdot T_2}\right] \quad \text{Equation 3-18}$$

3.2.4 Model application to rechlorination condition

When the model is applied to rechlorination conditions, the $k_{ov,TCM}$ and $k_{ov,TTHM}$ is independent of the booster chlorine concentration as it only related to the reactivity and concentration of the THM precursors (**Eq. 3-6**). Before and after the rechlorination point, both of concentration and reactivity of THM precursors are constant. Therefore, extra calibrations of two model parameters φ and χ are not needed under rechlorination conditions.

3.2.5 Statistical analysis

The proposed model requires calibration to obtain the optimal values for the model parameters φ and χ, which allows the model to best represent THM formation. The optimal parameters should be invariant for any ICC, which is an important criterion for a THM formation model to reduce the model recalibration and extend the model application.

The TCM model (**Eq. 3-9**) was first calibrated against each TCM formation data sets for HWT water samples by minimizing the sum of squared differences between the experimentally-determined TCM concentrations and simulations at corresponding times (SSE). Then, to validate that the parameters, which were obtained from different experiments with a particular ICC, were not significantly different for the identical water, the coefficient of variation (CV) was calculated. We accepted that the parameters were not significantly different from each other when the CV was less than 10%. After proofing that the model parameters were not different from each other, the average parameters for the corresponding type of water were then used

for model validation by predicting the TCM formation with a range of ICCs (8.5 to 51.8 µM).

The TTHM formation model (**Eq. 3-14**) was developed based on the TCM formation model, thus the model parameters (φ and χ) obtained from TCM formation model were further used for the TTHM formation model validation. The TTHM formation model was validated by predicting the formation pattern with a range of ICCs (8.5 to 51.8 µM, at different temperatures (10 and 20°C) and rechlorination. It is note that no additional model calibrations or parameter recalculations were required for rechlorination. Since the proposed model did not have an analytical solution, the Euler method was adopted to solve the model numerically with a numerical time interval of 10 min. The details of the calculation process are described elsewhere (Butcher 2008).

All models were evaluated by the coefficient of determination (R^2) and the root-mean-square error (RMSE) (Piñeiro et al. 2008). Furthermore, the model adequacy was evaluated by the *F* test for the goodness-of-fit (Otto 2007).

3.3 MATERIALS AND METHODS

3.3.1 Water samples

Treated water samples prior to final disinfection were collected from the Hosterwitz drinking water treatment (HWT) plant situated in the state of Saxony, Germany in the period from January to May 2013. The treatment train of HWT plant was introduced in **Chapter 2** (section 2.3). The characteristics of water samples are summarized in **Table 3-1**, which was comparable with the value in **Table 2-1**.

The measurement methods of water quality characteristics were the same as them addressed in **Chapter 2** (section 2.3). The Bromide concentration is under detection limit. As address previously, the initial bromine concentration considered to be equal to bromide concentration and equal to the minimum detective concentration. In other words, the initial bromine concentration was 0.1 mg/L (1.23 µM) in this study for the model simulation.

Table 3-1. Characteristics of water samples.

Abbr.	Sample description	pH	DOC	UV_{254}	$SUVA_{254}$	Chlorine demand	Br^-	THMFP
			mg/L	m^{-1}	L/mg/m	mg/L	mg/L	µM
HWT	Treated river water	7.1	1.7±0.1	1.95	1.14	3.50±0.4	< 0.1	0.6

3.3.2 Experimental plan

To obtain the best-fit model parameters and evaluate the model accuracy under different chlorination conditions, THM formation data sets were used. The THM formation data sets included experimentally determined concentrations of total and individual THM species. A preliminary experiment to determine the THMFP was performed according to the German standard operation procedure (DVGW W-295 1997). Samples were first spiked with 10 mg Cl_2/L in 250 mL chlorine-demand-free amber glass bottles at 20°C, then the TTHM concentration was determined 168 h later.

Chlorination was conducted in 250 mL, chlorine-demand-free, glass-stoppered bottles. Chlorine stock solution was made by diluting concentrated sodium hypochlorite solution (14% active chlorine, VWR) with ultrapure water. All samples were buffered with 1 mM phosphate at pH 7. Prior to chlorination, the ICC was determined using the ratio of ICC-to-DOC in the range of 0.5 to 2 mg/mg, yielding ICC of 8.5, 27.9, and 51.8 µM for chlorination in this study (Kastl et al. 2003). In total, five independent experiments were conducted with regards to chlorination of HWT samples with different ICCs. After being dosed with chlorine, samples were stored headspace-free in the dark at 20°C. Following each dosing, total and individual THM concentrations and free chlorine concentration were measured periodically during incubation time. The frequency of grab sampling was higher at the beginning and decreased gradually over time. The maximum incubation time was 500 hours. To clarify the impact of temperature on model accuracy, additional chlorination experiments were performed for HWT water samples at 5 and 12°C, separately.

Rechlorinations were conducted 36 hours after the initial chlorination. Time was chosen according to the previous studies (Lee et al. 2007, Mouly et al. 2010). Specifically, rechlorination experiments were conducted 36 hours after the initial chlorination with ICC of 27.9 µM. At the booster point, the rechlorination dose was calculated to increase the residual chlorine concentration of the water samples back to the ICC. All the rechlorination experiments were conducted in the dark at 20°C. The THM concentration was measured periodically after the booster time.

3.3.3 Sample analysis

Residual free chlorine concentration was determined according to a N, N-diethyl-p-Phenylenediamine (DPD) Standard Colorimetric Method 4500-Cl G (American Public Health Association 2005). The water sample, which used for the THM concentration determination, was firstly quenched by the addition of sodium thiosulfate solution. Then, the THM concentration was measured by the gas-chromatographic method according to the German Norm (DIN EN ISO 15680 2004).

3.4 RESULTS AND DISCUSSION

3.4.1 Model parameters estimation for TCM formation model

The optimal value of model parameter φ and χ, which obtained by applying respective formation data sets with a particular ICC, are shown in appendix **Table 7-3**. In total, three groups of φ and χ were determined for the HWT water sample chlorinated at ICCs of 8.5, 27.9 and 51.8 µM. As addressed in Section 3.2 of model development, the $k_{ov,TCM}$ is independent of ICC, i.e. the φ and χ were independent of ICC. Therefore, it is expected that the difference between the obtained group of parameters is negligible for identical water samples, which would confirm that the model parameters are independent of any ICC and further validate that the $k_{ov,TCM}$ is independent of the ICC.

As shown in appendix **Table 7-3**, the differences between the obtained groups of φ and χ were evaluated based on the CV. The results indicate that the CV with respect to φ and χ were smaller than 10%, which shows that there were no noticeable differences between the groups of optimal parameters for the same water sample

even if a relative wide range of ICC was applied. Thus, the $k_{ov,TCM}$ with respect to TCM formation was validated to be independent of the ICC. This results might be the reason for the previous experimental results reported by Gallard and von Gunten (2002b), which showed that the obtained second order rate constants varied insignificantly in the range of ICCs from 50 to 210 μM.

As the optimal φ and χ for the same water sample were not significantly different, the average values of parameters ($\bar{\varphi}$ and $\bar{\chi}$) were applied. The model accuracy and adequacy test results are also shown in appendix **Table 7-3**. For HWT water sample, the relationship between the measured and simulated results was satisfactory with R^2 ranging from 0.93 to 0.98. The obtained RMSE is of similar magnitude to the measurement error with a typical precision (95%), which indicates a good fit. As for the model adequacy *F*-test for the goodness-of-fit, all the *p* values were lower than the significance level of 0.05 (*Prob* > F) considered in this study, and the test is therefore significant, which gives additional evidence that the model provides an adequate fit to the experimental data.

Fig. 3-1 shows the goodness of curve fitting for TCM formation when chlorination of HWT water sample with different ICCs. It can be seen that the proposed TCM model described the experimental data well. On the basis of the graphical and quantitative analysis discussed above, the TCM model was confirmed to provide an adequate fit to the data.

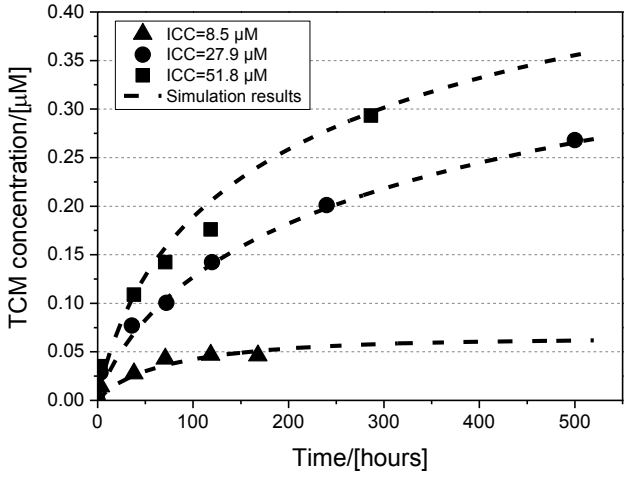

Figure 3-1. Time-course TCM formation of HWT water sample with different ICCs. Points represent experimental data; dash lines represent the calibration results.

3.4.2 TTHM formation model validation for chlorination at different initial chlorine concentrations

As discussed previously, the model parameters obtained from TCM model were further applied for TTHM formation model validation. The overall reaction rate coefficient with respect to THM formation $k_{ov,TCM}$, the model accuracy and adequacy were also shown in appendix **Table 7-3**. It can be seen that the range of $K_{ov,THM}$ over the long-term reaction periods was consistent with the conclusion that the second order rate constant for the long-term THM formation falls into the range of 0.05 to 0.2 $M^{-1}s^{-1}$ for drinking waters at 7.5 < pH < 8.5 (Gallard and von Gunten 2002a). Furthermore, as shown in appendix **Table 7-3**, $K_{ov,THM}$ at the end of reaction time was found to be lower when higher ICCs were applied. This might be explained by the fact that NOM with high reactivity is consumed faster when higher chlorine dose is applied.

The TTHM formation as a function of time is shown in **Fig. 3-2**. It can be seen that all THM formation profiles follow the same pattern, which was characterized by an initial fast formation stage and a later slower formation stage. A good agreement between the TTHM formation simulation was obtained for both samples with R^2 ranged from 0.91 to 0.97.

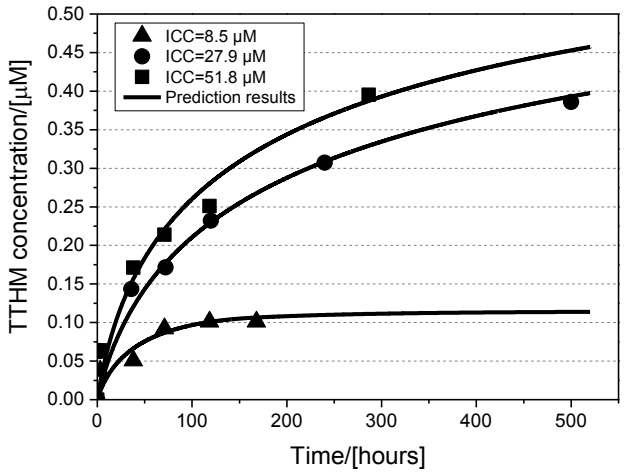

Figure 3-2. Time-course TTHM formation with different ICCs. Solid line indicates the prediction results by using invariant parameters obtained from TCM model calibration.

3.4.3 TCM and TTHM formation model validation for chlorination at different temperatures

In this study, several combinations of ICCs and temperatures referred to as ICC/temperature were conducted on the HWT water sample, which included 27.9 μM/10 °C, 51.8 μM/10 °C. The $k_{ov,TCM}$ and $k_{ov,THM}$ obtained from chlorination experiments conducted at 20 °C were used as a reference reaction rate coefficient of TCM formation (appendix **Table 7-3**). The optimum E_A/R was determined as 7810 for HWT sample.

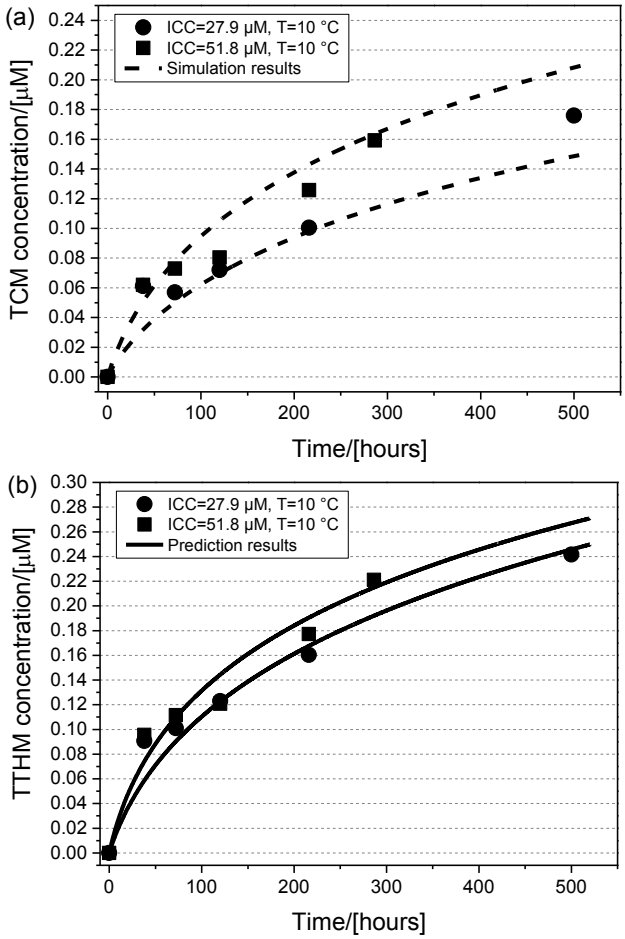

Figure 3-3. Time-course (a) TCM formation and (b) TTHM formation with different ICCs at 10 °C by using invariant parameters calibrated at 20 °C. Dash line and solid line indicate the simulation and prediction results respectively.

Fig. 3-2 illustrates the model predictions at different temperatures with invariant parameters of φ and χ. The model estimates for all ICCs and temperatures combination show a good agreement with experimentally determined TTHM concentrations, and with the average R^2 of 0.92. In terms of the model adequacy *F*-test for the goodness-of-fit, all the *p* values were lower than the significance level of 0.05 (*Prob*>F), and the test is therefore significant, which indicates that the model provides an adequate fit to the experimental data.

3.4.4 TCM and TTHM models validation for rechlorination condition

As mentioned before, the proposed TCM and TTHM models are able to predict TCM and TTHM concentrations under rechlorination condition without additional calibration.

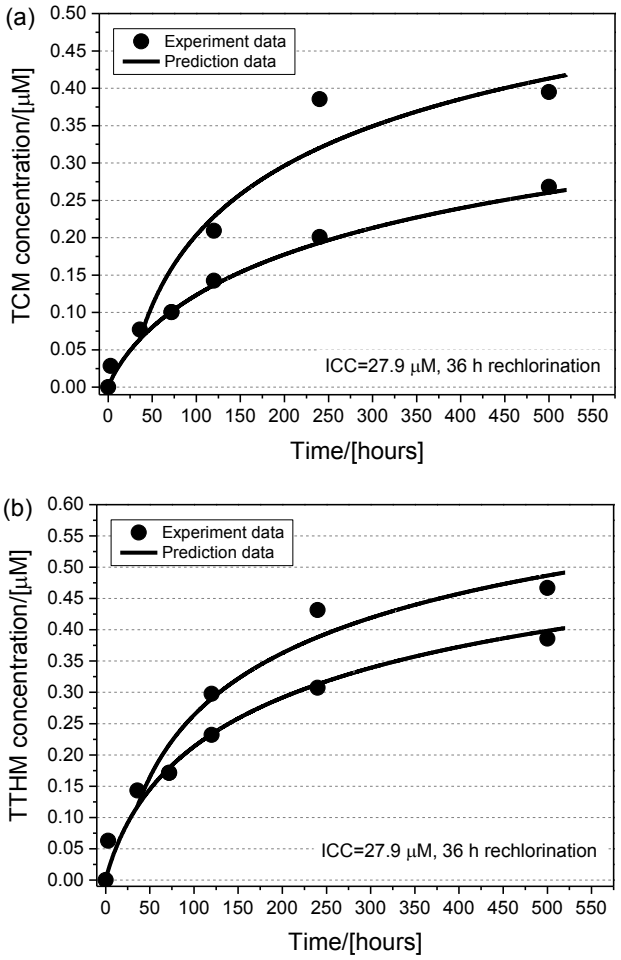

Figure 3-4. Time-course (a) TCM formation and (b) TTHM formation under rechlorination condition. Solid line indicates the prediction results by using invariant parameters obtained from TCM model calibration.

Fig. 3-3(a) and (b) illustrate the model accuracy with respect to TCM formation under rechlorination conditions 72 hours after the initial chlorination with ICC of 8.5 µM and 36 hours after the initial chlorination with ICC of 27.9 µM, respectively. **Fig. 3-3(c) and (d)** show the model accuracy with respect to TTHM formation. It can be seen that the TTHM formation resumed substantially after the rechlorination when a lower ICC of 8.5 µM was applied, while the TTHM moderately increased when higher ICC of 27.9 µM was applied. It suggests that with a lower ICC, the residual chlorine concentration is the limiting factor for the TTHM formation. Thus, the THM formation increased substantially when chlorine is applied at the rechlorination point. The model accuracy and adequacy evaluation are shown in **Table 3-2**, which shows that both TCM and TTHM models were able to provide reliable prediction results.

Table 3-2. The accuracy and adequacy of proposed models for TCM and TTHM predictions under chlorination at different temperatures and rechlorination.

Scenarios	Water sample	ICC	Booster Concen.	Rechlo. time	DBP	R^2	RMSE	F value
			µM	hours				
Chlorination at 10°C	HWT	27.9	-	-	TCM	0.902	0.016	83.6
		27.9	-	-	THM	0.928	0.013	97.9
	HWT	51.8	-	-	TCM	0.963	0.015	156.4
		51.8	-	-	THM	0.957	0.014	99.36
Rechlorination	HWT	27.9	27.9	36	TCM	0.914	0.045	44.0
					THM	0.920	0.033	101.8

3.5 SUMMARY AND CONCLUSIONS

In the present work, the kinetics of the TCM and TTHM formation was described by a second order kinetic model with a variable formation coefficient. Such a coefficient was able to describe the changing reactivity of THM precursors. Furthermore, it was depend on the water type but was independent of the dosed chlorine, which enables the model to predict a TTHM concentration with invariant parameters under

chlorination condition with different initial chlorine concentrations. In order to consider the influence of changing temperature in the distribution system, e. g. due to the seasons change, Arrhenius equation was approved to be suitable for both the TCM and TTHM models modification, and consequently, enabled the models provide reliable results for chlorination at different temperatures. The proposed models were also able to predict the TCM and TTHM concentrations under rechlorination conditions with invariant calibrated parameters. Generally, the proposed models have simplified calibration process and show good predictions for a wide application in the field of drinking water distribution systems.

REFERENCES

American Public Health Association, A.W.W.A.a.W.E.F. (2005) 4500-Cl G: Standard method for determination of chlorine (residual). In. Standard methods for the examination of water and wastewater 21st Edition. APHA-AWWA-WEF, Washington, D.C.

Boccelli, D.L., Tryby, M.E., Uber, J.G. and Summers, R.S. (2003) A reactive species model for chlorine decay and THM formation under rechlorination conditions. Water Research 37(11), 2654-2666.

Butcher, J.C. (2008) Numerical methods for ordinary differential equations. Second edition, John Wiley & Sons, West Sussex, England.

Chang, E.E., Chiang, P.C., Ko, Y.W. and Lan, W.H. (2001a) Characteristics of organic precursors and their relationship with disinfection by-products. Chemosphere 44(5), 1231-1236.

Chang, E.E., Lin, Y.P. and Chiang, P.C. (2001b) Effects of bromide on the formation of THMs and HAAs. Chemosphere 43(8), 1029-1034.

Chowdhury, S., Champagne, P. and McLellan, P.J. (2009) Models for predicting disinfection byproduct (DBP) formation in drinking waters: a chronological review. Science of The Total Environment 407(14), 4189-4206.

Clark, R.M. (1998) Chlorine demand and TTHM formation kinetics: a second-order model. Journal of Environmental Engineering 124(1), 16-24.

Deborde, M. and von Gunten, U. (2008) Reactions of chlorine with inorganic and organic compounds during water treatment—Kinetics and mechanisms: A critical review. Water Research 42(1–2), 13-51.

DIN EN ISO 15680 (2004) Gas-chromatographic determination of a number of monocyclic aromatic hydrocarbons, naphthalene and several chlorinated compounds using purge-and-trap and thermal desorption.

DVGW W-295, A. (1997) Determination of potentials of THM-formation of drinking water, water of swimming pools and baths. Technische Regeln. DVGW Regelwerk. Bonn.

Gallard, H., Leclercq, A. and Croué, J.-P. (2004) Chlorination of bisphenol A: kinetics and by-products formation. Chemosphere 56(5), 465-473.

Gallard, H. and von Gunten, U. (2002a) Chlorination of natural organic matter: kinetics of chlorination and of THM formation. Water Research 36(1), 65-74.

Gallard, H. and von Gunten, U. (2002b) Chlorination of phenols: Kinetics and formation of chloroform. Environmental Science & Technology 36(5), 884-890.

Gang, D., Clevenger, T.E. and Banerji, S.K. (2003) Relationship of chlorine decay and THMs formation to NOM size. Journal of Hazardous Materials 96(1), 1-12.

Golfinopoulos, S.K. and Arhonditsis, G.B. (2002) Multiple regression models: A methodology for evaluating trihalomethane concentrations in drinking water from raw water characteristics. Chemosphere 47(9), 1007-1018.

Hong, H.C., Liang, Y., Han, B.P., Mazumder, A. and Wong, M.H. (2007) Modeling of trihalomethane (THM) formation via chlorination of the water from Dongjiang River (source water for Hong Kong's drinking water). Science of The Total Environment 385(1-3), 48-54.

Hua, G. and Reckhow, D.A. (2012) Evaluation of bromine substitution factors of DBPs during chlorination and chloramination. Water Research 46(13), 4208-4216.

Hua, G., Reckhow, D.A. and Kim, J. (2006) Effect of Bromide and Iodide Ions on the Formation and Speciation of Disinfection Byproducts during Chlorination. Environmental Science & Technology 40(9), 3050-3056.

Kastl, G., Fisher, I., Jegatheesan, V., Chandy, J. and Clarkson, K. (2003) Prediction of chlorine and trihalomethanes concentration profile in bulk drinking water distribution systems from laboratory data. Water Science and Technology: Water Supply 3(1-2), 239-246.

Kumar, K. and Margerum, D.W. (1987) Kinetics and mechanism of general-acid-assisted oxidation of bromide by hypochlorite and hypochlorous acid. Inorganic Chemistry 26(16), 2706-2711.

Lee, J., Lee, D. and Sohn, J. (2007) An experimental study for chlorine residual and trihalomethane formation with rechlorination. Water science and technology 55(1-2), 307-313.

Li, X. and Zhao, H.B. (2006) Development of a model for predicting trihalomethanes propagation in water distribution systems. Chemosphere 62(6), 1028-1032.

Mouly, D., Joulin, E., Rosin, C., Beaudeau, P., Zeghnoun, A., Olszewski-Ortar, A., Munoz, J.F., Welté, B., Joyeux, M., Seux, R., Montiel, A. and Rodriguez, M.J. (2010) Variations in trihalomethane levels in three French water distribution systems and the development of a predictive model. Water Research 44(18), 5168-5179.

Nokes, C.J., Fenton, E. and Randall, C.J. (1999) Modelling the formation of brominated trihalomethanes in chlorinated drinking waters. Water Research 33(17), 3557-3568.

Obolensky, A. and Singer, P.C. (2005) Halogen Substitution Patterns among Disinfection Byproducts in the Information Collection Rule Database. Environmental Science & Technology 39(8), 2719-2730.

Otto, M. (2007) Chemometrics: Statistics and Computer Application in Analytical Chemistry, Wiley-VCH, Weinheim, Germany.

Piñeiro, G., Perelman, S., Guerschman, J.P. and Paruelo, J.M. (2008) How to evaluate models: Observed vs. predicted or predicted vs. observed? Ecological Modelling 216(3–4), 316-322.

Sohn, J., Amy, G., Cho, J., Lee, Y. and Yoon, Y. (2004) Disinfectant decay and disinfection by-products formation model development: chlorination and ozonation by-products. Water Research 38(10), 2461-2478.

Uyak, V., Ozdemir, K. and Toroz, I. (2007) Multiple linear regression modeling of disinfection by-products formation in Istanbul drinking water reservoirs. Science of The Total Environment 378(3), 269-280.

Yang, X., Shang, C., Lee, W., Westerhoff, P. and Fan, C. (2008) Correlations between organic matter properties and DBP formation during chloramination. Water Research 42(8–9), 2329-2339.

Zhang, X.L., Yang, H.W., Wang, X.M., Fu, J. and Xie, Y.F. (2013) Formation of disinfection by-products: Effect of temperature and kinetic modeling. Chemosphere 90(2), 634-639.

CHAPTER 4

Chlorine decay and trichloromethane formation in the presence of goethite and magnetite particles

---

THIS CHAPTER IS REPRODUCED BASED ON

Effects of pipe deposits on chlorine consumption and trihalomethane formation in drinking water distribution system

Hua P, Vasyukova E and Uhl W

IWA World Water Congress & Exhibition
September 2014, Lisbon, Portugal

4 CHLORINE DECAY AND TRICHLOROMETHANE FORMATION IN THE PRESENCE OF GOETHITE AND MAGNETITE PARTICLES

ABSTRACT

This study investigated the adsorption behavior of dissolved organic matter (DOM) components onto synthetic iron pipe corrosion scales, goethite and magnetite, as well as the influence of these synthetic pipe deposits (PDs) on the kinetics of chlorine decay and trichloromethane (TCM) formation in drinking water. Results show that goethite and magnetite selectively adsorb DOM molecules, namely those of high and intermediate molecular weight. The presence of goethite and magnetite resulted in a significant increase of chlorine consumption and TCM formation compared to the bulk water containing no PDs, supposedly due to the increased number of reactive sites. The previously suggested second order models with variable reaction rate coefficients were extended for simulating the residual chlorine and the TCM concentrations in the presence of goethite and magnetite. The models take into account not only the decreasing reactivity of DOM but also the influence of PDs on the reaction kinetics.

KEYWORDS

Chlorine decay; dissolved organic matter; kinetic models; pipe deposits; trichloromethane formation

4.1 INTRODUCTION

In the WDS, free chlorine reacts not only with DOM remaining in the bulk water, which is termed as the bulk reaction, but also with biofilm (Lu et al. 1999, Ndiongue et al. 2005), pipe materials (Al-Jasser 2007), and pipe deposits (PDs) (Hassan et al. 2006, Zhang and Andrews 2012) which is termed as the wall reaction. Comparing with the bulk reaction, there is growing evidence suggests that the wall reaction causes increased chlorine consumption and could potentially lead to a significant DBP formation (Digiano and Zhang 2005, Zhang and Andrews 2013, Zhang et al. 2008). Among the assessed DBP, THM is one of the first identified carcinogenic DBP and regulated by most of countries worldwide (USEPA 2009, WHO 2011).

Water quality models, which use the output of hydraulic models to predict the temporal and spatial distribution of chlorine and THM within a WDS, have been well developed during the past several years. Fisher et al. (2011) emphasized the advantages of the separate models of bulk and wall chlorine decay for planning and managing of WDS, e.g. minimizes calibration or scenario simulation efforts. However, the majority of predictive models developed at present are related to bulk reaction including the chlorine decay models (Fisher et al. 2011, Hua et al. 2015) and the THM formation models (Chowdhury et al. 2009). The progress of the kinetics models for the wall reaction still remains limited (Zhang et al. 2008). Therefore, developing models to simulate the kinetics of chlorine decay and THM formation in the presence of PDs became a driven force of this study.

Prior to the model development, investigating the adsorption behaviour of different DOM components onto the PDs was the first objective of this study. The knowledge of the preferential adsorption of DOM components onto PDs improves the understanding of the PDs effects on chlorine consumption and THM formation. With respect to the model development and application, two factors should be taken into account. First, the overall reactivity of DOM with chlorine decreases with the reaction progress, i.e. the reaction rate coefficient is variable (Hua et al. 2015, Jonkergouw et al. 2008). Second, the total (maximum) chlorine consumption and TCM formation potential (TCMFP) might increase in the presence of PDs compared

to the bulk water containing no PDs, even though the DOM concentration and composition were initially the same (Hassan et al. 2006). Therefore, developing second order models with variable reaction rate coefficients (VRRC) to simulate chlorine decay and TCM formation in the presence of PDs was the second objective of this study. Moreover, the applicability of models to the chlorination of a specific water containing either different PDs dosages or different initial chlorine concentrations (ICC) was evaluated. The investigated PDs in this study were synthetic iron pipe corrosion scales, goethite and magnetite.

4.2 MATERIAL AND METHODS

4.2.1 Materials

The raw surface water without treatment and the treated water prior to the final disinfection were collected between June and July 2013 from Altenberg water treatment (AWT) plant located in the state of Saxony, Germany. The AWT raw water was reservoir water characterized by a high content of dissolved organic carbon (DOC) of 11.2 ± 0.2 mg/L, low turbidity and slightly acid pH (~6.0). The treatment train comprised coagulation/flocculation with ferric chloride as coagulant and an anionic polymer as coagulation aid, followed by sedimentation, rapid sand filtration, ozonation, biological activated carbon filtration, and chlorine disinfection (Vasyukova et al. 2013). The DOC and pH of AWT treated water were 2.4 ± 0.1 mg/L and 7.3 ± 0.2, respectively. Samples were collected in pre-cleaned DOC free canisters and stored at 4°C until analysis.

The goethite and magnetite were both purchased from Sigma-Aldrich (Sigma Aldrich, USA). TCM standard solutions were prepared by diluting concentrated TCM standard (Sigma Aldrich, USA) with ultrapure water to the target aqueous phase concentration. The chlorine stock solution was prepared by diluting a concentrated commercial sodium hypochlorite solution (14% active chlorine, VWR) with ultrapure water (18.2 MΩ•cm at 25°C, Direct-Q system, Merck Millipore).

4.2.2 Adsorption experiments

The adsorption experiments were conducted in a series of 100 mL Pyrex conical flasks with stoppers to investigate the preferential adsorption of DOM components onto goethite and magnetite. The DOC of 11.2 mg/L in AWT raw water was adsorbed onto goethite or magnetite by shaking the suspensions at 100 rpm using an orbital shaker at room temperature (20 ± 1°C) for 5 days to achieve the equilibration. The suspended goethite and magnetite concentrations ranged from 0.5 to 5 g/L. The pH value was adjusted to 7.5 by 0.1 M NaOH (Chun et al. 2005). After 5 days, the suspensions were filtered through the 0.45 µm polycarbonate filters for DOC analysis. The amount of adsorbed DOC calculated as the final DOC in solution after 5 days adsorption minus the initial DOC concentration. The adsorption percentages were calculated as the absolute amount of adsorbed DOC (positive value) divided by the initial DOC concentration.

4.2.3 Chlorination experiments

A blank experiment was conducted in the absence of DOC, i.e. chlorination of ultrapure water with goethite or magnetite, to find out whether these PDs themselves consume chlorine.

The detailed experimental design regarding the chlorination of AWT treated water with and without PDs is shown in **Fig. 4-1**. With regard to the chlorine decay experiment with goethite (**Fig. 4-1(a)**), the ICC was initially constant at 4 mg/L, while the goethite dosages were varied between 0 and 2 g/L. The experiment in the absence of goethite (0 g/L goethite) was conducted to obtain the decay dataset of bulk reaction. In addition, the goethite dosage was kept constant at 1 g/L while the ICC was varied between 2 and 6 mg/L. In this way, the combined effects of ICC and PDs dosages on chlorine decay were investigated. Likewise, a similar experimental matrix was settled to determine the residual chlorine concentration in the presence of magnetite.

The experimental design for TCM determination is shown in **Fig. 4-1(b)**. Although the size of the experimental matrix for TCM was smaller than that for the residual

chlorine determination, the combined effect of ICC and PDs dosages on TCM formation was also investigated. Specifically, the goethite dosages were ranged from 0 g/L (bulk reaction) to 5 g/L while the ICC was fixed at 4 mg/L. Moreover, the ICC was set to 2 mg/L and 4 mg/L individually with an identical goethite concentration of 1 g/L. To compare the effects of goethite and magnetite on TCM formation, two independent experiments were conducted under the same chlorination condition, i.e. ICC of 4 mg/L and both goethite and magnetite dosages of 1 g/L.

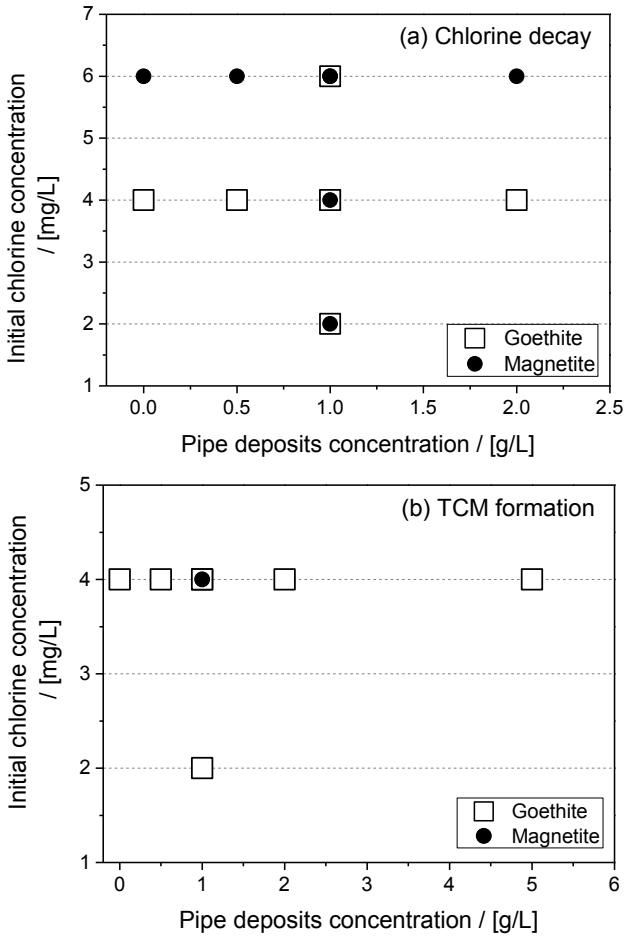

Figure 4-1. Experimental design regarding chlorination of AWT treated water (DOC = 2.4 mg *C*/L) in the presence of goethite and magnetite for (a) residual chlorine concentration determination and (b) TCM concentration determination.

Based on the experimental design, the AWT treated water was filled into 100 ml chlorine-demand free brown glass bottles containing PDs at planed dosages. Then, the chlorine stock solution was added to the bottles to achieve the target ICC. The

reaction time ranged from 10 min to maximum 168 hours. At the end of the reaction time, the water sample was filtrated through 0.45 µm polycarbonate filters and the residual chlorine and TCM concentrations were determined immediately. To take into account the loss of TCM caused by the sample filtration, TCM standard solutions with different PDs dosages were filtrated and TCM concentration remaining in solution after filtration were analysed. The loss factor was calculated as the remaining TCM after filtration divided by the initial TCM concentration. Therefore, the experimentally determined TCM concentrations in this study were modified by the loss factors. Temperature and pH of all experiments were kept constant at 20 °C and 7.5, respectively (Vikesland 2000).

4.2.4 Analytical methods

The determination methods of residual chlorine concentration and THM formation were described in Chapter 2 and Chapter 3 (section of material and methods), respectively.

The total DOC concentration including that of DOC components were determined by the LC-OCD (Huber et al. 2011). The compound-specific detection limit of DOC was <1–50 µg/L (http://www.doc-labor.de/Specs.html, accessed Jun. 2015). The mentioned DOM components in this study were based on the fractionation of liquid chromatographs with organic carbon detection (LC-OCD) (Huber et al. 2011), including Biopolymers (BP), Humic Substances (HS), Building Blocks (BB), Low Molecular Weight neutrals (LMW-neutrals), Low Molecular Weight Acid (LMW-acids) and Hydrophobic Organic Carbon (HOC). In this study, it was assumed that HS and BB have similar characteristics and can be treated as one component that refers to as HS+BB.

4.2.5 Model development

The main THM species in AWT treated water sample was TCM, which accounted for above 97% of the total THM concentration. Thus, the influece of bromide (bromine) on the kinetics of THM formation was ignored in this study and the focus was the kinetics formation of TCM.

Hua et al. (2015) developed a VRRC second order model, which initially applied for chlorine decay in bulk water. The VRRC model was based on an assumption that each reactive site provided by DOM exhibits its own characteristic or reactivity with chlorine. The overall VRRC of chlorine $k_{ov,Cl}$ with respect to all reactive sites was not constant but decreased during the whole reaction period. The $k_{ov,Cl}$ can be expressed as an exponential equation, and the detailed information can be found in Chapter 2 (**Eq. 2-13**):

In this chapter, the VRRC model was extended from bulk water to the water sample containing PDs. Specifically, the best-fit parameters were calibrated against the experiment datasets in the presence of PDs. Similar as the TCM formation model, it was hypothesized that the TCM formation model with a $k_{ov,TCM}$ can also be expressed as **Eq. 3-9** in **Chapter 3**.

4.2.6 Data analysis

The best-fit model parameters with respect to chlorine decay, i.e. α, β and $\Delta C_{Cl,max}$ were obtained by minimizing the sum of squared differences between the experimentally-determined residual chlorine concentrations and simulations at corresponding times, namely, sum of the squared errors (SSE). Likewise, the best-fit model parameters φ, χ and ΔC_{THMFP} were also obtained by minimizing SSE of experimentally-determined TCM concentration and corresponding simulation results.

It should be illustrated that these model parameters are related not only to the concentration and composition of DOM but also depends on the type and dosages of PDs. Thus, parameters were calibrated against all the datasets with respect to chlorination of AWT treated water at identical ICC but with different type or dosages of PDs. However, for AWT water containing a specific type of PDs at a constant PDs dosage, the parameters were expected to be invariable when different ICC was spiked. This is because, theoretically, the rate coefficient k_{ov} is only related to the concentration and reactivity of reactant but independent of ICC (Hua et al. 2015).

Since the proposed model does not have an analytical solution, the Euler method was adopted to solve the model numerically with a time interval of 0.5 hours. The

details of the calculation process are described elsewhere (Butcher 2008). Excel Solver, which is based on the generalized reduced gradient algorithm, was employed to obtain the best-fit model parameters. The models were evaluated by the coefficient of determination (R^2) and the root-mean-square error (RMSE). All the methods have often been used as measures of difference between the predicted data and those obtained experimentally (Piñeiro et al. 2008).

4.3 RESULTS AND DISCUSSION

4.3.1 Adsorption of DOM fractions on goethite and magnetite

The initial DOC concentration of AWT raw water sample (11.2 mg *C*/L) and the DOC of solution after 5 days adsorption onto different dosages of goethite and magnetite are shown in **Fig. 4-2**. For both goethite and magnetite, the total DOC decreased significantly with increasing PDs dosages supposedly due to the increased available adsorption sites (**Fig. 4-2(a)**). The concentrations of HS+BB and BP decreased substantially as shown in **Fig. 4-2(b)** and **(c)**, indicating that they were main components contributing to the reduction of the total DOC due to adsorption. Nevertheless, the decrease of LMW-neutrals was not significant until the goethite and magnetite dosages reached at 5 g/L (**Fig. 4-2(d)**). These results indicate the components of HS+BB and BP were removed by adsorption preferentially, whereas LMW-neutrals could only be removed when more adsorbent was dosed and more adsorption sites were available. These observations are in agreement with Safiur Rahman et al. (2013) who showed that the DOC of a larger molecular weight fraction decreased preferentially, while the DOC with low molecular weight fraction remained in solution. LMW-acids were not detected in raw water.

No clear trend was observed regarding HOC adsorption onto PDs (not shown), which might attributed to the analytical method. Specifically, HOC was the difference of the DOC between the total DOC and five components (BP, HS, BB, LMW-neutrals and LMW-acid), which was thought to be of hydrophobic character but was not the same as the hydrophobic matter obtained from resin adsorption. Possibly due to the

quantification difficulty, the obtained HOC concentration varied randomly and no conclusion can be drawn for HOC components.

Comparing the adsorption percentages of goethite and magnetite, it was found the DOC decreased by 78% in the presence of goethite compared with 42% for magnetite when both PDs concentrations were at 5 g/L. With respect to the model development, the different DOM adsorption abilities of PDs might lead to the different effects of PDs on the kinetics of chlorine decay and TCM formation.

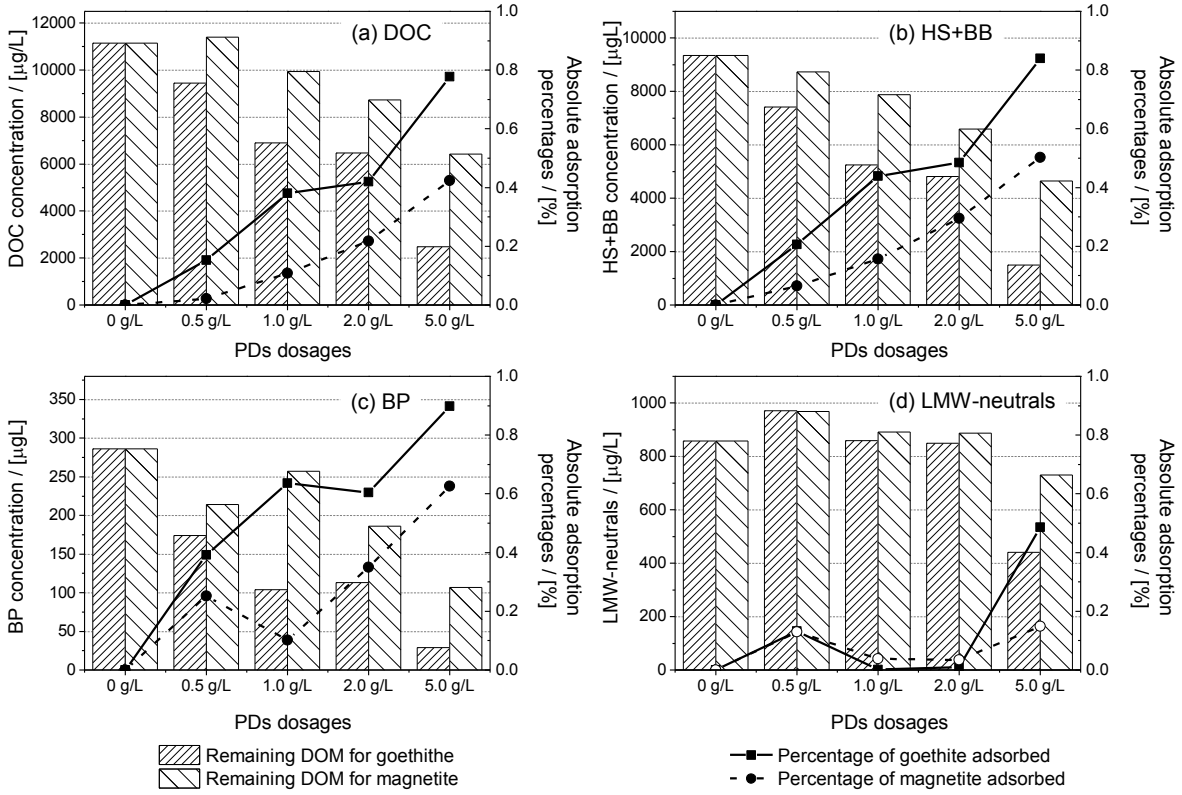

Figure 4-2. The remaining concentrations and absolute adsorption percentages of (a) DOC, (b) HS+BB, (c) BP, and (d) LMW-neutrals in AWT raw water (11.2 mg *C*/L) and in solution after 5 days adsorption onto different dosages of goethite and magnetite.

4.3.2 Chlorine decay in the presence of goethite and magnetite

A blank experiment in the absence of DOC was performed previously, i.e. ultrapure water containing 1 g/L of goethite or magnetite was spiked with ICC of 4 mg/L and incubated for 24 hours. Results show that 2.75% and 0.75% of the initial chlorine dosage were consumed by the goethite and magnetite, respectively. These low

losses suggest that the chlorine consumption of synthetic corrosion pipe scales themselves can be negligible.

However, in the presence of both DOM and PDs, chlorine consumption increased substantially compared with that of bulk water without PDs.

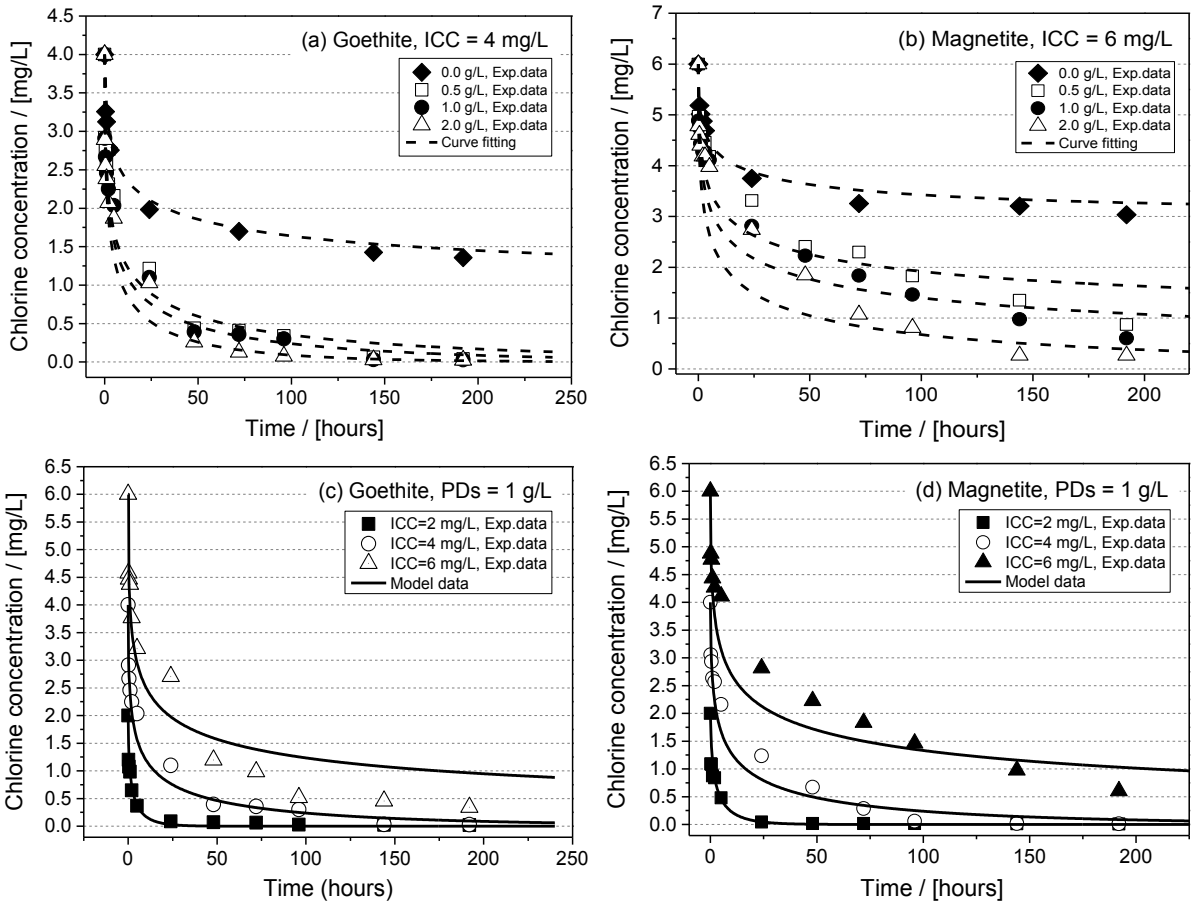

Figure 4-3. Chlorine decay test and curve fitting for AWT treated water chlorinated at (a) ICC of 4 mg/L in the presence of goethite, (b) ICC of 6 mg/L in the presence of magnetite, and AWT treated water chlorinated at different ICC containing (c) 1 g/L of goethite and (d) 1 g/L of magnetite. The dash lines represent the curve fitting (calibration) results, while the solid lines represent the model predition results.

Fig. 4-3 shows chlorine decay of AWT treated water containing different dosages of goethite spiked at ICC of 4 mg/L **(a)**, and containing different dosages of magnetite spiked with ICC of 6 mg/L **(b)**. Although no chlorine consumption was observed for both goethite and magnetite themselves, the chlorine consumption of AWT treated water significantly increased in the presence of PDs compared with that without PDs, even though an equal mass of DOM was present. The first reasonable

explanation might be the reactivity of DOM was modified due to the catalyst effects of goethite and magnetite (Schwarzenbach et al. 2005). The second reason is attributed to the increased total chlorine demand, i.e. the adsorption on scales lead to an increased number of DOM reactive sites making functional groups available for reactions that are not available in bulk water (Hassan et al. 2006).

For the model application (**Eq. 2-13**), the optimal α, β and $\Delta C_{Cl,max}$ were first calibrated against each datasets with respect to chlorination of AWT treated water at constant ICC but with different goethite or magnetite dosages. Taking goethite for example, four groups of α, β and $\Delta C_{Cl,max}$ were determined independently for four datasets presented in **Fig. 4-3(a)**, i.e. goethite dosages = 0, 0.5, 1, and 2 g/L with constant ICC = 4 mg/L. Likewise, four groups of parameters for magnetite were obtained individually for four datasets presented in **Fig. 4-3(b)**, i.e. magnetite dosages = 0, 0.5, 1, and 2 g/L with constant ICC = 6 mg/L. All the obtained best-fit parameters are shown in **Table 4-1**.

Table 4-1. Best-fit model parameters α, β and $\Delta C_{Cl,max}$ for each chlorine decay experiment dataset along with the corresponding R^2, SSE, RMSE.

Type of PDs	ICC	PDs concentration	α	β	$\Delta C_{Cl,max}$	R^2	SSE	RMSE
	mg/L	g/L	L/mg/h		mg/L			mg/L
Goethite	4	0.0*	0.14	-4.51	2.89	0.99	0.15	0.072
	4	0.5	0.18	-4.32	4.87	0.97	0.46	0.207
	4	1.0	0.19	-4.57	5.30	0.97	0.40	0.191
	4	2.0	0.19	-4.13	5.66	0.96	0.57	0.228
	2	1.0	0.19	-4.57	5.30	0.94	0.14	0.114
	6	1.0	0.19	-4.57	5.30	0.91	2.78	0.503
Magnetite	6	0.0*	0.14	-4.51	2.89	0.99	0.17	0.071
	6	0.5	0.14	-4.73	4.95	0.92	1.95	0.421
	6	1.0	0.14	-4.80	5.80	0.92	2.15	0.442
	6	2.0	0.14	-4.62	7.01	0.94	2.02	0.428
	2	1.0	0.14	-4.80	5.80	0.95	0.43	0.165
	4	1.0	0.14	-4.80	5.80	0.97	0.66	0.241

*: without PDs, bulk reaction

As addressed in the section of data analysis, the model parameters should be invariant for any ICC in the operation range. Therefore, when the type and dosages of PDs were invariable, the best-fit model parameters can be used to predict the chlorine decay of AWT treated water spiked at different ICC. Specifically, the best-fit α, β and $\Delta C_{Cl,max}$ for goethite, which were calibrated against the dataset of ICC = 4 mg/L and goethite dosage = 1 g/L, were further applied to predict the other two datasets presented in **Fig. 4-3(c)**, i.e. ICC = 2 and 6 mg/L, goethite dosage = 1 g/L. Similar with goethite, the model parameters for magnetite, which calibrated against the dataset of ICC = 6 mg/L and magnetite dosage = 1 g/L, were further used to predict the chlorine decay of AWT treated water spiked at 2 and 4 mg/L with 1 g/L magnetite (**Fig. 4-3(d)**). These invariant parameters are also shown in **Table 4-1**.

Fig. 4-3(a) and **(b)** show the goodness of curve fitting (calibration) for AWT treated water samples chlorinated with the identical ICC but containing different initial PDs dosages. **Fig. 4-3(c)** and **(d)** illustrate the model prediction results by using invariant parameters for AWT treated water containing constant PDs dosages but spiked at different ICC. Graphically, the proposed VRRC model described the experimental data well. Qualitatively, the relationships between the measured and simulated chlorine decay results were satisfactory with R^2 ranging from 0.91 to 0.99. The obtained RMSE is considered to be of a similar magnitude as the measurement error with a typical precision (95%), which indicates a good fit. Therefore, on the basis of the graphical and quantitative analysis discussed above, the VRRC model was able to provide a reasonable fit to the experimental datasets.

4.3.3 Trichloromethane formation in the presence of goethite and magnetite

Fig. 4-4(a) shows the TCM formation of AWT treated water spiked at ICC of 4 mg/L without goethite (bulk water) and with different dosages of goethite ranging from 0.5 to 2 g/L. The total TCM concentrations increased in the presence of goethite

compared with that of the bulk water containing no PDs. However, the influences of increased PDs dosages (from 0.5 to 2 g/L) on TCM formation were not significant.

Fig. 4-4(b) shows the results regarding AWT treated water spiked at ICC of 4 mg/L with 1 g/L goethite or magnetite. It was found that goethite leads to higher TCM formation compared with magnetite. A plausible explanation can be that the HS+BB component was more favorably adsorbed onto the goethite surface than onto that of magnetite, which observed in the adsorption experiments (**Fig. 4-2**). Because the HS+BB contain more aromatic and hydrophobic matters that are considered to be an important precursor for TCM formation, the preferential adsorption of HS+BB, which in turn, leads to an increased TCM formation.

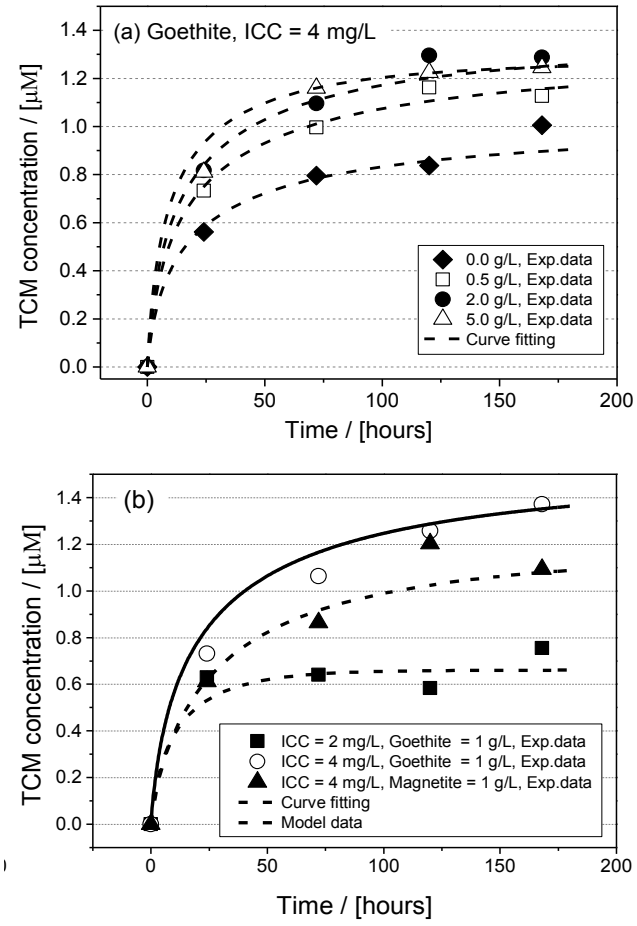

Figure 4-4. AWT water sample chlorinated at (a) ICC of 4 mg/L with different dosages of goethite and (b) ICC of 4 mg/L with 1 g/L goethite or magnetite and ICC of 2 mg/L with 1 g/L goethite The dash lines represent the curve fitting (calibration) results, while the solid lines represent the model predition results.

Fig. 4-4(b) also shows that the TCM concentration increased significantly in AWT treated water containing 1 g/L goethite chlorinated at ICC = 4 mg/L compared with the same sample chlorinated at ICC = 2 mg/L. This can be attributed to the fact that the ICC was completely consumed within the first 24 hours of reaction (**Fig. 4-3(c)**). Therefore, no significant TCM formation was observed after 24 hours when ICC of 2 mg/L was applied.

For the model application (**Eq. 3-9**), the optimal φ, χ and ΔC_{THMFP} were calibrated against each datasets with respect to chlorination of AWT treated water at constant ICC of 4 mg/L but with different goethite dosages. **Table 4-2** shows the best-fit parameters for each datasets as well as the model accuracy evaluation. Specifically, the R^2 ranged from 0.74 to 0.98 indicating a moderate to excellent match with experiment data. **Fig. 4-4** represents the graphical agreement between experimentally-determined and simulated TCM concentrations. Generally, the VRRC model was able to provide a reasonable fit to the experimental datasets of TCM formation.

Table 4-2. The best-fit model parameters φ, χ and ΔC_{THMFP} for each TCM formation experimental dataset along with the corresponding R^2, SSE, RMSE.

Type of PDs	ICC	PDs concen.	φ	χ	ΔC_{TCMFP}	R^2	SSE	RMSE
	mg/L	g/L	L/mol/s		µmol/L			mg/L
Goethite	4	0.0*	0.52	-1.21	1.04	0.86	0.014	0.058
	4	0.5	0.52	-1.21	1.33	0.97	0.010	0.052
	4	1.0	0.52	-1.21	1.51	0.90	0.070	0.133
	4	2.0	0.52	-1.21	1.61	0.97	0.019	0.069
	4	5.0	0.55	-1.21	1.67	0.98	0.009	0.049
	2	1.0	0.52	-1.21	2.28	0.74	0.021	0.072
Magnetite	4	1.0	0.61	-1.09	1.45	0.81	0.035	0.088

*: without PDs, bulk reaction

4.4 CONCLUSION

The adsorption behavior of dissolved organic matter (DOM) components onto synthetic pipe corrosion scales, goethite and magnetite, was evaluated initially. The results showed that high and intermediate molecular weight DOM components, e.g. Biopolymers, Humic acid and Building Blocks were preferentially adsorbed onto the goethite and magnetite. Whereas LMW-neutrals could only be removed when more adsorbent was used to provide a higher number of adsorption sites.

The influences of goethite/magnetite-adsorbed DOM on the chlorine consumption and trichloromethane (TCM) formation in drinking water were then evaluated. It was found that the chlorine consumption and TCM formation were increased in the presence of the pipe deposits (PDs) compared to the bulk water containing no PDs, even though the DOM concentration and composition was initially the same.

The second order models with variable reaction rate coefficients, which initially used to predict chlorine decay and TCM formation in the bulk water, were further applied under the condition that the PDs were present. The model was shown to be generally effective for describing chlorine decay and TCM formation for chlorination of AWT treated water containing both different PDs dosages and different initial chlorine concentrations.

REFERENCES

Al-Jasser, A.O. (2007) Chlorine decay in drinking-water transmission and distribution systems: Pipe service age effect. Water Research 41(2), 387-396.

Butcher, J.C. (2008) Numerical methods for ordinary differential equations. Second edition, John Wiley & Sons, West Sussex, England.

Chowdhury, S., Champagne, P. and McLellan, P.J. (2009) Models for predicting disinfection byproduct (DBP) formation in drinking waters: a chronological review. Science of The Total Environment 407(14), 4189-4206.

Chun, C.L., Hozalski, R.M. and Arnold, W.A. (2005) Degradation of Drinking Water Disinfection Byproducts by Synthetic Goethite and Magnetite. Environmental Science & Technology 39(21), 8525-8532.

Digiano, F.A. and Zhang, W. (2005) Pipe section reactor to evaluate chlorine-Wall reaction. Journal - American Water Works Association, 74-85.

Fisher, I., Kastl, G. and Sathasivan, A. (2011) Evaluation of suitable chlorine bulk-decay models for water distribution systems. Water Research 45(16), 4896-4908.

Hassan, K.Z., Bower, K.C. and Miller, C.M. (2006) Iron oxide enhanced chlorine decay and disinfection by-product formation. Journal of Environmental Engineering 132(12), 1609-1616.

Hua, P., Vasyukova, E. and Uhl, W. (2015) A variable reaction rate model for chlorine decay in drinking water due to the reaction with dissolved organic matter. Water Research 75(0), 109-122.

Huber, S.A., Balz, A., Abert, M. and Pronk, W. (2011) Characterisation of aquatic humic and non-humic matter with size-exclusion chromatography – organic carbon detection – organic nitrogen detection (LC-OCD-OND). Water Research 45(2), 879-885.

Jonkergouw, P.M.R., Khu, S.-T., Savic, D.A., Zhong, D., Hou, X.Q. and Zhao, H.-B. (2008) A variable rate coefficient chlorine decay model. Environmental Science & Technology 43(2), 408-414.

Lu, W., Kiéné, L. and Lévi, Y. (1999) Chlorine demand of biofilms in water distribution systems. Water Research 33(3), 827-835.

Ndiongue, S., Huck, P.M. and Slawson, R.M. (2005) Effects of temperature and biodegradable organic matter on control of biofilms by free chlorine in a model drinking water distribution system. Water Research 39(6), 953-964.

Piñeiro, G., Perelman, S., Guerschman, J.P. and Paruelo, J.M. (2008) How to evaluate models: Observed vs. predicted or predicted vs. observed? Ecological Modelling 216(3–4), 316-322.

Safiur Rahman, M., Whalen, M. and Gagnon, G.A. (2013) Adsorption of dissolved organic matter (DOM) onto the synthetic iron pipe corrosion scales (goethite and magnetite): Effect of pH. Chemical Engineering Journal 234(0), 149-157.

Schwarzenbach, R.P., Gschwend, P.M. and Imboden, D.M. (2005) Environmental organic chemistry, John Wiley & Sons.

USEPA (2009) National primary drinking water regulations. EPA 816-F-09-0004.

Vasyukova, E., Proft, R., Jousten, J., Slavik, I. and Uhl, W. (2013) Removal of natural organic matter and trihalomethane formation potential in a full-scale drinking water treatment plant. Water Science & Technology: Water Supply 13(4).

Vikesland, P.J. (2000) The role of the pipe water interface in DBP formation and disinfectant loss, American Water Works Association, U.S.A.

WHO (2011) Guidelines for drinking-water quality, 4th edition, Geneva.

Zhang, H. and Andrews, S.A. (2012) Catalysis of copper corrosion products on chlorine decay and HAA formation in simulated distribution systems. Water Research 46(8), 2665-2673.

Zhang, H. and Andrews, S.A. (2013) Effects of pipe materials, orthophosphate, and flow conditions on chloramine decay and NDMA formation in modified pipe loops. Journal of Water Supply: Research and Technology—AQUA 62(2), 107-119.

Zhang, Z., Stout, J.E., Yu, V.L. and Vidic, R. (2008) Effect of pipe corrosion scales on chlorine dioxide consumption in drinking water distribution systems. Water Research 42(1–2), 129-136.

CHAPTER 5

Reaction kinetics of chlorine with synthetic human body fluids and humic acid present in swimming pool water

---

THIS CHAPTER IS REPRODUCED BASED ON

Reaction kinetics of chlorine with human body fluids present in swimming pool water

Hua P, X. Chen, Vasyukova E and Uhl W

Book Chapter Disinfection byproducts in drinking water

ISBN:978-1-78262-0884, pages 322-329

The Royal Society of Chemistry

5 REACTION KINETICS OF CHLORINE WITH SYNTHETIC HUMAN BODY FLUIDS AND HUMIC ACID IN SWIMMING POOL WATERS

ABSTRACT

The reactivity of substances remaining in swimming pool waters towards chlorine consumption and trichloromethane (TCM) formation were investigated by conducting laboratory experiments. The investigated substances include body fluid analogue (BFA) representing swimmer excretions and humic acid (HA) representing natural organic matters in filling water. Based on the results obtained from chlorine demand and TCM formation potential tests, urea, which is one of the main BFA components, exhibited the highest TOC-related specific chlorine demand. Citric acid showed a considerable higher specific TCM formation potential than it of other BFA components. BFA was more reactive than HA towards chlorine consumption, whereas HA was more reactive towards TCM formation than BFA. Based on the results of kinetics experiments, the second order variable reaction rate coefficients towards chlorine decay and TCM formation were calculated for each individual substance separately. Uric acid exhibited the highest reactivity towards chlorine decay while urea exhibited the highest reactivity towards TCM formation. According to the rate coefficients for individual substances, the overall rate coefficients for the BFA (mixture) and a mixture of BFA and HA were calculated. Therefore, the chlorine consumption and TCM formation for mixtures were predicted by the proposed second order models. It was found that the models provide good simulation results.

KEYWORDS

Body fluid analogue (BFA); chlorine; reaction rate; swimming pool

5.1 INTRODUCTION

Bathers introduce considerable amounts of organic matter in the form of body fluids such as sweat, urea and saliva as well as some synthetic chemicals originating from perfumes or deodorants into swimming pool (SP) water (Keuten et al. 2014, Keuten et al. 2012). In order to ensure microbial safety, a disinfectant residual is required, as which usually chlorine is used. However chlorine reacts with organic substances introduced by the bathers as well as with organic matter already present in the filling water. The products of these reactions are the so-called disinfection by-products (DBPs) which are potentially harmful substances including inorganic chloramines and numerous organohalogenated DBPs (Richardson et al. 2010, Zwiener et al. 2007). Richardson *et al.* (2010) identified more than a hundred DBPs in swimming pool waters. Among those the group of trihalomethanes (THM) is the one studied most intensively. Trichloromethane (TCM) is the most prevalent THM formed during chlorine disinfection, beyond dibromochloromethane, bromodichloromethane and tribromomethane. The brominated species are of importance when saltwater is used as pool water, otherwise they play a minor role.

THM concentrations are regulated worldwide for drinking water, (USEPA 2009, WHO 2011) and in many countries for SP water as well (DIN 19643 2012, Simard et al. 2013). However, considerably high THM concentrations are still found in SP waters (Li and Blatchley 2007, Weaver et al. 2009), resulting in health risks mainly due to inhalation and dermal uptake during swimming rather than to ingestion (Lindstrom et al. 1997). In order to minimize health risks, a proactive control of THM concentrations in pool waters is required. To do so, a better understanding of the kinetics of DBP formation in swimming pools is advantageous.

THM formation in swimming pool water is mainly attributed to: (i) the chlorine residual level kept in the pool water to guarantee the microbial safety, (ii) the continuous introduction of human body fluids by the bathers and (iii) the continuous introduction of natural organic matter (NOM) when some of the pool water is replaced with filling water which usually is drinking water (Kanan and Karanfil 2011).

The chemical composition of human body fluids introduced into swimming pools is represented by a so-called body fluid analogue (BFA), because it is not feasible to collect and preserve large amounts of human body fluids. In the literature, several mixtures of organic and inorganic compounds at typical ratios or concentrations were described (Borgmann-Strahsen 2003, Goeres et al. 2004, Judd and Bullock 2003). The NOM in filling water can be surrogated by humic acid (HA).

Individual BFA components and HA have very different characteristics, i.e. exhibit different reactivity towards chlorine. Efforts have been made to understand the mechanisms for chlorination of individual BFA components, such as urea (Blatchley and Cheng 2010, De Laat et al. 2011), uric acid (Lian et al. 2014) and some organic-nitrogen DBP precursors such as creatinine and L-histidine (Li and Blatchley 2007). However, comparably less attention was paid to the kinetics of the reactions of BFA components with chlorine in SP waters (Kanan 2010).

Regarding the models for predicting DBPs in swimming pools, not many models are available to date (Chowdhury et al. 2014), especially the kinetic models with regards to chlorine consumption and DBP formation in SP water are not available. Adversely, intensive models are available for the simulation of residual chlorine and THM concentrations in drinking water (Chowdhury et al. 2009, Fisher et al. 2011, Hua et al. 2015, Sadiq and Rodriguez 2004). Therefore, it was one of the objectives of this study to develop a model, by which the kinetics of chlorine consumption and THM formation with regard to SP water can be described.

Consequently, this study was composed of two steps. The first step was conducting chlorination experiments to qualitatively analyze the reactivity of pool water substances; the second step was to develop models to simulate and predict the chlorine consumption and THM formation under pool conditions. The detailed focuses were to: (i) determine the specific chlorine demand and specific THMFP of HA and each BFA component, (ii) evaluate the time-course contributions of individual components to the total chlorine consumption and THM formation, (iii) determine the reaction rate coefficients of chlorine consumption and TCM formation for HA and each BFA component, and (iv) simulate the kinetics of chlorine consumption and

THM formation of BFA and a mixture of BFA and HA (BFA+HA) based on the proposed kinetic models.

5.2 DEVELOPMENT OF KINETIC MODELS FOR CHLORINE CONSUMPTION AND THM FORMATION

5.2.1 Overall reaction rate coefficients for individual substances

As addressed above, there are many different substances in SP waters. Each specific substance may provide one or more reactive sites to react with chlorine. The reaction between chlorine and a single reactive site can be expressed as follows:

$$Cl + R_{i,Cl}^{S_j} \xrightarrow{k_{i,Cl}^{S_j}} \nu_i P_i$$

$$Cl + R_{i,TCM}^{S_j} \xrightarrow{k_{i,TCM}^{S_i}} \delta_i TCM_i$$

Equation 5-1

where *Cl* represents chlorine either in the form of dissolved chlorine (Cl_2, aq), hypochlorous acid (HOCl) or hypochlorite ions (OCl^-). $R_{i,Cl}^{S_j}$ and $R_{i,TCM}^{S_j}$ represent the reactive site *i* provided by the substance S_j with respect to chlorine consumption and TCM formation, respectively (*i* = 1, 2, … , *n; j = 1, 2, …, m*). P_i denotes a product. TCM_i denotes the TCM formation from the i^{th} reaction. ν_i and δ_i are the stoichiometric coefficients for the product P_i and TCM_i, respectively. As $R_{i,Cl}^{S_j}$ and $R_{i,TCM}^{S_j}$ represent a single reactive site, the stoichiometric coefficients are equal to one. $k_{i,Cl}^{S_j}$ is the rate constant of chlorine decay, and $k_{i,TCM}^{S_j}$ is the rate constant of TCM formation regarding the i^{th} reactive site provided by the substance S_j.

As a substance can comprise several reactive sites, an overall reaction rate coefficient $k_{ov,Cl}^{S_j}$ of chlorine decay is introduced (Hua et al. 2015, Jonkergouw et al. 2008). By analogy with chlorine decay, the overall reaction rate coefficient of TCM formation is defined as $k_{ov,TCM}^{S_j}$.

For a specific individual substance S_j, introducing the respective overall rate coefficients into second order models of chlorine decay (Clark and Sivaganesan

2002) and TCM formation (Gallard and von Gunten 2002), the following equations are obtained:

$$\frac{dc_{Cl}^{S_j}(t)}{dt} = -k_{ov,Cl}^{S_j}(t) \cdot c_{Cl}(t) \cdot c_{S_j,Cl}(t) \qquad \text{Equation 5-2}$$

$$\frac{dc_{TCM}^{S_j}(t)}{dt} = k_{ov,TCM}^{S_j} \cdot c_{Cl}(t) \cdot c_{S_j,TCM}(t) \qquad \text{Equation 5-3}$$

Herein $c_{Cl}(t)$ is the chlorine concentration at time t in mg/L. $c_{Sj,Cl}(t)$ and $c_{Sj,TCM}(t)$ are the concentrations of all reactive sites provided by substance S_j at time t towards chlorine consumption and TCM formation, respectively.

With respect to the overall reaction rate coefficient of chlorine, Hua et al. (2015) (**Chapter 2**) proposed to describe an overall rate coefficient according to:

$$k_{ov,Cl}^{S_j} = \alpha_{S_j} \cdot e^{-\beta_{S_j} \cdot \left[\frac{-\Delta c_{Cl}(t)}{\Delta c_{Cl,\max,S_j}}\right]} = \alpha_{S_j} \cdot e^{-\beta_{S_j} \cdot [X_{Cl}(t)]} \qquad \text{Equation 5-4}$$

where α_{Sj} and β_{Sj} are model parameters, which should be positive. The unit of α is L/mg/h. β is dimensionless. $\Delta c_{Cl}(t)$ is the consumed chlorine at time t, mg/L, which is negative. $\Delta c_{Cl,max,Sj}$ is the maximum chlorine consumption of the substance S_j (mg/L), i.e. the maximum chlorine demand. More detailed derivation process and discussion can be found in Hua et al. (2015) (**Chapter 2**). $X_{Cl}(t)$ is the fractional conversion ranging from 0 to 1, which indicates the reaction progress of chlorine consumption. When $X = 0$, α_{Sj} indicates the initial rate coefficient at the beginning of reaction ($t = 0$).

Similar to chlorine decay, it is hypothesized that the overall rate coefficient of TCM formation $k_{ov,TCM}^{S_j}$ can also be expressed as follows. More detailed derivation process and discussion can be found in **Chapter 3**:

$$k_{ov,TCM}^{S_j}(t) = \varphi_{S_j} \cdot e^{-\chi_{S_j} \cdot \left[\frac{\Delta c_{TCM}(t)}{\Delta c_{TCMFP,S_j}}\right]} = \varphi_{S_j} \cdot e^{-\chi_{S_j} \cdot [X_{TCM}(t)]} \qquad \text{Equation 5-5}$$

where φ_{Sj} and χ_{Sj} are model parameters, which should be positive. The unit of φ is L/μmol/h. χ is dimensionless. $X_{TCM}(t)$ is the fractional conversion ranging from 0 to 1, which indicates the TCM formation progress. $\Delta c_{TCM}(t)$ is the TCM concentration formed at time t (μM). $\Delta c_{TCMFP,Sj}$ is TCMFP for the j^{th} substance (S_j ,μM).

Based on the principle of mass conservation as well as the assumption that the stoichiometric coefficients for chlorine and reactive sites are equal to one. The following relationships are established:

$$c_{Cl}(t) = c_{Cl}(0) + \Delta c_{Cl}(t)$$

$$c_{S_{j,Cl}}(t) = c_{S_{j,Cl}}(0) + \Delta c_{Cl}(t)$$

Equation 5-6

$$c_{S_{j,TCM}}(t) = c_{S_{j,TCM}}(0) - \Delta c_{TCM}(t)$$

Equation 5-7

where $c_{Sj,Cl}(0)$ is the initial concentration of chlorine-reactive sites provided by S_j at time $t = 0$. $c_{Cl}(0)$ is the ICC. In this study, the $c_{Sj,Cl}(0)$ was surrogated by the chlorine demand of $\Delta c_{Cl,max,Sj}$. $c_{Sj,TCM}(0)$ was represented by the TCMFP of $\Delta c_{TCMFP,Sj}$, i.e. $c_{Sj,Cl}(0) = \Delta c_{Cl,max,Sj}$ and $c_{Sj,TCM}(0) = \Delta c_{TCMFP,Sj}$.

Substituting **Eq. 5-4** and **5-6** to **Eq. 5-2**, **Eq. 5-5** and **5-7** to **Eq. 5-3**, yields:

$$\frac{dc_{Cl}^{S_j}(t)}{dt} = -\alpha_{S_j} \cdot e^{-\beta_{S_j} \cdot [X_{Cl}(t)]} \cdot c_{Cl} \cdot \left[\Delta c_{Cl,\max,S_j} + \Delta c_{Cl}(t)\right]$$

Equation 5-8

$$\frac{dc_{TCM}^{S_j}(t)}{dt} = \varphi_{S_j} \cdot e^{-\chi_{S_j} \cdot [X_{TCM}(t)]} \cdot c_{Cl}(t) \cdot \left[\Delta c_{TCMFP,S_j}(t) - \Delta c_{TCM}(t)\right]$$

Equation 5-9

Eq. 5-8 and **5-9** are related to the specific and single substance S_j. By fitting **Eq. 5-8** and **5-9** to the experiment datasets, the model parameters for individual substance S_j can be obtained.

5.2.2 Determination of reaction rate coefficients for mixtures

In this study, we surrogated substances introduce to the pool water by the swimmers with a body fluid analogue as described in more detail below. The organic matter introduced to the pool by the filling water was surrogated with humic acid (HA). The BFA included six organic components and ammonium chloride. Based on **Eq. 5-2 and 5-3**, summing up the concentrations of all individual substances, the chlorine decay and TCM formation of mixtures, i.e. $\sum_7$BFA and BFA+HA, can be expressed as follows:

$$\frac{\sum_{j=1}^{m} dc_{Cl}^{S_j}(t)}{dt} = \frac{dc_{Cl}(t)}{dt} = -\sum_{j=1}^{m} k_{ov,Cl}^{S_j} \cdot c_{Cl}(t) \cdot c_{S_j,Cl}(t) \qquad \text{Equation 5-10}$$

$$\frac{\sum_{j=1}^{m} dc_{TCM}^{S_j}(t)}{dt} = \frac{dc_{TCM}(t)}{dt} = \sum_{j=1}^{m} k_{ov,TCM}^{S_j} \cdot c_{Cl}(t) \cdot c_{S_j,TCM}(t) \qquad \text{Equation 5-11}$$

where m= 7 or m= 8, depending on either a mixture of the seven BFA components or of BFA+HA is considered.

Considering a second order model for the mixtures, the rates of chlorine decay and TCM formation can be expressed as follows:

$$\frac{dc_{Cl}(t)}{dt} = -k_{mix,Cl}(t) \cdot c_{Cl}(t) \cdot c_{mix,Cl}(t) \qquad \text{Equation 5-12}$$

$$\frac{dc_{TCM}(t)}{dt} = k_{mix,TCM}(t) \cdot c_{Cl}(t) \cdot c_{mix,TCM}(t) \qquad \text{Equation 5-13}$$

where $c_{mix,Cl}(t)$ and $c_{mix,TCM}(t)$ are the total reactive sties provided by the mixtures towards chlorine consumption and TCM formation, respectively. $k_{mix,Cl}$ and $k_{mix,TCM}$ are the overall rate coefficients of chlorine decay and TCM formation for mixtures, respectively.

Combining **Eq. 5-10** and **5-12**, the reaction rate coefficient of chlorine decay for substance mixture is expressed as follows:

$$k_{mix,Cl}(t) = \frac{\sum_{j=1}^{m}\left[k_{ov,Cl}^{S_j} \cdot c_{S_{j,Cl}}(t)\right]}{c_{mix,Cl}(t)}$$ Equation 5-14

Principally, the **Eq. 5-14** has the identical form as **Eq. 2-17** when all the substances completely mixed with V:V =1:1. Similarly, combining **Eq. 5-11** and **5-13**, the reaction rate coefficient of TCM formation for substance mixtures is expressed as follows:

$$k_{mix,TCM}(t) = \frac{\sum_{j=1}^{m}\left[k_{ov,TCM}^{S_j} \cdot c_{S_{j,TCM}}(t)\right]}{c_{mix,TCM}(t)}$$ Equation 5-15

It can be seen from **Eq. 5-14** and **5-15** that the rate coefficients for mixtures ($k_{mix,Cl}$ or $k_{mix,TCM}$) were related to the reactivity of individual substances and the concentration of residual reactive sites at time *t*. For the real pool waters, which are an aqueous with different substances, it is assumed that the individual substance reacts independently in the mixtures. When $k_{ov,Cl}^{S_j}$ and $k_{ov,TCM}^{S_j}$ were determined for the individual substance S_j according to **Eq. 5-8** and **5-9**, the rate coefficients for mixtures can be calculated based on **Eq. 5-12** and **5-13**. Then, it is able to simulate the kinetics of chlorine decay and TCM formation for the substance mixtures by using the following equations:

$$\frac{dc_{Cl}(t)}{dt} = -k_{mix,Cl}(t) \cdot c_{Cl}(t) \cdot \left[\Delta c_{Cl,\max} + \Delta c_{Cl}(t)\right]$$ Equation 5-16

$$\frac{dc_{TCM}(t)}{dt} = k_{mix,TCM}(t) \cdot c_{Cl}(t) \cdot \left[\Delta c_{THMFP} - \Delta c_{TCM}(t)\right]$$ Equation 5-17

where $\Delta c_{Cl,max}$ and Δc_{THMFP} are the total chlorine demand and TCMFP of mixtures.

5.3 MATERIALS AND METHODS

5.3.1 Preparation of the BFA solution

All solutions were prepared with ultrapure water (18.2 MΩcm at 25°C, Direct-Q system, Merck Millipore). The constituents of body fluids introduced into pools by

swimmers were surrogated according to the recipe given by Judd and Bullock (2003), which is composed of six organic and an inorganic components (referred to as $\sum_7$BFA in this study). The used BFA components and their grade of purity are given in **Table 5-1**. The percentages of carbon and nitrogen in the BFA solution originating from the individual BFA constituents are also given in **Table 5-1**.

Stock solutions of the individual organic BFA constituents as well as of the BFA organic substances mixture were prepared at pH = 12. The ammonium chloride stock solution was prepared separately at pH = 2. pH was adjusted by using H_2SO_4 (1 mol/L) and NaOH (2 mol/L) The $\sum_7$BFA solution at target concentration was prepared by mixing the stock solution of BFA organic substances with the stock solution of ammonium chloride at vol:vol 1:1. Specifically, preparing a BFA organic solution and a ammonium chloride solution with a concentration that two times higher than target concentration at pH = 12 and pH = 2, respectively.

Table 5-1. Carbon and nitrogen concentrations of individual BFA components, and their corresponding contribution percentages to $\sum_7$BFA.

BFA components	Concentration	Carbon	Carbon percentages contribution	Nitrogen	Nitrogen percentages contribution	Supplier and Grade
	mg/L	mg/L	%	mg/L	%	
Urea	14800	2960	51.48	6900	85.17	Merck Millipore, GR
L-histidine	1210	560	9.74	320	3.95	Alfa Aesar, 98%
Hippuric acid	1710	1040	18.09	134	1.65	Alfa Aesar, 98%
Uric acid	490	180	3.13	160	1.98	Alfa Aesar, 99%
Citric acid	640	240	4.17	-	-	Alfa Aesar, 99%
Creatinine	1800	770	13.39	67	0.83	Alfa Aesar, 98%
Ammonium Chloride	2000	-	-	520	6.42	Merck Millipore, GR
$\sum_7$BFA	-	5750	100	8101	100	-

Note: The theoretical values of concentration, carbon and nitrogen are those from Judd and Bullock (2003).

5.3.2 Surrogates for swimming pool water

As a surrogate for NOM in filling water, commercial humic acid (HA) sodium salt (Sigma-Aldrich, US) was used (Kanan and Karanfil 2011). The HA stock solution at a concentration of 28 mg/L was prepared by dissolving the HA sodium salt in ultrapure water, under stirring at room temperature for 3 h and then filtering the solution through a 0.45-µm polycarbonate filter (Nuclepore Track-Etch Membrane, Whatman, Germany) to remove suspended solids.

In preliminary analysis of swimming pool water from 6 swimming pools located in the city of Dresden, Germany, by size-exclusion chromatography-organic carbon detection (LC-OCD) (Huber et al. 2011), it was found that the HA fraction accounted for 20-30% of the total organic carbon (TOC). De Laat et al. (2011) reported that 4 mg *C*/L falls in the TOC range of SP water. Consequently, the surrogate for SP water was composed such that the TOC consisted of 3 mg/L originating from BFA and 1 mg/L was contributed by HA. In other words, the selected ratio of $\sum_7$BFA:HA was 3:1 in this study by assuming the real pool waters were composed of body fluids and NOM in filling water.

The mixture of BFA and HA to surrogate the composition of SP water, which is referred to as (BFA+HA) in this study, was prepared by mixing the respective BFA and HA stock solutions and diluting it to the target TOC concentration.

5.3.3 Experimental procedures

5.3.3.1 Chlorine demand and THMFP tests

For chlorination experiments, a chlorine stock solution at a concentration of 15.5 mM was prepared with ultrapure water by diluting the commercial sodium hypochlorite solution (14% active chlorine, VWR). Until use, the solution was stored in the refrigerator at 4°C.

Preliminary experiments were conducted to determine the total chlorine demand and THMFP of all substances, including BFA organic components, $\sum_7$BFA and HA. The TOC of each BFA components were 2 mg *C*/L, which prepared independently by diluting their respective stock solution. The TOC of $\sum_7$BFA was set to be 3 mg *C*/L by diluting the $\sum_7$BFA stock solution. HA solution had a TOC of 1 mg *C*/L. The BFA+HA had a TOC of 4 mg *C*/L, of which 3 mg *C*/L was contributed by $\sum_7$BFA and 1 mg *C*/L was contributed by HA.

The TOC of each BFA component used for chlorine demand and TCMFP was 2 mg/L. Chlorine demand tests were conducted based on a Standard Method 2350 B (APHA 2005a). For THMFP test, the chlorine stock solution was spiked to each sample at the same initial chlorine concentration (ICC) of 50 mg/L to provide chlorine concentration in excess for 168 h. All chlorinated samples were incubated in head-space free amber glass bottles at 28°C. According to the typical swimming pool operation condition, pH was fixed at 7.2±0.1 by the addition of phosphate buffer.

5.3.3.2 Kinetics experiments

As shown in **Table 5-2**, two different experiment series were conducted. The experiment series *I* was performed to investigate the time-course contribution of individual components to the total chlorine consumption and total THM formation. The designed theoretical values of TOC, nitrogen, solution concentrations of BFA components, $\sum_7$BFA, HA and BFA+HA are also shown in **Table 5-2**.

Table 5-2. Experimental design.

Substance	Experiment series *I*			Experiment series *II*		
	TOC	Total Nitrogen	Solution concentration	TOC	Total Nitrogen	Solution concentration
	mg/L	mg/L	µmol/L	mg/L	mg/L	µmol/L
Urea	1.54	3.59	128.20	2.00	4.66	166.68
L-histidine	0.29	0.17	4.03	2.00	1.17	27.78
Hippuric acid	0.54	0.07	5.00	2.00	0.26	18.52
Uric acid	0.09	0.08	1.50	2.00	1.87	33.33
Citric acid	0.13	NA	1.80	2.00	NA	27.78
Creatinine	0.40	0.35	8.33	2.00	0.74	41.67
Ammonium Chloride	NA	0.27	19.41	NA	0.27	19.41
$\sum_7$BFA	3.00	NM	NM	NC	NC	NC
HA	1.00	NM	NM	NC	NC	NC
BFA+HA	4.00	NM	NM	NC	NC	NC

Note: NA indicates no contribution; NM indicates not measured; NC indicates not conducted.

Similar to the chlorine demand and THMFP tests, the TOC of $\sum_7$BFA was 3 mg *C*/L. Then, the concentrations of individual BFA components were calculated based on the defined carbon contribution ratio as shown in **Table 5-1**. In other words, the TOC concentration of $\sum_7$BFA is a summation of individual BFA components.

Experiment series *II* was conducted to determine the reaction rate coefficients of individual BFA components and HA. Batch tests were conducted for the chlorination of each BFA component with an identical TOC of 2 mg *C*/L. To make sure the chlorine concentration is not a limitation for reaction, i.e. enough free chlorine remains in the water sample after a maximum reaction time of 168 h. An ICC of 50 mg Cl_2/L was chosen for both Experiment series *I* and *II*. pH was fixed at 7.2±0.1. Temperature was kept constant at 28°C.

5.3.4 Analytical methods

TOC concentration was determined by the catalytic combustion method using a LiquiTOC II organic carbon analyzer (Elementar Analysensystem GmbH, Germany). All the samples were measured by LiquiTOC II before chlorination. Free chlorine concentration was determined according to the N, N-diethyl-p-Phenylenediamine (DPD) Standard Colorimetric Method 4500-Cl G (APHA 2005b). pH was measured by a pH meter 340i (Wissenschaftlich-Technische-Werkstätten, Germany). THM concentrations were determined by membrane inlet mass spectrometry (MIMS) 2000 (Mikrolab Aarhus, Denmark), which comprising a Prisma QME 220 PT mass spectrometer (Pfeiffer Vacuum, Germany) equipped with electron ionization. THM standards were purchased from Sigma-Aldrich. Before measurement, THM without purification were diluted with ultrapure water to the target solution concentrations and measured for the MIMS calibration. Water samples were firstly analysed in mass spectrum scan mode (49-m/z-215). Then the THM concentration was quantified with a selected ion monitoring. As all the synthesized samples were prepared with ultrapure water, which does not contain bromide, of all THM species only TCM was detected. Ions at m/z 83 were chosen to quantify TCM with a quantification limit of 2.5 µg/L. More detailed operation conditions for MIMS can be found elsewhere (Shang and Blatchley 1999, Yang et al. 2012).

5.3.5 Model calibration and statistical analysis

Data obtained from Experiment series *II* were used to determine the best-fit parameters of α_{Sj} and β_{Sj} (towards chlorine decay) as well as φ_{Sj} and χ_{Sj} (towards TCM formation) for each individual substance (S_j). Specifically, Excel Solver, which based on the generalized reduced gradient algorithm, was employed to solve **Eq. 5-8** and **5-9**. They were calculated numerically with a time interval of 0.5 h by minimizing the differences (sum of the squared errors) between the experimentally-determined chlorine or TCM concentrations and simulations at corresponding times. Once the best-fit parameters were determined, the rate coefficients for mixtures can be calculated following **Eq. 5-14** and **15**. Furthermore, the kinetics of chlorine decay and

TCM formation with respect to mixtures were predicted according to **Eq. 5-16** and **5-17** with a time interval of 0.5 h.

The accuracy of model simulation was evaluated by the coefficient of determination (R^2) and the root-mean-square error (RMSE), as these methods are often used as measures of difference between the predicted data and those obtained experimentally (Piñeiro et al. 2008). R^2 shows the unexplained variance of model. While RMSE evaluates the prediction capability of the model, with a smaller RMSE value indicating a greater predictive capability. The obtained RMSE is also expected to be of similar magnitude to the measurement error which indicates a reasonable fit.

5.4 RESULTS AND DISCUSSION

5.4.1 Chlorine consumption

5.4.1.1 Specific chlorine demand

The reactivity of the investigated substances towards chlorine consumption was firstly evaluated by conducting chlorine demand test. Experiment datasets were interpreted in the forms of the solution concentration-related and TOC-related specific chlorine demands. The solution concentration-related specific chlorine demand was calculated as the chlorine demand of the individual substances, also known as the maximum chlorine consumption, divided by corresponding solution concentrations (mol Cl_2/mol substance). The TOC-related specific chlorine demand was calculated as the chlorine demand of individual substances divided by their TOC concentrations (mg Cl_2/mg C).

Fig. 5-1(a) shows the concentration-related specific chlorine demand. The horizontal axis shows the ratios of ICC to the initial solution concentration of individual BFA components, which were referred to as the specific chlorine doses (ICC/solution concentration, mol Cl_2/mol BFA component). It can be seen that the solution concentration-related specific chlorine demand reached a plateau at the specific chlorine doses above 20 mol Cl_2/mol BFA. The highest specific chlorine demand was observed for L-histidine, which almost reached at 14 mol Cl_2/mol histidine, followed

by uric acid with 10.5 mol Cl_2/mol uric acid and creatinine with 7.5 mol Cl_2/mol creatinine. The results were consistent with an assumption reported by Hong et al. (2009) that chlorine demand was related to the structure of the compounds, i.e. the more electro-donating functional groups (-NH_2 and -OH) and double bonds in the structure, the more chlorine demand. Specifically, as shown in **Fig. 5-1(a)**, L-histidine and creatinine, which contain aromatic ring and functional group of -NH_2, showed higher specific chlorine demand than hippuric acid which has no functional groups on its ring. Hippuric acid had the lowest demand compared with other BFA components. The demand of urea was 3.3 mol Cl_2/mol urea, which fall into the theoretical chlorine demand that ranges between 3 and 8 mol Cl_2/ mol of urea (De Laat et al. 2011).

Fig. 5-1(b) presents the TOC-related specific chlorine demand. The specific chlorine dose shown in horizontal axis was calculated as ICC divided by the initial TOC of individual BFA components (ICC/TOC, mg Cl_2/mg *C*). The TOC-related specific chlorine demand increased with an increasing specific chlorine dose and reached a plateau at specific chlorine doses above 20 mg Cl_2/mg *C*. Urea exhibited the highest demand of 19.5 mg Cl_2/mg *C*, followed by L-histidine with 13.5 mg Cl_2/mg *C* and uric acid with 12.0 mg Cl_2/mg *C*. These three BFA components are organic-nitrogen compounds, which could reasonably explain the higher TOC-related specific chlorine demand. As urea exhibited the highest demand, it confirmed that the importance of informing swimmers not to urinate in the pools.

Data shown in **Fig. 5-1(c)** are TOC-related specific chlorine demands of $\sum_7$BFA and HA. As for $\sum_7$BFA, it reached the highest plateau level of 14 mg Cl_2/ mg C.

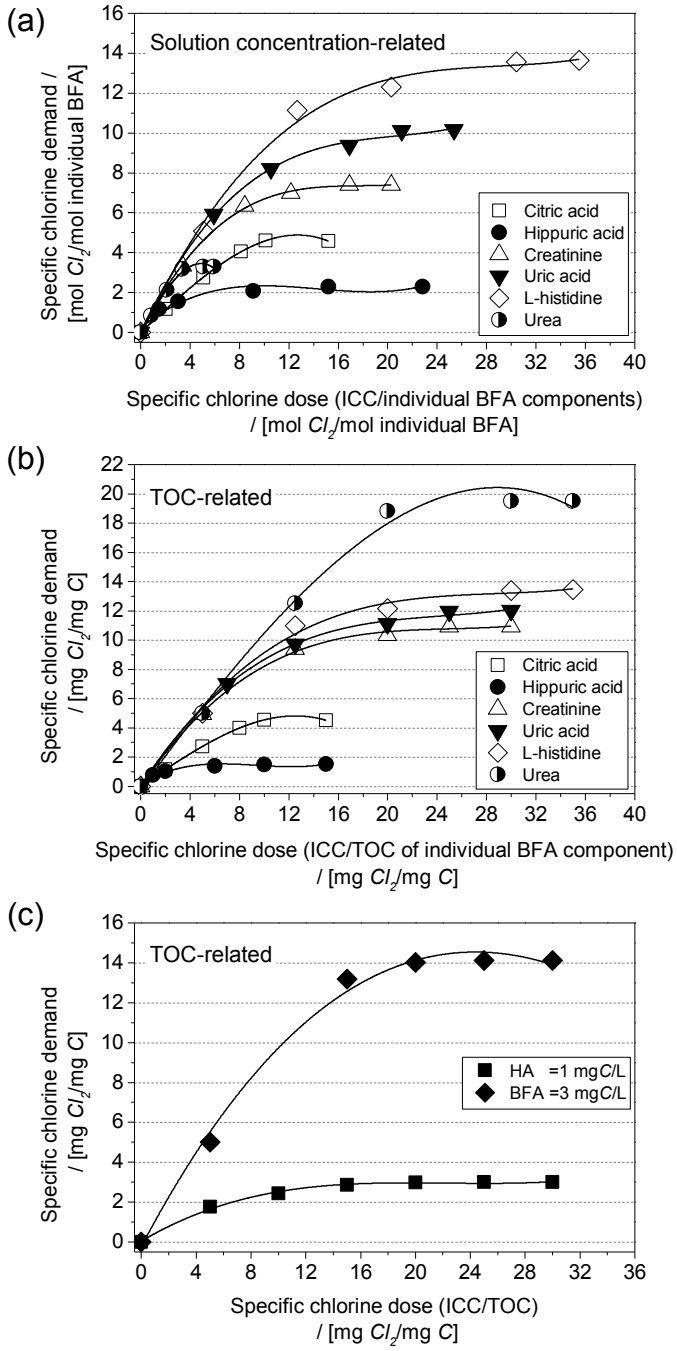

Figure 5-1. (a) Solution concentration-related, (b) TOC-related specific chlorine demand of organic BFA components, and (c) TOC-related specific chlorine demands of $\sum_7$BFA and HA. Tests were performed with 168 h, pH = 7.2±0.1. Solid line represents the trend of polynomial approximation.

However, HA exhibited at 3 mg Cl_2/mg C, which was nearly five times lower than that of BFA. The result agrees with the conclusions reported in Kanan and Karanfil (2011) that BFA is more reactive towards chlorine consumption than HA.

5.4.1.2 Kinetic chlorine consumption of substances with individual TOC concentration

Based on the results of Experiment series *I* (**Table 5-2**), **Fig. 5-2** shows the kinetic chlorine consumptions of seven BFA components and HA with their respective TOC concentration. It can be seen that the chlorine consumption of urea was significantly higher than it of other substances over the whole reaction period. This is due to a fact that urea accounted for the highest percentage of total TOC of $\sum_7$BFA (**Tabel 5-1**) and also showed the highest TOC-related specific chlorine demand. Conversely, hippuric acid showed the very low chlorine consumption, although it had the second highest TOC concentration. The result agrees with the findings presented in **Fig. 5-1** that hippuric acid exhibited the lowest TOC-related specific chlorine demand.

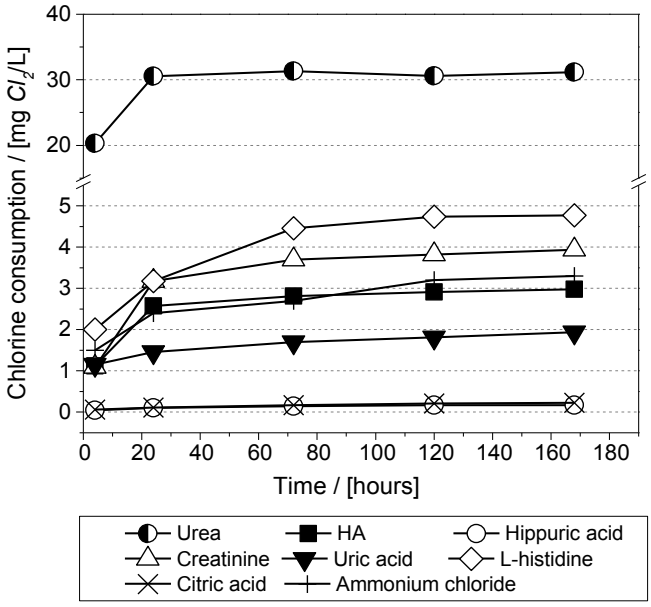

Figure 5-2. Time-course chlorine consumption of individual BFA components with their respective initial TOC (Table 5-1, Experiment series I), HA (TOC = 1 mg *C*/L).

From kinetics stand point of view, the chlorine consumption of urea reached a plateau at 24 h whereas the consumption of L-histidine increased with increasing reaction time and reached a plateau at 120 h. The results indicate that individual substances show different reactivity with chlorine and therefore play different role in the kinetic chlorine consumption of mixture. For more clear illustration, a so called time-course contribution percentages were calculated, i.e. the chlorine consumption

of individual substances divided by the summation of all substance consumption (total consumption) at the corresponding time. The results are shown in **Fig. 5-3**.

As shown, urea contributed 78.9% to the total consumption at 4 h, while 70.4% at 168 h. Uric acid also showed decreasing percentages, i.e. from 4.5% at 4 h to 4.3% at 168 h. The decreasing percentages might indicate that urea and uric acid are responsible for the total chlorine consumption at the early phase of reaction. Conversely, the total chlorine consumption contributed by creatinine, HA and L-histidine were slightly increased until 72 h and kept fairly stable to 168 h, which indicates that they are responsible for the total chlorine consumption at the later reaction phase. Therefore, the reactivity of chlorine with creatinine, HA and L-histidine might be slower than it with urea. These hypotheses will be further discussed in the section 5.4.1.3 by deriving the reaction rate coefficient for each substance.

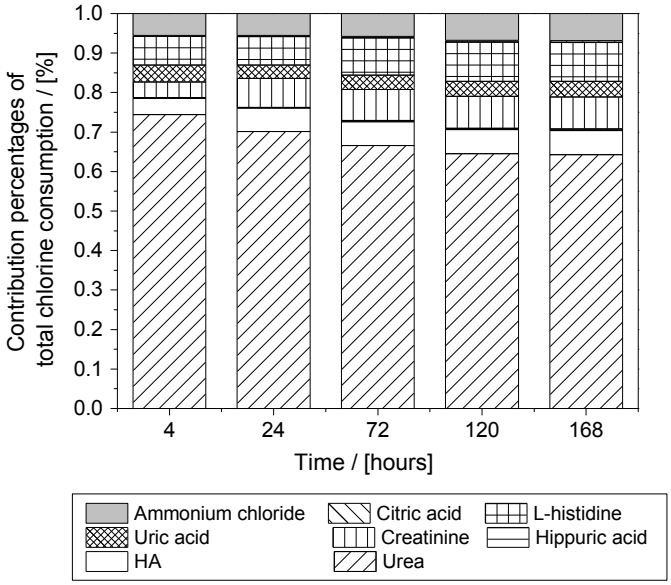

Figure 5-3. Time-course contribution percentages of individual substances to the chlorine consumption of BFA+HA.

5.4.1.3 Derivation of rate coefficient for individual substances

To determine the reaction rate coefficient of chlorine decay for each substance, the proposed model (**Eq. 5-8**) was applied individually to the decay dataset obtained from Experiment series *II*.

Table 5-3. Best-fit model parameters α and β, overall reaction rate coefficient of chlorine decay, chlorine demand, and corresponding R^2 and RMSE with respect to individual substances and substance mixture.

Substance (S_j)	α_{Sj}	β_{Sj}	$k_{ov,Cl}^{S_j}$	$\Delta c_{Cl,max,Sj}$	R^2	RMSE
	L/mg/h		L/mg/h	mg/L		mg/L
Uric acid	2.81E-2	3.85	2.81E-2 – 6.06E-4	24.05	0.998	0.092
Urea	6.73E-3	0.14	6.73E-3 – 5.85E-3	38.68	0.996	0.329
L-histidine	4.22E-3	0.32	4.22E-3 – 3.07E-3	26.91	0.999	0.095
Creatinine	2.85E-3	0.59	2.85E-3 – 1.58E-3	21.85	0.990	0.519
Humic acid	2.81E-3	0.97	2.81E-3 – 1.07E-3	2.97	0.991	0.064
Hippuric acid	1.39E-3	2.30	1.39E-3 – 1.58E-4	3.02	0.996	0.053
Citric acid	3.69E-4	0.49	3.69E-4 – 3.38E-4	9.02	0.993	0.261
Ammonium chloride	7.10E-3	3.67	7.10E-3 – 1.94E-4	3.30	0.964	0.123
Substance mixture	α	β	$k_{mix,Cl}$	$\Delta c_{Cl,max}$	R^2	RMSE
	L/mg/h		L/mg/h	mg/L		mg/L
$\sum_7$BFA	-	-	7.01E-3 – 1.97E-4	42.32	0.994	1.122
BFA+HA	-	-	6.71E-3 – 2.06E-4	47.80	0.994	1.155

Note: the range of $k_{ov,Cl}^{S_j}$ and $k_{mix,Cl}$ indicates the changes of rate coefficient from t = 0 h to 240 h; α and β for substance mixture are not needed; TOC of individual substance were 2 mg *C*/L; TOC of BFA was 3 mg *C*/L while it of BFA+HA was 4 mg *C*/L.

The chlorine demand $c_{Cl,max,Sj}$ of S_j, required by **Eq. 5-8** was calculated as the TOC concentration of S_j (TOC = 2 mg/L, Experiment series *II*) multiply the corresponding specific chlorine demand that shown in **Fig. 5-1(b)**. By conducting the curve fitting, the best-fit parameters of α_{Sj} and β_{Sj} for each substance S_j were obtained. The

variable reaction rate coefficient $k_{ov,Cl}^{S_j}$ of chlorine with respect to S_j was calculated following

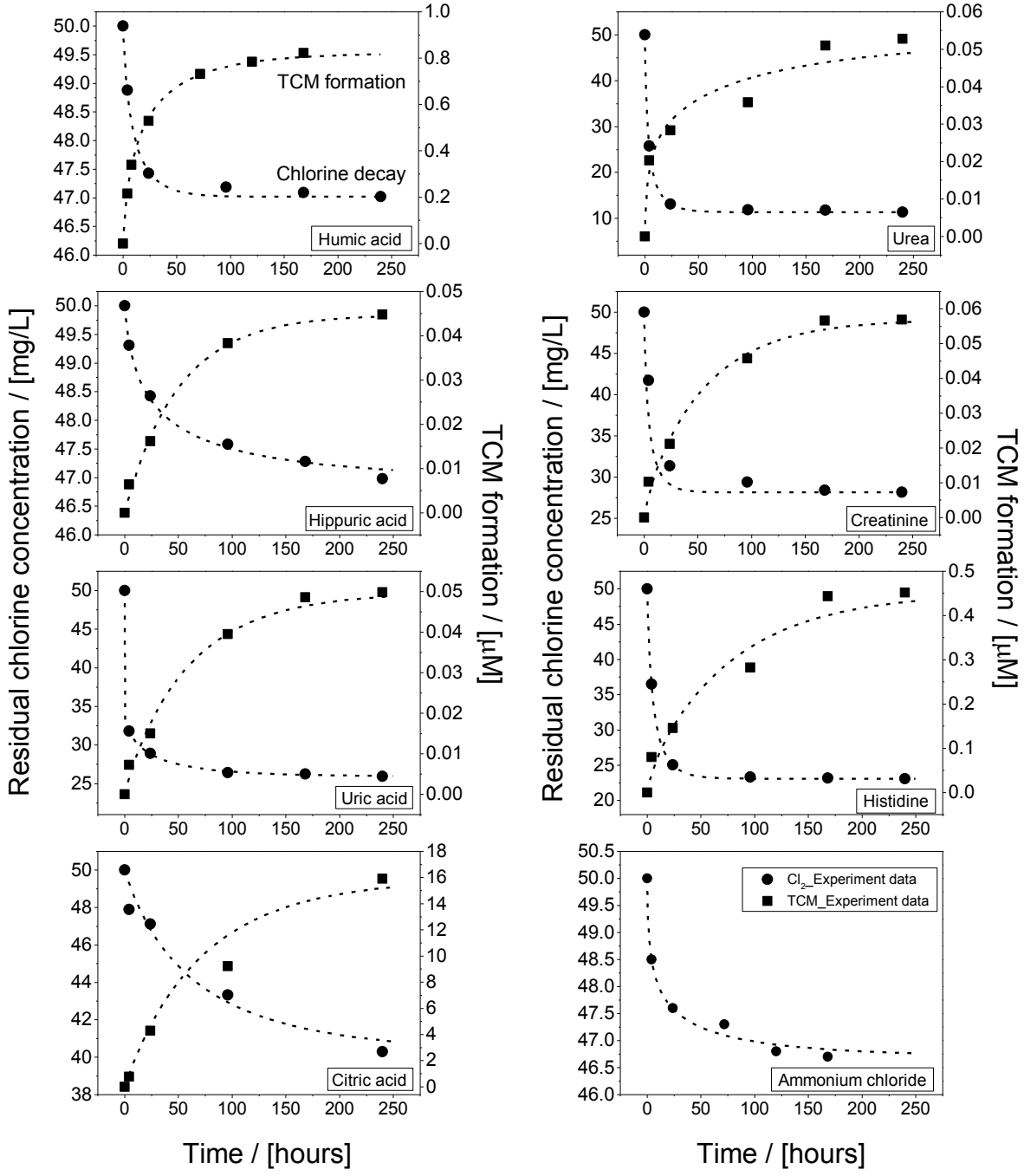

Figure 5-4. Curve fitting for individual BFA components and HA with respect to chlorine decay and TCM formation.

Eq. 5-4. The values of best-fit parameters α_{Sj} and β_{Sj}, chlorine demand $c_{Cl,max,Sj}(0)$ and rate coefficient $k_{ov,Cl}^{S_j}$ for individual substances are shown in **Table 5-3**.

As shown in **Table 5-3**, α_{Sj} was equal to initial $k_{ov,Cl}^{S_j}(0)$, indicating α reflects the initial rate coefficient at $X(t) = 0$. Uric acid exhibited the highest $\alpha_{uric\ acid}$, which is consistent with the conclusions in literature that uric acid appeared to consume free chlorine faster than the most other organic-N precursors (Li and Blatchley 2007, Lian et al. 2014). Ammonium chloride and urea showed the second and third highest value of α_{Sj}, which were an order of magnitude lower than $\alpha_{uric\ acid}$. Moreover, the calculated α_{urea} confirmed the assumption derived from the results of Experiment series *I*, i.e. the reactivity of chlorine with urea may faster than them of creatinine, HA and L-histidine. α values of hippuric acid and citric acid showed the lowest reactivity towards chlorine consumption compared with the other BFA components.

Fig. 5-4 shows the measured datasets and curve fitting results for all substances. Except for few data points, the chlorine decay of substances was reasonably described by the curve. **Table 5-3** also summarized the model evaluation results. R^2 ranges from 0.96 to 0.99 and RMSE were observed from 0.1 to 0.5 mg/L, indicating the model successfully simulated the experimental datasets.

5.4.1.4 Prediction of chlorine for mixture

As model parameters α_{Sj} and β_{Sj} for individual substance S_j were determined, the reaction rate coefficients for mixture ($k_{mix,Cl}$) can be calculated according to **Eq. 5-14**. Following that, the kinetic of chlorine decay with respect to the mixtures of $\sum_7$BFA and BFA+HA can be predicted by applying **Eq. 5-16.** However, the chlorine consumption is a more interesting factor than the residual chlorine concentration in pool waters as the latter should be kept constant to ensure the microbial safety. Therefore, the time-course chlorine consumption was calculated as ICC of 50 mg/L minus the residual chlorine concentration at the corresponding time, which is shown in **Fig. 5-5**. It can be seen that the chlorine consumption profiles of both $\sum_7$BFA and BFA+HA follow the same pattern, which is characterized by an initial fast consumption stage and a later slower formation stage. As the chlorine-reactive

substances from swimmer are continuously introduced into the pool waters, it is therefore required to chlorination continuously to ensure the microbial safety. Based on kinetics results, it illustrates that effective hygiene practices by swimmers, such as pre-swim shower, is important to reduce the chlorine doses, and also helpful to decrease the THM formation.

Fig.5-5 also shows the predicting results of chlorine consumptions for $\sum_7$BFA and BFA+HA as a function of time. Graphically, the model results showed a good simulation. Quantitatively, the values of R^2 for the model accuracy evaluation was 0.99, i.e. 1% of variance is unexplained. RMSE was 1.12 for BFA while 1.16 for BFA+HA. These results prove that the model provides a very good prediction of experimental data.

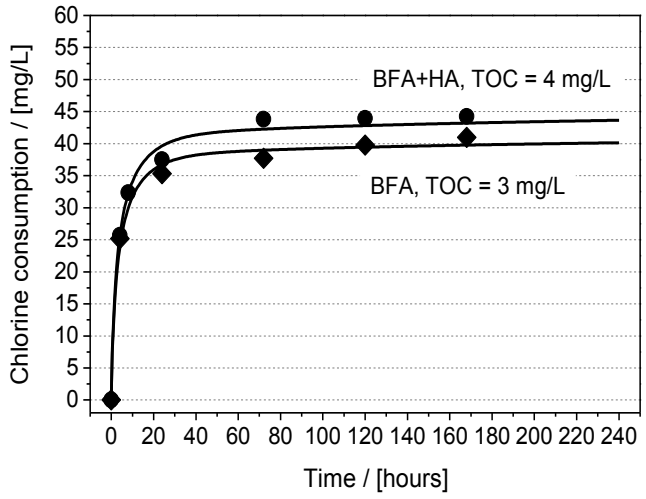

Figure 5-5. Chlorine consumption experiment and model simulation results for $\sum_7$BFA and BFA+HA.

5.4.2 Trichloromethane formation

5.4.2.1 Specific trichloromethane formation potential

As all the synthesized samples were prepared with ultrapure water, which does not contain bromide, of all THM species only TCM was detected. The specific TCMFP were calculated as TCMFP divided by the corresponding TOC concentration (μmol TCM/mg *C*). It was found that citric acid exhibited considerably higher specific

TCMFP at 10.6 µmol/mg *C* than all the other individual BFA components despite its low chlorine consumption (**Fig. 5-1**). Followed by citric acid, HA shows the second highest values of specific TCMFP at 0.82 µmol/mg *C* which was about 2.5 times higher than that of BFA at 0.45 µmol/mg *C*. It indicates that HA results in more TCM formation than BFA. Therefore, controlling the organic precursor in filling water is helpful to decrease TCM formation in pool waters.

5.4.2.2 Kinetic TCM formation of substances with individual TOC concentration

Based on the results of Experiment series *I* (**Table 5-2**), **Fig. 5-6** presents the TCM formation as a function of time with regards to organic BFA components and HA with their different TOC concentration.

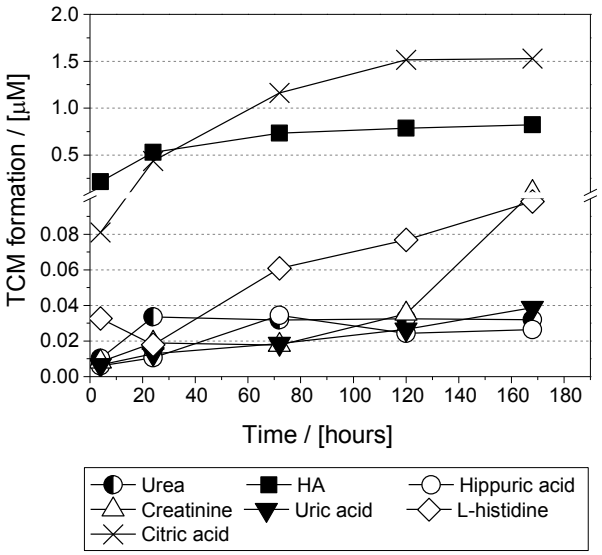

Figure 5-6. Time-course TCM formation of individual BFA components with their respective TOC (Experiment series *I*), HA (TOC = 1 mg C/L).

It can be seen from **Fig. 5-6** that citric acid showed the highest TCM formation followed by HA, which consists with the observation of TCMFP test. Moreover, the TCM formation of citric acid increased until 120°h, whereas it of HA reached a plateau at 24 h. The results indicate the substances exhibited different reactivity towards TCM formation, and therefore may contribute differently to the TCM formation of mixture. Similar as the interpretation of chlorine consumption results,

the time-course contribution percentage of TCM formation were calculated. They were calculated as the TCM concentration of individual substances to the summation of all substance TCM formation (total TCM) at corresponding time. The results are shown in **Fig. 5-7(a)**.

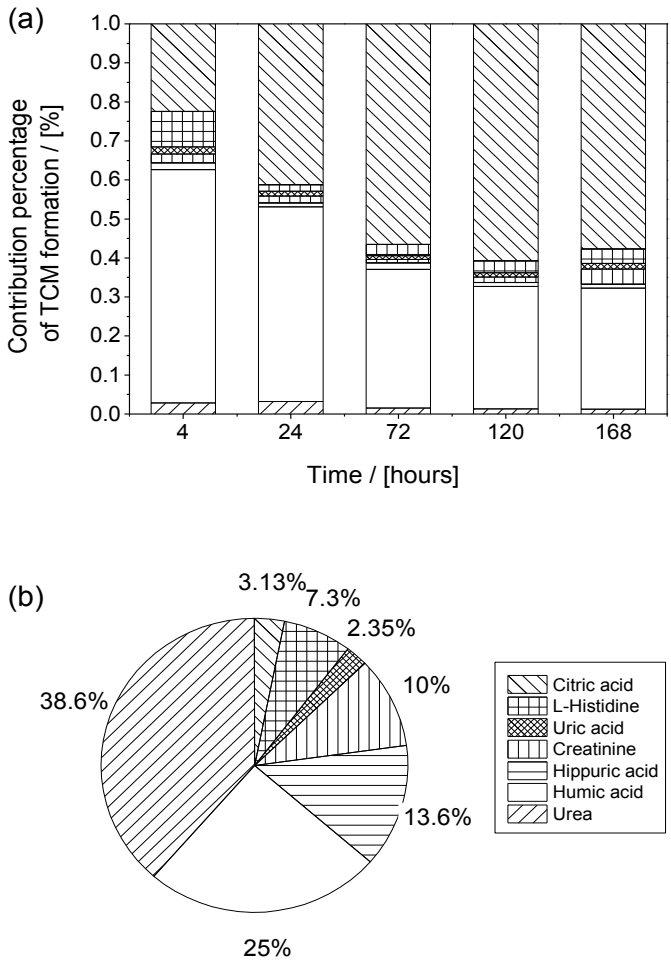

Figure 5-7. (a) Time-course contribution percentages of individual substances to the total TCM formation, and (b) the TOC percentage contributions of individual organic substances to total TOC of 4 mg C/L.

As shown in **Fig. 5-7(a)**, although citric acid contributed the lowest to the chlorine consumption, over 50% of the total TCM was formed due to the presence of citric acid. Approximately 90% of the total TCM formations were attributed to the presence of citric acid and HA. However, the time-course contribution of HA and citric acid to the total TCM formation showed adverse trend. Specifically, the contribution percentage with regard to HA decreased, while it with regards to citric

acid increased with increasing reaction time. It suggests that HA might responsible for the total TCM formation at the early phase of reaction. This hypothesis will be further confirmed by deriving their corresponding reaction rate coefficients, which means the initial reaction rate coefficient of HA is higher than citric acid. **Fig. 5-7(b)** shows the TOC contributions of organic BFA components and HA to the total TOC. It concludes that urea, hippuric acid and creatinine were totally responsible for 64% of the total TOC of BFA+HA. However, less than 10% of TCM formation was caused by these components.

5.4.2.3 Reaction rate coefficient of TCM formation for individual substances

The proposed model (**Eq. 5-9**) was applied to each TCM formation datasets of individual substance obtained from Experiment series *II*. The best-fit parameters of φ_{Sj} and χ_{Sj} for the substance S_j were determined by conducting the curve fitting as shown in **Fig. 5-4**. The TCMFP $\Delta c_{TCMFP,Sj}$ of the substance S_j was experimentally determined. Applying the best-fit parameters into **Eq. 5-5**, the variable reaction rate coefficient of TCM formation $k_{ov,TCM}^{S_j}$ was calculated. The value of the best-fit parameters, $\Delta c_{TCMFP,Sj}$ and $k_{ov,TCM}^{S_j}$ were shown in **Table 5-4**.

As shown in **Table 5-4**, φ_{Sj} was equal to initial $k_{ov,TCM}^{S_j}(0)$, indicating φ reflects the initial rate coefficient at $X(t) = 0$. Urea showed the highest initial rate coefficient (φ_{urea}) followed by HA, which were an order of magnitude higher than them of the other BFA components. Moreover, the initial φ_{HA} was higher than that of citric acid, which agrees with the observation and assumptions obtained from Experiment series *I* (section 5.4.2.2), i.e. HA might have a higher reactivity towards TCM formation than citric acid. Although citric acid exhibited the highest specific TCMFP, the rate coefficient was not high. The result implies that citric acid might be responsible for the TCM formation at the slow-phase when the circulation time of swimming pool water is long.

The goodness of curve fitting can be found in **Fig. 5-4** for the TCM formation of all substances. Graphically, the model described the experimental data well. The values of R^2 were ranging from 0.85 to 0.99 indicating a moderate to good simulation (**Table**

5-4). RMSE were observed from 0.002 to 0.064 µmol/L. These results indicate that the model successfully simulated the experimental datasets.

Table 5-4. Best-fit model parameters φ and χ, overall reaction rate coefficient of TCM formation, TCMFP, and corresponding R^2 and RMSE with respect to individual substances and substance mixture.

Substance (S_j)	φ_{Sj} L/µmol/h	χ_{Sj}	$k_{ov,TCM}^{S_j}$ L/µmol/h	$\Delta c_{TCMFP,Sj}$ µmol	R^2	RMSE µmol/L
Uric acid	6.95E-5	0.00	6.95E-5 – 6.95E-5	0.05	0.983	0.003
Urea	4.47E-4	2.08	4.47E-4 – 6.51E-5	0.05	0.850	0.005
L-histidine	6.34E-5	0.00	6.34E-5 – 6.34E-5	0.45	0.938	0.042
Creatinine	7.52E-5	0.04	7.52E-5 – 7.22E-5	0.06	0.984	0.003
HA	2.23E-4	1.70	2.23E-4 – 4.11E-5	0.82	0.997	0.012
Hippuric acid	4.89E-5	0.01	4.89E-5 – 4.84E-5	0.05	0.990	0.002
Citric acid	3.55E-5	0.00	3.55E-5 – 3.55E-5	1.53	0.988	0.064
Substance mixture	φ L/µmol/h	χ	$k_{mix,TCM}$ L/µmol/h	Δc_{TCMFP} µmol	R^2	RMSE µmol/L
$\sum_7$BFA	-	-	5.55E-5 – 4.89E-5	1.75	0.981	0.069
BFA+HA	-	-	8.36E-5 – 6.95E-5	2.60	0.959	0.124

Note: the range of $k_{ov,TCM}^{S_j}$ and $k_{mix,TCM}$ indicates the changes of rate coefficient from t = 0 h to t = 240 h; the φ and χ for substance mixture are not needed; TOC of individual substance was 2 mg *C*/L; TOC of BFA was 3 mg *C*/L while it of BFA+HA was 4 mg *C*/L.

5.4.2.4 Prediction of TCM formation for mixtures

As model parameters φ_{Sj} and χ_{Sj} for individual substance were determined, the reaction rate coefficients for substance mixture $k_{mix,TCM}$ can be calculated according to **Eq. 5-15**. Then, the kinetics of TCM formation with respect to $\sum_7$BFA and BFA+HA can be predicted by applying **Eq. 5-17**. The TCMFP used for model prediction is shown in **Table 5-4.**

Figure 5-8 shows the experiment and predicting results of TCM formation for $\sum_7$BFA and BFA+HA as a function of time. It can be seen that the TCM formation profiles is

characterized by an initial fast consumption stage and a later slower formation stage. Good agreement of TCM concentration was found between experimental data and model predictions for $\sum_7$BFA and BFA+HA with R^2 values of 0.96 and 0.98, respectively. RMSE ranged from 0.07 to 0.12 μmol/L. According to the graphical and quantitative analysis, it confirms accuracy fit to the experiment data.

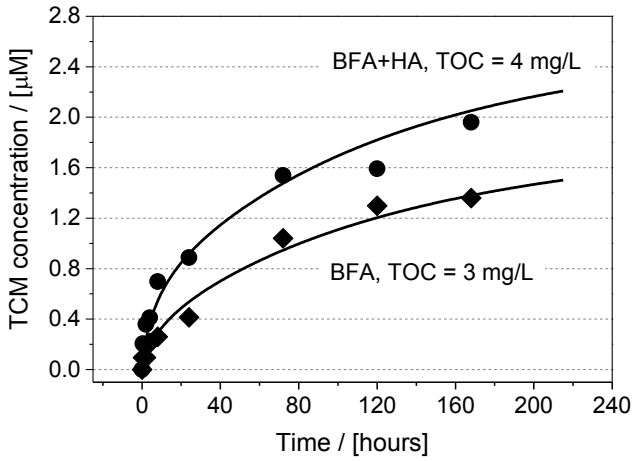

Figure 5-8. TCM formation experiment results and model simulation results for $\sum_7$BFA and BFA+HA.

5.5 CONCLUSIONS

The reactivity of substances remaining in swimming pool waters towards chlorine consumption and trichloromethane (TCM) formation were investigated by conducting laboratory experiments.

The chlorine demand and TCM formation potential tests established the following conclusions. Urea exhibited the highest TOC-related chlorine demand and body fluid analogue (BFA) was more reactive than humic acid (HA) towards chlorine consumption. These results confirm the importance of informing swimmers to have effective hygiene practices, such as not to urinate in the pools and to have a pre-swim shower. Citric acid had the highest specific TCM formation potential compared with other BFA components. HA is more reactive towards TCM formation than BFA.

Kinetics experiments were conducted to derive the second order reaction rate coefficients of chlorine decay and TCM formation for individual substances,

respectively. Uric acid exhibited the fastest initial rate coefficient of chlorine decay. Urea and HA were attributed to the fast reacting TCM formation precursors, which show the reaction coefficients a magnitude higher than that of other substances.

As the individual reaction rate coefficients for individual substances were derived, the chlorine consumption and TCM formation with respect to the mixtures of $\sum_7$BFA and BFA+HA were predicted by the proposed second order models. The models comprised overall (variable) reaction rate coefficients. The models were validated by predicting the kinetics of chlorine consumption and TCM formation with respect to $\sum_7$BFA and BFA+HA. It was found that the model provides very good simulation results.

REFERENCES

APHA (2005a) 2350 B: Standard Method for determination of chlorine demand, American Water Works Association and Water Environment Federation, Washington, D.C.

APHA (2005b) 4500-Cl G: Standard method for determination of chlorine (residual), American Water Works Association and Water Environment Federation, Washington, D.C.

Blatchley, E.R. and Cheng, M. (2010) Reaction Mechanism for Chlorination of Urea. Environmental Science & Technology 44(22), 8529-8534.

Borgmann-Strahsen, R. (2003) Comparative assessment of different biocides in swimming pool water. International Biodeterioration & Biodegradation 51(4), 291-297.

Chowdhury, S., Alhooshani, K. and Karanfil, T. (2014) Disinfection byproducts in swimming pool: Occurrences, implications and future needs. Water Research 53(0), 68-109.

Chowdhury, S., Champagne, P. and McLellan, P.J. (2009) Models for predicting disinfection byproduct (DBP) formation in drinking waters: a chronological review. Science of The Total Environment 407(14), 4189-4206.

Clark, R.M. and Sivaganesan, M. (2002) Predicting Chlorine Residuals in Drinking Water: Second Order Model. Journal of Water Resources Planning and Management 128(2), 152-161.

De Laat, J., Feng, W., Freyfer, D.A. and Dossier-Berne, F. (2011) Concentration levels of urea in swimming pool water and reactivity of chlorine with urea. Water Research 45(3), 1139-1146.

DIN 19643 (2012) Treatment of swimming pool water (in German). Beuth Verlag GmbH, Berlin.

Fisher, I., Kastl, G. and Sathasivan, A. (2011) Evaluation of suitable chlorine bulk-decay models for water distribution systems. Water Research 45(16), 4896-4908.

Gallard, H. and von Gunten, U. (2002) Chlorination of phenols: Kinetics and formation of chloroform. Environmental Science & Technology 36(5), 884-890.

Goeres, D.M., Palys, T., Sandel, B.B. and Geiger, J. (2004) Evaluation of disinfectant efficacy against biofilm and suspended bacteria in a laboratory swimming pool model. Water Research 38(13), 3103-3109.

Hong, H.C., Wong, M.H. and Liang, Y. (2009) Amino acids as precursors of trihalomethane and haloacetic acid formation during chlorination. Archives of environmental contamination and toxicology 56(4), 638-645.

Hua, P., Vasyukova, E. and Uhl, W. (2015) A variable reaction rate model for chlorine decay in drinking water due to the reaction with dissolved organic matter. Water Research 75(0), 109-122.

Jonkergouw, P.M.R., Khu, S.-T., Savic, D.A., Zhong, D., Hou, X.Q. and Zhao, H.-B. (2008) A variable rate coefficient chlorine decay model. Environmental Science & Technology 43(2), 408-414.

Judd, S.J. and Bullock, G. (2003) The fate of chlorine and organic materials in swimming pools. Chemosphere 51(9), 869-879.

Kanan, A. (2010) Occurrence and formation of disinfection byproducts in indoor swimming pools water, Clemson University,, Clemson, SC, USA.

Kanan, A. and Karanfil, T. (2011) Formation of disinfection by-products in indoor swimming pool water: The contribution from filling water natural organic matter and swimmer body fluids. Water Research 45(2), 926-932.

Keuten, M.G.A., Peters, M.C.F.M., Daanen, H.A.M., de Kreuk, M.K., Rietveld, L.C. and van Dijk, J.C. (2014) Quantification of continual anthropogenic pollutants released in swimming pools. Water Research 53(0), 259-270.

Keuten, M.G.A., Schets, F.M., Schijven, J.F., Verberk, J.Q.J.C. and van Dijk, J.C. (2012) Definition and quantification of initial anthropogenic pollutant release in swimming pools. Water Research 46(11), 3682-3692.

Li, J. and Blatchley, E.R. (2007) Volatile Disinfection Byproduct Formation Resulting from Chlorination of Organic−Nitrogen Precursors in Swimming Pools. Environmental Science & Technology 41(19), 6732-6739.

Lian, L., E, Y., Li, J. and Blatchley, E.R. (2014) Volatile Disinfection Byproducts Resulting from Chlorination of Uric Acid: Implications for Swimming Pools. Environmental Science & Technology 48(6), 3210-3217.

Lindstrom, A.B., Pleil, J.D. and Berkoff, D.C. (1997) Alveolar breath sampling and analysis to assess trihalomethane exposures during competitive swimming training. Environmental Health Perspectives 105(6), 636.

Piñeiro, G., Perelman, S., Guerschman, J.P. and Paruelo, J.M. (2008) How to evaluate models: Observed vs. predicted or predicted vs. observed? Ecological Modelling 216(3–4), 316-322.

Richardson, S.D., DeMarini, D.M., Kogevinas, M., Fernandez, P., Marco, E., Lourencetti, C., Ballesté, C., Heederik, D., Meliefste, K. and McKague, A.B. (2010) What's in the Pool? A Comprehensive Identification of Disinfection By-products and Assessment of Mutagenicity of Chlorinated and Brominated Swimming Pool Water. Environmental Health Perspectives 118(11), 1523.

Sadiq, R. and Rodriguez, M.J. (2004) Disinfection by-products (DBPs) in drinking water and predictive models for their occurrence: a review. Science of The Total Environment 321(1–3), 21-46.

Shang, C. and Blatchley, E.R. (1999) Differentiation and Quantification of Free Chlorine and Inorganic Chloramines in Aqueous Solution by MIMS. Environmental Science & Technology 33(13), 2218-2223.

Simard, S., Tardif, R. and Rodriguez, M.J. (2013) Variability of chlorination by-product occurrence in water of indoor and outdoor swimming pools. Water Research 47(5), 1763-1772.

USEPA (2009) National primary drinking water regulations. EPA 816-F-09-0004.

Weaver, W.A., Li, J., Wen, Y., Johnston, J., Blatchley, M.R. and Blatchley Iii, E.R. (2009) Volatile disinfection by-product analysis from chlorinated indoor swimming pools. Water Research 43(13), 3308-3318.

WHO (2011) Guidelines for drinking-water quality, 4th edition, Geneva.

Yang, X., Peng, J., Chen, B., Guo, W., Liang, Y., Liu, W. and Liu, L. (2012) Effects of ozone and ozone/peroxide pretreatments on disinfection byproduct formation during subsequent chlorination and chloramination. Journal of Hazardous Materials 239–240(0), 348-354.

Zwiener, C., Richardson, S.D., De Marini, D.M., Grummt, T., Glauner, T. and Frimmel, F.H. (2007) Drowning in disinfection byproducts? Assessing swimming pool water. Environmental Science & Technology 41(2), 363-372.

CHAPTER 6

Summary and general conclusion

6 SUMMARY AND GENERAL CONCLUSION

An important aspect of modeling water quality in water distribution system (WDS) is the ability to predict the temporal and spatial distribution of disinfectant residuals and the formation of disinfection byproducts. Although the water quality modeling techniques have been applied for several decades, a universal model for different scenarios of chlorination is, however, lacking. Especially the calibration is the most challenging task for water quality modeling application, as the over-simplification of the conventional approaches must be compensated by the calibration of over-parametrized models. Thus, to decrease the number of model parameter and apply the model under different chlorination conditions with invariant parameters becomes a driven force of this research (**Chapter 1**).

Chapter 2 focuses on the development of a chlorine decay model with respect to the bulk reaction. The developed second order model took into account the variable reactivity of reactive sites which provided by NOM. Naturally, species with higher reactivity were converted firstly and then those with low reactivity. Thus, the overall reactivity was decreasing continuously with the reaction progress and expressed by the variable second order rate coefficient. The overall (variable) reaction rate coefficient was described by an exponential function, which was maximum at the beginning of the reaction and was approaching to zero when the maximum accumulative chlorine demand has been turned over. Only two parameters were needed for calculation of overall reaction coefficient, which save the efforts for model calibration. Moreover, the model was shown to describe the chlorine decay rate as a function of conversion or time with a high quality applying statistical goodness-of-fit test for different waters. Without any further calibration, the model had the capability to describe chlorine decay rates after rechlorination and after water mixing, as well as to consider different temperature effects and initial chlorine concentration.

By applying the same idea and assumption, which was established in **Chapter 2**, **Chapter 3** describes the development of a THM formation model with a variable

reaction rate coefficient for the bulk reaction. The coefficient reflects the different reactivity of NOM to form THM. As THM contains the trichloromethane (TCM) and brominated THM, therefore, the model also considered the bromide (bromine) effects on the kinetics of THM. The proposed model was proven to be able to predict the TCM and TTHM concentrations with constant parameters under different initial chlorine concentrations, rechlorination conditions. Arrhenius equation was approved to be suitable for both the TCM and TTHM models modification, and consequently, enable the model to provide reliable results for chlorination at different temperatures. Generally, with the proposed models, the calibration process was simplified and show good predictions for a wide application in the field of WDS.

Different from the first two chapters which are related to the bulk reaction, in **Chapter 4**, the models are extended to simulate the wall reaction. Therefore, in an experiment synthesized pipe deposits, goethite and magnetite, were dosed into water sample. To investigate the influence of the pipe deposits on the reactivity of NOM, adsorption experiments were conducted in advance. The results showed that high and intermediate molecular weight NOM components, e.g. biopolymers, humic acid, and building blocks were preferentially adsorbed onto the goethite and magnetite. These fractions of NOM also contributed to the THM formation. As for the chlorination experiments, it was found that the chlorine consumption and TCM formation were increased in the presence of pipe deposits compared to the bulk water containing no pipe deposits, even though the NOM concentration and composition was initially the same. The second order models with variable reaction rate coefficients, which were initially used to predict chlorine decay and TCM formation in the bulk water, were further extended for the conditions where pipe deposits were present. The model was shown to be able to describe chlorine decay and TCM formation for chlorination of treated water containing both different pipe deposits dosages and different initial chlorine concentrations with constant parameters.

Chapter 5 focuses on the application of the model described in **Chapter 2** and **3** to swimming pool water chlorination. The chlorine demand and TCM formation

potential tests were initially conducted to investigate the reactivity of each specific substance in the swimming pool water. The conclusions indicate that urea exhibited the highest total organic carbon-related chlorine demand and body fluid analogue was more reactive than humic acid towards chlorine consumption. These results confirm the importance of informing swimmers to have effective hygiene practices. Citric acid had the highest specific TCM formation potential compared with the other BFA components. HA is more reactive toward TCM formation than BFA. Kinetics experiments were conducted to derive the second order reaction rate coefficients of chlorine decay and TCM formation for individual substances. Uric acid exhibited the fastest initial rate coefficient of chlorine decay. Urea and HA were attributed to the fast reacting TCM formation precursors, which were a magnitude high than the other substances. As the individual reaction rate coefficients for individual substances were derived, the overall rate coefficients of chlorine consumption and TCM formation with respect to the mixture of substances present in the real swimming pool water were derived. In other words, the rate coefficients reflect the reaction progress and were calculated based on the rate coefficients of individual substances and the concentrations of the substances remaining in water. The models were validated by predicting the kinetics of chlorine consumption and TCM formation with respect to BFA mixture and a mixture of BFA and HA. It was found that the model provides good simulation results.

In general, the models developed in this study have wider applications potential as the number of model parameters is decreased and the re-calibration is not required. By using the model, it is possible to simulate chlorine and THM concentration in many different chlorination scenarios.

CHAPTER 7

Appendix

7 APPENDIX

7.1 EQUATIONS

7.1.1 Differentiation of Eq. 2-7 / derivation of Eq. 2-8

$$k_{ov,Cl}(t)=\frac{\sum_{i=1}^{n}\left[k_{i,Cl}\cdot c_{R_{i,Cl}}(t)\right]}{\sum_{i=1}^{n}c_{R_{i,Cl}}(t)} \qquad \text{Equation. 2-8}$$

$$\frac{dk_{ov,Cl}(t)}{dt}=\frac{\left[\sum_{i=1}^{n}\left[k_{i,Cl}\cdot c_{R_i}(t)\right]\right]'\cdot\sum_{i=1}^{n}c_{R_{i,Cl}}(t)-\sum_{i=1}^{n}\left[k_{i,Cl}\cdot c_{R_{i,Cl}}(t)\right]\cdot\left[\sum_{i=1}^{n}c_{R_{i,Cl}}(t)\right]'}{\left[\sum_{i=1}^{n}c_{R_{i,Cl}}(t)\right]^2} \qquad \text{Equation 7-1}$$

Among them, k_i is constant for individual chlorine-reactive site, therefore, yields:

$$\frac{d\sum_{i=1}^{n}\left[k_{i,Cl}\cdot c_{R_{i,Cl}}(t)\right]}{dt}=\sum_{i=1}^{n}k_{i,Cl}\cdot\frac{dc_{R_{i,Cl}}(t)}{dt}=\sum_{i=1}^{n}k_{i,Cl}\cdot\left[-k_i\cdot c_{Cl}(t)\cdot c_{R_{i,Cl}}(t)\right] \qquad \text{Equation 7-2}$$

$$\frac{d\sum_{i=1}^{n}c_{R_{i,Cl}}(t)}{dt}=\sum_{i=1}^{n}\left[-k_{i,Cl}\cdot c_{Cl}(t)\cdot c_{R_{i,Cl}}(t)\right] \qquad \text{Equation 7-3}$$

Substituting **Eq. 7-2** and **Eq. 7-3** to the **Eq. 7-1**, yields,

$$\frac{dk_{ov,Cl}(t)}{dt}=\frac{\sum_{i=1}^{n}k_{i,Cl}\cdot\left[-k_{i,Cl}\cdot c_{Cl}(t)\cdot c_{R_{i,Cl}}(t)\right]\cdot\sum_{i=1}^{n}c_{R_{i,Cl}}(t)-\sum_{i=1}^{n}\left[k_{i,Cl}\cdot c_{R_{i,Cl}}(t)\right]\cdot\sum_{i=1}^{n}\left[-k_{i,Cl}\cdot c_{Cl}(t)\cdot c_{R_{i,Cl}}(t)\right]}{\left[\sum_{i=1}^{n}c_{R_{i,Cl}}(t)\right]^2} \qquad \text{Equation 7-4}$$

$$\frac{dk_{ov,Cl}(t)}{dt}=c_{Cl}(t)\cdot\left[\frac{-\sum_{i=1}^{n}\left[{k_{i,Cl}}^2\cdot c_{R_{i,Cl}}(t)\right]}{\sum_{i=1}^{n}c_{R_{i,Cl}}(t)}+\frac{\left[\sum_{i=1}^{n}\left[k_{i,Cl}\cdot c_{R_{i,Cl}}(t)\right]\right]^2}{\left[\sum_{i=1}^{n}c_{R_{i,Cl}}(t)\right]^2}\right] \qquad \text{Equation 7-5}$$

According to **Eq. 2-7**,

$$\left[\sum_{i=1}^{n}\left[k_{i,Cl}\cdot c_{R_{i,Cl}}(t)\right]\right]^2 = k_{ov,Cl}^2\cdot\left[\sum_{i=1}^{n}c_{R_{i,Cl}}(t)\right]^2 \qquad \text{Equation 7-6}$$

Thus, substituting **Eq. 7-6** to **Eq. 7-5**:

$$\frac{dk_{ov,Cl}(t)}{dt} = c_{Cl}(t)\cdot\left[k_{ov,Cl}^2(t) - \frac{\sum_{i=1}^{n}\left[{k_{i,Cl}}^2\cdot c_{R_{i,Cl}}(t)\right]}{\sum_{i=1}^{n}c_{R_{i,Cl}}(t)}\right] \qquad \text{Equation 7-7}$$

Hence, the **Eq. 7-7** is the **Eq. 2-8** in the manuscript. It can be seen that:

$$k_{ov,Cl}^2(t) \le \frac{\sum_{i=1}^{n}\left[{k_{i,Cl}}^2\cdot c_{R_{i,Cl}}(t)\right]}{\sum_{i=1}^{n}c_{R_{i,Cl}}(t)} \qquad \text{Equation 7-8}$$

This is because

$$\left[\sum_{i=1}^{n}\left[k_{i,Cl}\cdot c_{R_{i,Cl}}(t)\right]\right]^2 \le \sum_{i=1}^{n}\left[{k_{i,Cl}}^2\cdot c_{R_{i,Cl}}(t)\right]\cdot\sum_{i=1}^{n}c_{R_{i,Cl}}(t) \qquad \text{Equation 7-9}$$

Eq. 7-9 can be further expressed as follows:

$$\left[\sum_{i=1}^{n}\left[k_{i,Cl}\cdot c_{R_{i,Cl}}(t)\right]\right]^2 =$$

$$\sum_{i=1}^{n}\left[k_{i,Cl}\cdot c_{R_{i,Cl}}(t)\right]^2 + 2\cdot(k_1c_1k_2c_2+\ldots+k_1c_1k_nc_n+k_2c_2k_3c_3+\ldots+k_2c_2k_nc_n+k_3c_3k_4c_4+\ldots+k_3c_3k_nc_n+\ldots)$$

$$\sum_{i=1}^{n}\left[{k_{i,Cl}}^2\cdot c_{R_{i,Cl}}(t)\right]\cdot\sum_{i=1}^{n}c_{R_{i,Cl}}(t) =$$

$$\sum_{i=1}^{n}\left[k_{i,Cl}\cdot c_{R_{i,Cl}}(t)\right]^2 + k_1^2c_1c_2+k_1^2c_1c_3+\ldots+k_1^2c_1c_n+k_2^2c_2c_1+k_2^2c_2c_3+\ldots+k_2^2c_2c_n+k_3^2c_3c_1+k_3^2c_3c_2+\ldots)$$

Comparing above two equations, it can be seen that:

$$2 \cdot k_1 c_1 k_2 c_2 \le k_1^2 c_1 c_2 + k_2^2 c_2 c_1 \qquad \text{.i.e., } 0 \le (k_1 - k_2)^2$$

$$2 \cdot k_2 c_2 k_3 c_3 \le k_2^2 c_2 c_3 + k_3^2 c_3 c_2 \qquad \text{i.e., } 0 \le (k_2 - k_3)^2$$

and so on.

Equation 7-10

According to **Eq. 7-10**, **Eq. 7-9** was validated. Therefore, the change rate of $k_{ov,Cl}$ i.e. $\frac{dk_{ov,Cl}(t)}{dt}$ is negative. In other words, the $k_{ov,Cl}$ is decreasing with reaction time.

Furthermore, $\frac{dk_{ov,Cl}(t)}{dt}$ is second order respect to the $k_{ov,Cl}$ and related to the chlorine concentration.

7.1.2 Differentiation of Eq. 2-9 / derivation of Eq. 2-10

$$k_{ov,Cl}(t) = \alpha \cdot e^{-\beta \cdot \left[\frac{\Delta c_{Cl}(t)}{\Delta c_{Cl,\max}}\right]}$$

Eq. 2-9

$$\Delta c_{Cl}(t) = c_{Cl}(0) - c_{Cl}(t)$$

$$\frac{dk_{ov,Cl}(t)}{dt} = -\alpha \cdot e^{-\beta \cdot \left[\frac{\Delta c_{Cl}(t)}{\Delta c_{Cl,\max}}\right]} \cdot \left(-\frac{\beta}{\Delta c_{Cl,\max}} \cdot \frac{d\left[c_{Cl}(0) - c_{Cl}(t)\right]}{dt}\right)$$

Equation 7-11

$$\frac{dk_{ov,Cl}(t)}{dt} = \alpha \cdot e^{-\beta \cdot \left[\frac{\Delta c_{Cl}(t)}{\Delta c_{Cl,\max}}\right]} \cdot \left[\frac{\beta}{\Delta c_{Cl,\max}} \cdot -k_{ov,Cl}(t) \cdot c_{Cl}(t) \cdot c_R(t)\right]$$

Equation 7-12

$$\frac{dk_{ov,Cl}(t)}{dt} = -\frac{\beta}{\Delta c_{Cl,\max}} \cdot k_{ov,Cl}^2(t) \cdot c_{Cl}(t) \cdot c_R(t)$$

Equation 7-13

Hence, the **Eq. 7-13** is the **Eq. 2-10** in the manuscript.

It can be seen that $\frac{dk_{ov,Cl}(t)}{dt}$ is negative in authors' model, and it is related to $C_{Cl}(t)$ and $k_{ov,Cl}^2$, which is satisfied with the characteristics of $k_{ov,Cl}$ obtained theoretically.

7.2 TABLES

Table 7-1. Calculated initial VRRC and the value of VRRC at the end of experimental time.

Waters	ICC	Temperature	α	Maximum experimental reaction time	Corresponding conversion fraction	Corresponding k_{ov} (X)
	mg/L	° C	L/mg/h	h	%	L/mg/h
AWT	0.6	20	0.140	36	64.5	9.55E-3
	2.0		0.140	36	42.5	1.09E-2
HWT	0.6	20	0.210	72	17.0	1.46E-2
	2.0	20	0.210	72	32.9	1.20E-3
	4.0	20	0.210	72	38.9	4.65E-4
	0.6	12	0.080	96	16.4	6.77E-3
	0.6	5	0.038	96	14.9	3.71E-3
	2	5	0.038	120	27.1	5.98E-4
	4	5	0.038	120	32.5	2.37E-4
PDW	2.1		0.100	168	35.7	6.62E-3
	4.5		0.100	168	60.8	1.17E-3
	6.7	-	0.100	168	67.9	5.70E-4
	8.8		0.100	168	71.9	4.00E-4
	11.2		0.100	168	75.5	3.10E-4
PRW	3	15	0.180	117.83	95	2.39E-3
	3	20	0.324	72.80	95	2.94E-3
	3	25	0.495	74.38	95	4.99E-3
	3	30	0.884	46.17	95	9.25E-3
	3	35	1.184	22.82	95	1.29E-2
	3	40	1.730	21.92	95	2.17E-2
CWT	3.6	-	0.070	120	70.4	4.79E-3

Waters	ICC	Temperature	α	Maximum experimental reaction time	Corresponding conversion fraction	Corresponding k_{ov} (X)
	mg/L	° C	L/mg/h	h	%	L/mg/h
GWT	4.0	-	0.060	120	76.3	3.98E-3
LWR	12.2	-	0.020	120	64.9	1.04E-3

Continue Table 7-1

Table 7-2. Calibrated model parameters, number of measurement (n) and model accuracy for the proposed VRRC model for chlorination at different temperatures, water mixing and rechlorination conditions.

Scenarios	Water	ICC mg/L	Booster Concentr-ation mg/L	Rechlorinati-on /Mixing time hours	Temper-ature °C	α L/mg/h	β	R^2	SSE	RMSE mg/L	F value	p value	n
Chlorination at different temperatures	HWT	0.6	-	-	20	0.19	15.60	0.98	0.04	0.05	201.6	5.8E-7	10
		0.6	-	-	12	0.09	15.60	0.94	0.080	0.06	105.2	7.01E-6	10
		0.6	-	-	5	0.04	15.62	0.98	0.01	0.03	278.1	1.42E-5	8
		2.0	-	-	5	0.04	15.62	0.98	0.01	0.05	246.6	1.90E-5	7
		4.0	-	-	5	0.04	15.62	0.95	0.19	0.12	97.9	1.79E-4	7
	PRW	3.0	-	-	15	0.18	4.55	0.95	1.40	0.20	135.5	1.58E-7	15
		3.0	-	-	20	0.32	4.95	0.93	1.69	0.25	266.6	4.8E-10	13
		3.0	-	-	25	0.49	4.84	0.97	0.37	0.14	479.2	4.8E-11	15
		3.0	-	-	30	0.88	4.80	0.98	0.22	0.14	487.2	1.8E-10	13
		3.0	-	-	35	1.18	4.76	0.97	0.17	0.12	324.5	9.2E-8	11
		3.0	-	-	40	1.73	4.61	0.98	0.21	0.13	529.6	1.2E-10	14
Mixing	AWT	1.9	-	36	20	0.13	4.51	0.97	0.01	0.03	539.8	3.5E-13	17
	HWT	0.6	-	1:1(v:v)	20	0.19	15.59						
	AWT	2.5	-	36	20	0.13	4.51						
	HWT	0.6	-	2:1(v:v)	20	0.21	15.72						
Rechlorination	HWT	0.6	0.65	24	20	0.21	15.72	0.98	0.02	0.02	481.8	1.9E-10	21
	HWT	0.6	0.40	36	20	0.21	15.72						

Table 7-3. Best-fit model parameters φ and χ for each formation data set, average parameters ($\overline{\varphi}$ and $\overline{\chi}$), and corresponding R^2, RMSE, and F value.

DBP	Water sample	DBP FP	ICC	φ $k_{ov,TCM}(0)$	χ	BSF	R^2	RMSE	*F* value	*Range of* $k_{ov,THM}$
		μM	μM	$M^{-1}s^{-1}$						$M^{-1}s^{-1}$
TCM	HWT	0.60	8.5	0.067	-2.22	-	0.938	0.005	61.55	-
	HWT		27.9	0.063	-2.51	-	0.987	0.010	884.28	-
	HWT		51.8	0.056	-2.70	-	0.972	0.015	213.68	-
	Coefficient of variation			9.4%	-9.8%					-
	Average parameters*			0.063	-2.47		0.960	0.017	388.6	-
Total THM	HWT	0.60	8.5	0.067	-2.22	0.27	0.911	0.016	41.24	0.217 – 0.04
	HWT		27.9	0.063	-2.51	0.01	0.972	0.019	342.16	0.109 – 0.04
	HWT		51.8	0.056	-2.70	0.01	0.973	0.024	179.85	0.076 – 0.02

7.3 FIGURES

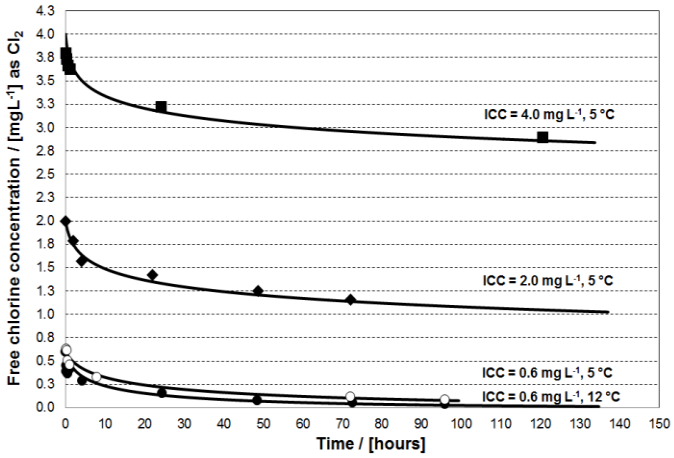

Figure 7-1. Decay test and VRRC model simulation for HWT water sample at different ICCs (0.6, 2 and 4 mg/L) and temperatures (12 and 5°C). Points represent experimental data and solid curves are the respective VRRC model predicting results.

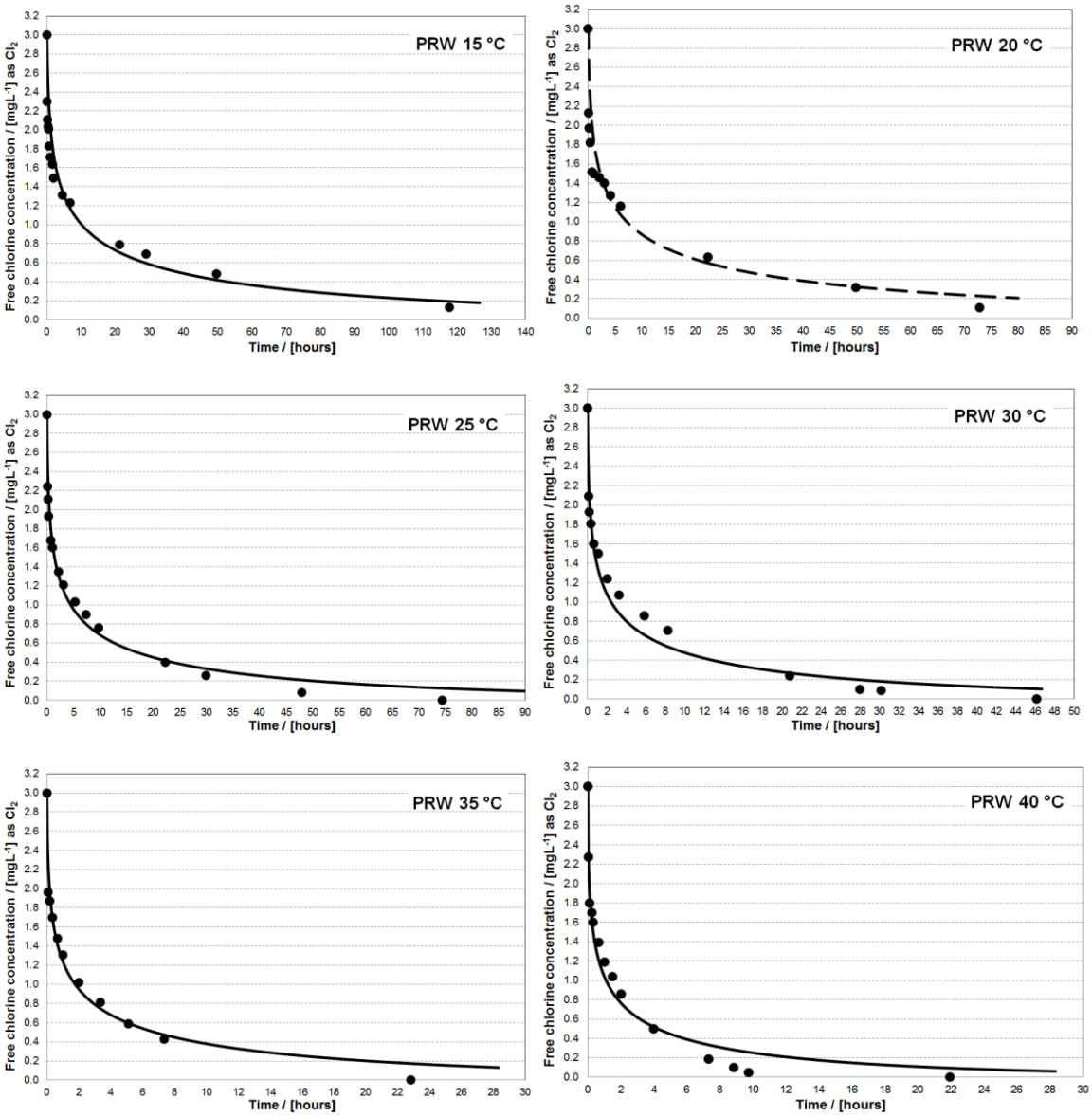

Figure 7-2. Decay test and VRRC model simulation for PRW water sample at ICC of 3 mg/L, and temperatures ranging from 15 to 40°C. Points represent experimental data, dash line represents VRRC model fitted to the experimental data, and solid curves are the respective VRRC model predicting results.

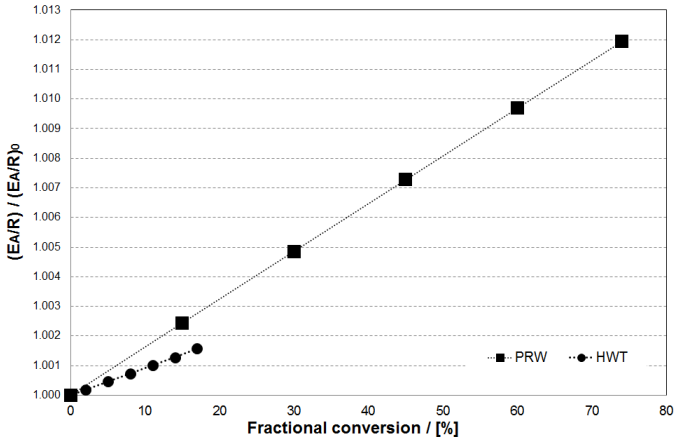

Figure 7-3. The ratio of E_A/R to initial E_A/R increasing with fraction conversion based on the data obtained from PRW and HWT water sample.